PONTIFÍCIA UNIVERSIDADE CATÓLICA DO PARANÁ
ESCOLA POLITÉCNICA
PROGRAMA DE PÓS-GRADUAÇÃO EM TECNOLOGIA EM SAÚDE
YALE UNIVERSITY
NEUROLOGY DEPARTMENT

MARIANA DE MELLO GUSSO ESPINOLA

DOCTORATE THESIS

More than a feeling: scalp EEG and eye correlates of conscious tactile perception

CURITIBA/ NEW HAVEN
2020

MARIANA DE MELLO GUSSO ESPINOLA

More than a feeling: scalp EEG and eye correlates of conscious tactile perception

Doctoral thesis presented to the Graduate Program on Health Technology from the Pontifical Catholic University of Paraná.

Mentor: Prof. Dr. Percy Nohama (PUCPR)
Co-mentor: Prof. Dr. Hal Blumenfeld (Yale University)

CURITIBA/ NEW HAVEN

2020

Dados da Catalogação na Publicação
Pontifícia Universidade Católica do Paraná
Sistema Integrado de Bibliotecas – SIBI/PUCPR
Biblioteca Central
Edilene de Oliveira dos Santos CRB-9/1636

Espinola, Mariana de Mello Gusso
E77m More than a feeling : scalp EEG and eye correlates of conscious tactile
2020 perception / Mariana de Mello Gusso ; Mentor, Percy Nohama ; co-mentor, Hal Blumenfeld. -- 2020
121 f. : il. ; 30 cm

Tese (doutorado) – Pontifícia Universidade Católica do Paraná, Curitiba, 2020
Bibliografia: f.93-102

1. Tecnologia médica. 2. Neurologia. 3. Consciência. 4. Percepção do tato. 5. Eletroencefalografia. I. Nohama, Percy. II. Blumenfeld, Hal. III. Pontifícia Universidade Católica do Paraná. Programa de Pós-Graduação em Tecnologia em Saúde. IV. Título

CDD. 20.ed. – 610.28

Pontifícia Universidade Católica do Paraná
Escola Politécnica
Programa de Pós-Graduação em Tecnologia em Saúde

STATEMENT OF THESIS APPROVAL No. 014

The Doctoral Thesis entitled "**MORE THAN A FEELING: SCALP EEG AND EYE CORRELATES OF CONSCIOUS TACTILE PERCEPTION**" was presented during a virtual viva public session by the candidate **Mariana de Mello Gusso Espinola** on **September 30, 2020**. Therefore, it was judged to obtain the title of Doctor in Health Technology, and it was approved in its final form by the Graduate Program in Health Technology.

BOARD OF EXAMINERS:

Prof. Dr. Percy Nohama – Supervisor and President – PUCPR
Prof. Dr. Alberto Cliquet Junior - UNICAMP
Prof. Dr. Amer Cavalheiro Hamdan - UFPR
Prof. Dr. Guilherme Nunes Nogueira Neto - PUCPR
Prof. Dr. Michael Joseph Crowley - Yale University

The original copy of this document with the signature of the PPGTS Coordinator, after the delivery of the final version of the work, is filed at the Program Secretariat.

Curitiba, October 23rd, 2020.

TERMO DE APROVAÇÃO DE TESE Nº 014

A Tese de Doutorado intitulada "**MAIS QUE UMA SENSAÇÃO: EEG E CORRELATOS OCULARES DA PERCEPÇÃO TÁTIL CONSCIENTE**" defendida em sessão pública pelo(a) candidato(a) **Mariana de Mello Gusso Espinola** no dia **30 de setembro de 2020**, foi julgada para a obtenção do título de Doutor em Tecnologia em Saúde, e aprovada em sua forma final, pelo Programa de Pós-Graduação em Tecnologia em Saúde.

BANCA EXAMINADORA:

Prof. Dr. Percy Nohama – Orientador e Presidente – PUCPR
Prof. Dr. Alberto Cliquet Junior - UNICAMP
Prof. Dr. Amer Cavalheiro Hamdan - UFPR
Prof. Dr. Guilherme Nunes Nogueira Neto - PUCPR
Prof. Dr. Michael Joseph Crowley - Yale University

A via original deste documento encontra-se arquivada na Secretaria do Programa, contendo a assinatura do Coordenador após a entrega da versão corrigida do trabalho.

Curitiba, 23 de outubro de 2020.

Prof. Dr. Percy Nohama
Head of PPGTS PUCPR
Coordenador do PPGTS PUCPR

Rua Imaculada Conceição, 1155, Prado Velho, CEP 80215-901, Curitiba – PR, Brasil
Telefone: +55 41 3271-1657
E-mail: ppgts@pucpr.br

ACKNOWLEDGEMENTS

I would like to thank the financial support from Betsy and Jonathan Blattmachr Family, the Loughridge Williams Foundation, Coordenação de Aperfeiçoamento de Pessoal de Nível Superior (CAPES), and Fundação Araucária and for the finantial support.

My profound appreciation goes to my mentors: Dr. Percy Nohama and Dr. Hal Blumenfeld. Dr. Percy Nohama introduced me to science and has been my guide since my masters, always encouraging me to take the next step and go after my dreams. Dr. Hal Blumenfeld received me with open arms and has been a great source of knowledge and learning.

My gratitude to the members of both laboratories (Blumenfeld Lab and Laboratório de Engenharia de Reabilitação), the ones who have directly helped me with this research: Sharif Kronemer, Ganesh Chandrasekaran, and Julia Ding. The undergrads that have helped me find my role as a mentor: Arielle Schutt (a highschooler then), David Zuckerman, Dante Lass, Gabriele Serur (now a master's student), João Pedro Leme da Silva, Mariany Zanchetta, and Renata Cavalheiro. Moreover, especially to Kate Christison-Lagay, who was not only a collaborator to this whole process, but also an editor, an encourager, and a friend.

I am also really grateful for our support staff: Ana Claudia Kampa, Kathy Polak, and Rosa Ortiz. You all moved mountains so I could be here! Thank you.

Thank you to my thesis committee for being available and willing to participate. It is a challenging time around the world, and being willing to help is a real gift.

My gladness goes to my family, especially my husband, that has been my support and agreed on joining me on this journey.

Thank you to God, that has blessed me so far.

GUSSO, Mariana de Mello. **More than a feeling: scalp EEG and eye correlates of conscious tactile perception.** 117p. Tese de Doutorado. Programa de Pós-Graduação em Tecnologia em Saúde (PPGTS). Pontifícia Universidade Católica do Paraná (PUCPR). Curitiba, 2020.

ABSTRACT

Understanding the neural basis of consciousness is a fundamental goal of neuroscience, and one path towards this goal is to focus on the mechanisms of conscious perception. However, to understand the multimodal nature of conscious perception, multiple sensory modalities have to be used, and the majority of studies focus on visual or auditory perception, with significantly fewer involving tactile perception. With the goal of investigating the Event-Related Potential (ERP) oscillations and eye-metrics related to tactile conscious perception (and as specific goals to evaluate conscious perception through a threshold tactile task; to identify the mechanisms responsible for tactile conscious perception through EEG signals; to identify the indirect correlates of tactile conscious perception of eye-metrics; and to relate the tactile conscious perception's eye-metric findings with auditory ones), we developed a novel tactile threshold task that we conducted in conjunction with high-density scalp electroencephalography (hdEEG) and eye-metric recordings. The neurophysiological signals of 23 adult participants (10 male; 6 left-handed) and the eye-metric recordings of 10 adult participants (4 male; 3 left-handed) were analyzed. Participants were delivered threshold-level vibrations to one of the four non-thumb fingers and were asked to report their perception using a response box. With false discovery rate (FDR) procedures, we found a significant P60 contralaterally, P100 ipsilaterally, and P200 and P3b bilaterally for perceived vibrations; significant contralateral P100 and bilateral P3b were found for not perceived vibrations, and a significant frontal contralateral N140 was discovered when comparing signals associated with perceived versus not perceived trials. Additionally, we found that pupil diameter and blink rate increase and microsaccades decrease following vibrations perceived relative to those not perceived. This study represents the first instance of a tactile-threshold task to study ERPs that differ due to perceptual status. While many of the signals are consistent with ERP-findings across sensory modalities, our results indicate a significant P3b in not-perceived trials raises more questions regarding P3b's perceptual meaning. Additionally, our findings on the dynamics of eye metrics are consistent with eye metrics as a measure of physiological arousal as pertains to conscious perception and may represent a path toward creating tactile no-report tasks in the future.

Keywords: tactile perception, consciousness, electroencephalogram, event-related potentials, pupillometry

GUSSO, Mariana de Mello. **More than a feeling: scalp EEG and eye correlates of conscious tactile perception.** 117p. Tese de Doutorado. Programa de Pós-Graduação em Tecnologia em Saúde (PPGTS). Pontifícia Universidade Católica do Paraná (PUCPR). Curitiba, 2020.

RESUMO

Compreender as bases neurais da consciência é uma das metas principais das neurociências, um dos caminhos para alcançá-la é compreender os mecanismos da percepção consciente. No entanto, para entender a natureza multimodal da percepção consciente, várias modalidades sensoriais precisam ser usadas, e a maioria dos estudos foca na percepção visual e auditiva, com poucos estudos focando na percepção tátil. Com o objetivo de investigar as oscilações de potenciais relacionados a eventos (PRE) e métricas oculares relacionadas com a percepção consciente tátil (e como objetivos específicos avaliar a percepção consciente através de uma tarefa tátil no limiar perceptivo; identificar os mecanismos responsáveis pela percepção consciente tátil através de sinais de eletroencefalograma (EEG); identificar os correlatos indiretos da percepção consciente tátil através dos achados de métrica ocular; e relacionar as métricas oculares da percepção consciente tátil com as da percepção consciente auditiva), nós desenvolvemos uma nova tarefa de limiar tátil realizada com eletroencefalograma de escalpe de alta densidade e métricas oculares. Os sinais neurofisiológicos de 23 adultos (10 homens, 6 canhotos) e as gravações de métricas oculares de 10 participantes (4 homens, 3 canhotos) foram analisados. Participantes receberam vibrações no nível do limiar da percepção em um dos quatro dedos (não polegar) e reportaram a sua percepção através de um acionador. Com procedimentos de taxa de detecção falsa (FDR), nós encontramos sinais significativos no P60 contralateral, P100 ipsilateral e P200 e P3b bilateralmente para vibrações percebidas; P100 contralateral e P3b bilateral para as vibrações não percebidas e um N140 contralateral frontal quando comparando os sinais percebidos e não percebidos. Adicionalmente, nós percebemos que há um aumento no diâmetro da pupila e na taxa de piscadas e uma diminuição nas microssacadas posteriormente a vibrações percebidas se comparadas com as não percebidas. Esse estudo representa a primeira vez que se é usada uma tarefa no limiar tátil com PRE que diferem devido aos seus status perceptivo. Enquanto muitos sinais são consistentes com achados de PRE de outras modalidades sensoriais, o achado do nosso estudo de um aumento significativo no P3b em vibrações não percebidas gera mais dúvidas sobre o significado perceptual do P3b. Nossos resultados na dinâmica das métricas oculares são consistentes com as métricas oculares serem consideradas uma medida de excitação relativa à percepção consciente e pode representar um caminho para a criação de testagens táteis sem respostas no futuro.

Palavras chave: percepção tátil, consciência, eletroencefalograma, potenciais relacionados a eventos, pupilometria

ILLUSTRATIONS LIST

Figure 1 – Neuron structure....18
Figure 2 – Brain hemispheres and its main structures....20
Figure 3 – Brain hemispheres division....21
Figure 4 – Default mode and task-related maps in healthy controls....25
Figure 5 – Subliminal and conscious processing according to the “global neuronal workspace” model....28
Figure 6 – Wyart and Tallon-Baudry Experimental Design....29
Figure 7 – Visual paradigms to evoke “transient blindness” in neurologically intact observers....30
Figure 8 – Switch and wave of neuronal activity in the first second of conscious perception....31
Figure 9 – Thresholds of hearing sensitivity for various frequencies....33
Figure 10 – Traditional fMRI Results on auditory trials for left stimulus....34
Figure 11 – Receptors mediating tactile senses....36
Figure 12 – Grand averaged somatosensory ERPs....37
Figure 13 – EEG electrode placing....38
Figure 14 – Scalp maps of event related potentials elicited by visible and invisible words....40
Figure 15 – Evoked and reset phase model....41
Figure 16 – Fixational eye movements and visual fading....44
Figure 17 – Tactile threshold task and experimental set-up.....48
Figure 18 – 256 electrodes net positioning – superior view....56
Figure 19 – Tactile data collection set-up....67
Figure 20 – Tactile behavioral results....70
Figure 21 – Auditory behavioral results....71
Figure 22 – EEG before and after applying the high-pass filter and the CleanLine procedure....72
Figure 23 – 30 Hz channels flagged for deletion....72
Figure 24 – 30 Hz electrodes after deletion and interpolation....73
Figure 25 – Examples of components identified by ICA method....73
Figure 26 – ICA deletion results....74
Figure 27 – Data before and after 25 Hz low-pass filter....75

Figure 28 – Electrical potential difference (μV) topographic maps. 76
Figure 29 – Electrical potential difference time courses. 77
Figure 30 – Electrical potential difference topographic maps without mirroring.....78
Figure 31 – Eye-Metrics' results 80

TABLE LIST

Table 1 – Categories of neuroglia 19
Table 2 – Primary afferent fibers and their roles.....35
Table 3 – Tactile task’s participant demographic information.....47
Table 4 – Auditory eye-metrics’ participant demographic information 58
Table 5 – Original (O) and New (N) electrodes mapping.....64
Table 6 – Activities schedule.....69

ABBREVIATIONS LIST

CAPES	Coordenação de Aperfeiçoamento de Pessoal de Nível Superior
CNS	Central Nervous System
DMN	Default Mode Network
EEG	Electroencephalography
ERP	*Event-Related Potential*
FDR	False Discovery Rate
fMRI	Functional Magnetic Resonance Imaging
GNW	Global Neuronal Workspace
hdEEG	High-Density Scalp Electroencephalography
ICA	Independent Component Analysis
icEEG	Intracranial Electroencephalography
IR	Infrared
LC	*Locus Coeruleus*
MEG	Magnetoencephalography
MUA	Mass Univariate Analysis
PC	Pacinian Corpuscle
PCA	Principal Component Analysis
PNS	Peripheral Nervous System
RA	Rapidly Adapting
SA	Slowly Adapting
SEM	Standard Errors of the Means
SNR	Signal-to-Noise Ratio

SUMMARY

1 INTRODUCTION 10
1.1 RESEARCH PROBLEM 12
1.2 HYPOTHESIS 12
1.3 OBJECTIVES 13
1.3.1 Main Goal 13
1.3.2 Specific Goals 13
1.4 JUSTIFICATION 13
1.5 THESIS OVERVIEW 14
2 THE HUMAN BRAIN 15
2.1 THE ANATOMY OF THE NERVOUS SYSTEM 17
2.2 BRAIN FUNCTIONS 22
2.2.1 Consciousness 24
2.2.2 Perception 27
2.2.2.1 Visual conscious perception 28
2.2.2.2 Auditory conscious perception 32
2.2.2.3 Somatosensory conscious perception 34
2.3 BRAIN DATA ACQUISITION 37
2.3.1 Electroencephalography 38
2.3.1.1 Event-Related Potentials 40
2.3.2 Eye-metrics 41
2.3.2.1 Pupillometry 42
2.3.2.2 Microsaccades 43
2.3.2.3 Blink Rate 44
3 METHODOLOGY 46
3.1 EXPERIMENT 1 46
3.1.1 Participants 46
3.1.2 Task Design 46
3.1.3 Experimental Design 51
3.2 EXPERIMENT 2 57
3.2.1 Participants 57
3.2.2 Task design 57
3.2.3 Experimental design 61

3.3 DATA ANALYSIS FOR BOTH TASKS 61
3.3.1 Behavioral analysis 61
3.3.2 *Event-Related Potential (ERP) analysis* 62
3.3.3 *Eye metrics analyses* 64
3.4 FUNDING SOURCE 66
3.5 RESOURCES 66
3.6 SCHEDULE 68
4 RESULTS 70
4.1 BEHAVIORAL RESULTS 70
4.1.1 Experiment 1 70
4.1.2 Experiment 2 71
4.2 EEG FILTERING PROCESS 71
4.3 EVOKED POTENTIALS 75
4.4 EYE METRICS 79
5 DISCUSSION 81
5.1 STUDY LIMITATIONS 85
5.2 NEXT STEPS 85
6 CONCLUSION 87
6.1 HIGHLIGHTS 87
REFERENCES 89

1 INTRODUCTION

One of the biggest challenges in modern science is understanding the neural basis of consciousness (Michel et al., 2019; Miller, 2005, p. 1436). Most studies have approached this through the lens of perceptual processing, using a combination of perceptual, behavioral tasks coupled with various brain recording techniques, such as scalp and intracranial electroencephalography (EEG), magnetoencephalography (MEG), functional magnetic resonance imaging (fMRI), and direct neural recordings in both humans and animal models (Del Cul, Baillet, & Dehaene, 2007a; Gaillard et al., 2009; Q. Li, Hill, & He, 2014; Michael A Pitts, Metzler, & Hillyard, 2014; Wyart & Tallon-Baudry, 2008). Although there are several conflicting theories about what gives rise to consciousness itself, studies spanning recording techniques and behavioral paradigms find characteristic activity in sensory areas followed by widespread activity in higher-level associative cortex, including frontal and parietal cortices.

One key feature of conscious experience is multimodal phenomenology, where several sensory domains are simultaneously present in perception. These studies have forwarded debate on the distribution of the neural basis for consciousness, either as a global architecture dynamic for all the sensory system or distributed among local foci, specific to each sensory modality. Discriminating between a global versus local neural mechanism of consciousness requires evaluating perceptual signals from each sensory system. Previous conscious perception studies emphasize visual perception, followed by auditory and finally, tactile or somatosensory paradigms (though, notably, there is an extensive literature on pain perception that stands somewhat separate) (Babiloni et al., 2001; Buchgreitz, Egsgaard, Jensen, Arendt-Nielsen, & Bendtsen, 2008; Douros, Karrer, & Rosenfeld, 1994; Egsgaard et al., 2012; McDowell et al., 2006; Truini et al., 2004). An expanded and rigorous study of the neural basis of consciousness among all sensory modalities is necessary to truly understand whether there are common mechanisms of conscious perception across sensory modalities.

The existing literature on somatosensory perception has mainly focused on using masking or oddball paradigms (Eimer, Forster, & Van Velzen, 2003; Kida, Wasaka, Nakata, Akatsuka, & Kakigi, 2006; Schubert, Blankenburg, Lemm, Villringer, & Curio, 2006); or studies involving multiple sensory modalities (Eimer et al., 2003; Montoya & Sitges, 2006). Although valuable to the perception field, these studies almost always present *different and additional* masking stimuli to control whether a

target is perceived, which adds a potential confound: was brain activity across masked and unmasked conditions different because of the perceptual difference or because of differential stimuli (i.e., two stimuli in a masked condition vs. one in an unmasked one)?

The use of a threshold detection task eliminates this potential confound because of identical (or functionally identical, as is the case with a perceptual threshold that changes over time) presentation of the stimuli: only the percept changes, either perceived or not perceived. Threshold detection tasks have successfully been used in vision (Herman et al., 2019; Pins & Ffytche, 2003; Ress & Heeger, 2003; Wyart & Tallon-Baudry, 2008) and audition (Christison-Lagay et al., 2018; Colder & Tanenbaum, 1999). To our knowledge, there is only one such tactile task published, but this task required participants to immediately move the stimulated finger (Palva, Linkenkaer-Hansen, Näätänen, & Palva, 2005); the immediate behavioral response complicates the interpretation of brain activity, as perceptual and motor components happen mostly at the same time.

Despite these caveats regarding previous studies, previous tactile studies have shown robust evidence that perception can modulate the electrophysiology demarcated by the event-related potentials of the P60, P100, N140, P200, and P3B. There is evidence that the P100 and N140 are the first indicators of perception, while an increase in the P200 has been related to the need of complex cognitive function and the P3B to the allocation of attention resources, awareness, conscious perception, perception report, and port-perceptual processing (Donchin & Coles, 1988; Kida et al., 2006; Koivisto, Salminen-Vaparanta, Grassini, & Revonsuo, 2016; Montoya & Sitges, 2006; Muñoz, Reales, Sebastián, & Ballesteros, 2014; Michael A Pitts et al., 2014; Railo, Koivisto, & Revonsuo, 2011; Schubert et al., 2006; Ye, Lyu, Sclodnick, & Sun, 2019).

To fully isolate the neural signatures of conscious perception itself, there is an increasing call in the field to move toward tasks that do not require a perceptual report at all, as the need to report perception involves additional cognitive processing such as retaining percepts in working memory, the preparation of a motor plan, and others. Although perceptual threshold tasks are particularly useful in identifying brain activity caused by perceptual differences (as opposed to changes correlated with physically different stimuli), such tasks pose a particular challenge in removing perceptual reports, as the only differences between trials are, in fact, the participant's perception.

Therefore, the development of covert measures of conscious perception is particularly important.

One promising avenue of study is using pupil diameter, blink, and microsaccade rates to covertly measure changes in physiological arousal, which in turn correlate with changes in cognitive engagement and perception (Eckstein, Guerra-Carrillo, Singley, & Bunge, 2017; Einhauser, Koch, & Carter, 2010; Kang & Wheatley, 2015; Laeng & Endestad, 2012; Piquado, Isaacowitz, & Wingfield, 2010). As with other methodologies, eye metrics have most frequently been used with visual paradigms; there exist fewer auditory and fewer still tactile paradigms with concurrent eye-metric measures. However, isolated studies have shown differences in pupil diameter (Lee & Margolis, 2016; van Hooijdonk et al., 2019) and microsaccade rate (Badde, Myers, Yuval-Greenberg, & Carrasco, 2020; Dalmaso, Castelli, Scatturin, & Galfano, 2017) associated with tactile perception; though again, these studies come with the same caveats and confounding factors discussed before.

Here, we present findings for a novel tactile threshold task, which we conducted with concurrent high-density scalp EEG and eye-metric recordings. To our knowledge, this is the first time that someone performed a tactile threshold task using both pupillometry and high-density scalp EEG to help elucidate the underlying mechanisms of consciousness.

1.1 RESEARCH PROBLEM

There are well-established studies about neural-correlates for visual and auditory conscious perception; nonetheless, tactile perception has been neglected. To better comprehend the brain mechanisms involved in the perception of tactile stimuli, it is necessary to have a task that avoids confounders and collect neurophysiological data through exams like EEG and eye-metrics. This research tries to find a solution for three research problems: the lack of tactile threshold tasks, the necessity to find the neural-correlates of tactile conscious perception, and to validate the use of eye-metrics as a tool for assessing perception.

1.2 HYPOTHESIS

We investigated the hypothesis that one can find relations between the two methods: high-density scalp electroencephalography (hdEEG) and pupillometry, when

assessing tactile conscious perception, and, with it, enhance the knowledge about how the brain processes tactile stimuli.

1.3 OBJECTIVES

1.3.1 Main Goal

The main goal of this research was to investigate the ERP oscillations and eye-metrics related to tactile conscious perception.

1.3.2 Specific Goals

To achieve the primary goal, the specific aims were:

a) To evaluate conscious perception through a threshold tactile task;
b) To identify the mechanisms responsible for tactile conscious perception through EEG signals;
c) To identify the indirect correlates of tactile conscious perception of eye-metrics;
d) To relate the tactile conscious perception's eye-metric findings with auditory ones.

1.4 JUSTIFICATION

Conscious perception is multimodal, but its study has been focused on the visual and auditory fields (Del Cul et al., 2007a; Gaillard et al., 2009; Q. Li et al., 2014; Michael A Pitts et al., 2014; Wyart & Tallon-Baudry, 2008). New paradigms and tasks are also needed to encompass tactile conscious perception, so the neural correlates of consciousness can be understood.

As Herman et al. (2019) state, it is crucial to find paradigms that do not use different or masking stimuli to control the target perception and other confounders that are usually used when trying to understand tactile perception (Eimer et al., 2003; Kida et al., 2006; Schubert et al., 2006). The use of a threshold detection task eliminates this potential confound.

There is also a need for no-report tasks that would prevent that signals associated with memory and readiness to interfere with the signal acquired, and this may be done through the use of eye-metrics (Eckstein et al., 2017; Einhauser et al., 2010; Kang & Wheatley, 2015; Laeng & Endestad, 2012; Piquado et al., 2010).

This being said, the study of tactile conscious perception using hdEEG and eye-metrics may enhance the knowledge about how the brain's networks function. It may support further studies about altered states of consciousness by establishing biomarkers of how conscious perception happens. These biomarkers may help the medical, scientific, legal, and ethical fields, as detection of consciousness in anesthetized or non-communicating patients, diagnosis and treatment of neurologic and psychiatric diseases, and assessment of moral responsibility (Michel et al., 2019).

1.5 THESIS OVERVIEW

The next section covers the essential concepts to understand this study. It is followed by section 3, which describes the methodology applied to get to the results presented in section 4. In section 5, the results are discussed considering related works found in the literature. After that, a conclusion is presented in section 6. Appendix 1 shows the ethics committee approval for the experimental protocol, Appendix 2 presents the PsychStairCase pipeline, used to get to the perception threshold, and the task timeline checklist is the next appended document (3)**.**

2 THE HUMAN BRAIN

The brain is considered the most complex organ of the body; it is the only organ capable of studying itself (Koch & Laurent, 1999). The relation between the brain and the human mind has posed a challenge for both philosophers and physicians. Theories vary about its origin, its materiality, its location, and its causality.

In the 17th century, Descartes defended the substance dualism: he thought that a substance has an essence, and the essence of mind is consciousness and of the body is the physical space in which each of us is a mind inhabiting a machine – our body. This way of viewing the world brings the question of how something in the body may cause something in the mind since they are entirely different things. For Descartes, the answer is that the mind is suffused throughout the body (Berrios, 2018; Lopez-Ibor, Ortiz, & Lopez-Ibor, 2011; Searle, 2004).

The dualists Popper and Eccles evolved Descartes' thinking. They explained dualism by saying that there are three worlds: one of the physical objects, one of consciousness, and a third of culture in all its manifestations. Each would be a separate and distinct world that interacts with others (Eccles, 1982; Rubinstein, 1997; Searle, 2004).

With the lack of evidence from the dualism, philosophers tried to explain the mind in a monistic way. So, two explanations appeared: idealism and materialism. The idealism states that everything is mental or spiritual; the only thing that exists is ideas. Materialists, on the other hand, believe that all that exists is physical. Both theories fail to thoroughly explain how the human mind works (Rose & Brown, 2015; Searle, 2004).

Searle (2004) proposes a third hypothesis: that we must abandon the assumptions that mind and body are distinct entities and the causality view that we are predetermined just by our genes. Instead, we should assume “mental” as a feature (at the system level) of the physical structure of the brain. Moreover, causally speaking, there are not two independent phenomena; there is just the brain system, where the system is conscious and consciously trying to do something.

Since man has attributed the mental faculties to the nervous system, there have been changes in viewing it. In the middle age, philosophers inferred that the three cerebral ventricles hold the mental faculties. At the beginning of the 19th century, Gall described the difference between the gray and white matter; he attributed the human faculties to specific and strict places. For him, those places, when developed, would

also develop touch-sensible cranial prominences (Luria, 1981; Zola-Morgan, 1995). His study was called phrenology. In his system of correspondent areas to brain functions, occipital regions, that nowadays are well known for their neural correlates to the visual perception, for which he related to (1) instinct of reproduction, (2) love of offspring, and (3) affection. Some were classified near to what is thought today, like frontal region 10 – corresponding to circumspection and forethought (Gall, 1825; Luria, 1981; Zola-Morgan, 1995).

In 1861, a French anatomist called Broca described an individual that had an essential disablement of the expressive speech due to a lesion in the third posterior part of the left (for the majority of the right-handed) inferior frontal brain gyrus. He refused the phrenological view that place the ability to speak in the area slightly anterior to the brain, in one of the convolutions resting on the orbital arch, and contributed to show the differences between the brain's hemispheres in several functions, starting to enhance the bonds between neurology and science (Broca, 2011; Luria, 1981).

Two decades later, Wernicke found a different brain region responsible for comprehending the speech located in the posterior section of the left (mostly) superior temporal gyrus. Those two discoveries led several other authors to create a map of the brain functions and to think that they had solved the problem of the functional structure of the brain as the correspondent organ of the mental activity – localizationist theory (Luria, 1981; Wernicke, 1969).

Scientists started to question the current understanding of the brain on the transition to the 20th century. Neurologists started to say that they should study the brain in a brain organization, through its construction and not its localization. They postulated that complex brain phenomena should be the result of the whole brain function rather than one area alone (Luria, 1981).

Luria (1981) evolved those thinking, considering that the brain is an integrated organ and has three central functional unities: (1) for the regulation of tone and arousal; (2) for the reception; and (3) for the execution – that helps on the planning of tasks. The three unities are integrated and inseparable, as being so, they need to be stimulated together in order to occur full learning and development of cognitive functions.

The first functional unity is essential since only in excellent awakened condition, one may receive and analyze information. Those structures are in the subcortex and the brainstem, and they influence all the cerebral cortex (ascending reticular system)

and, at the same time, are subject to its regulatory influence (descending reticular system) (Luria, 1981).

The lateral neocortex regions, including the occipital, temporal, and parietal regions, hold the second functional unity, responsible for the reception, analysis, and storage of information. This unity ranges from highly specific sensory neurons, circumspect by gnostic areas to integrational ones – less specialized (Luria, 1981).

For Luria (1981), the conscious activity occurs on the third functional unity. It gives the capacity to plan, intent, inspect, realize, and regulate one's action, and to verify one's conscious activity, comparing the effects of their action with their original intentions, correcting any mistakes that they would have made.

This model defends that the brain is a functional system with a complex structure, and its parts can change. That means that, given the same original task and result, this system can find different ways to achieve it since it can rearrange itself, called brain plasticity (Luria, 1981). The complex function can not be localized because these regions are highly interconnected and indivisible. Instead, this movement investigates how each function is processed and related to different brain areas (Lefèvre, 1989).

An improvement of this concept is the *Distributive Code.* This theory affirms that even in specialized zones, where there supposedly has a great specialization of neurons, they may take on other functions that not the original, or even execute two functions at the same time. Even with a limited number of direct neuronal connections, they are enough to enable millions of alternatives for the exchange of information between the brain regions that do not have direct connections (Nicolelis, 2011).

In this perspective, plasticity and resilience are the foundation of the brain's networks. The brain is considered dynamic; its whole is bigger than the sum of the individual parts. The human nervous system can look for information and have the consciousness that would be the point of view of the brain itself (Nicolelis, 2011).

2.1 THE ANATOMY OF THE NERVOUS SYSTEM

The nervous system comprises two broad categories of cells: nerve cells (also called neurons) and glial cells (also called neuroglia or glia). Most of the neurons are specialized for electrical signaling over long distances and intercellular communication through synapses. Although, in the beginning, neuroglial cells were thought only to

give support to the nervous system, they have several functions, including information transmission (Pliszka, 2004; Purves et al., 2018; Stehno-Bittel, 2013a).

Figure 1 shows the parts of a multipolar neuron. The body cell (soma) and the dendrites are part of the input zone. The nucleus of the cell is in the soma, and the dendrites are protoplasmic extensions with spikes that allow them to connect to other neurons' axons. The axon is the place where the conduction occurs. In the human nervous system, axons can be 100 μm up to around 1 m long. The electrical through the neuron conduction occurs mainly through exchanges of potassium (K^+) and sodium (Na^+) between the intra- and extracellular sites. The neuron ends in the presynaptic terminal responsible for sending signals for the next postsynaptic neurons through electrical or chemical signaling (Pliszka, 2004; Purves et al., 2018; Stehno-Bittel, 2013a, 2013b).

Figure 1 – Neuron structure

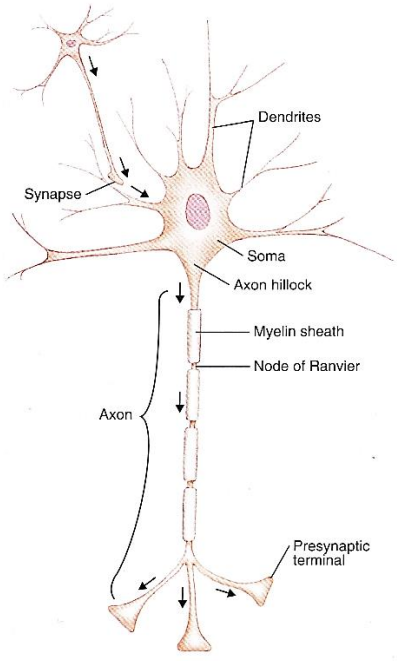

Multipolar neuron with its parts. The synapses happen between the presynaptic terminal and the dendrites and travel though the soma and axon to the next presynaptic terminal.
Source: Stehno-Bittel (2013a)

There are two kinds of synapses: electrical or chemical. The electrical synapses occur through the gap junction, where there are intercellular specializations called connexons that allow the ion current to flow freely through those ion channels.

The electrical synapse is faster than the chemical one; it has a more considerable space between neurons called the synaptic cleft. The synaptic vesicles

are small, membrane-bounded organelles, filled with neurotransmitters that activate postsynaptic neurotransmitter receptors that are very selective to neurotransmitters but less selective for the ions, what means that it is necessary to a specific neurotransmitter to open it, but, once opened, it is permeable to multiple kinds of ions (Pliszka, 2004; Purves et al., 2018; Stehno-Bittel, 2013b).

The second kind of nervous system cells is the neuroglia. As shown in Table 1, they can be divided between macroglial and microglial cells. They are responsible for supporting metabolic and signaling, synaptic plasticity, myelin axon insulation, blood-brain barrier, inflammatory response, scar formation, maintaining the ionic milieu of nerve cells, modulating the rate of nerve signal propagation, modulating synaptic action. They provide a scaffold for some aspects of neural development, aiding recovery from neural injury, doing the interface between brain and immune system, and cleaning the brain during sleep – what facilitates the connective flow of interstitial fluid (Purves et al., 2018; Stehno-Bittel, 2013a).

Table 1 – Categories of neuroglia

Category	Macroglial cells				Microglias	
Classification	Astrocytes		Oligodentrocytes		Sch-wann Cells	
Location	CNS		CNS		PNS	CNS
Function	Mantain chemical enviro-nment	Enhace synapses	Produce stem cells	Myelin = speed up electrical signals	Produce stem cells	Speed up electrical signals	Remove cellular debris	Modulate inflamation

The two neuroglia categories (macroglial and microglial cells) with their respective classification, location, and function. Unlike what was believed, the neuroglia can assume different functions as speeding electrical signals and brain protection.
Source: the author

Two subsets categorize the nervous system: peripheral nervous system (PNS) and central nervous system (CNS). The PNS comprises axons, sensory nerve endings, glial cells, entire neurons, synapses, and ganglia; it has afferent and efferent neurons. The afferent (somatosensory) neurons are responsible for carrying information from peripheral receptors (as pain, mechanical, and chemical receptors) to the CNS. Efferent axons carry information away from the CNS, enabling movement and visceral control (Lundy-Ekman, 2013; Purves et al., 2018).

The CNS is composed of spinal, brainstem, cerebellar, and cerebrum regions. The spinal region is within the vertebral column; it has the spinal cord, which has 31 segments with a pair of spinal nerves arising from each one, surrounded by the meninges. It has the function of conveying information among the neurons connected to peripheral structures and the brain, and processing information (Lundy-Ekman, 2013; Purves et al., 2018).

The brainstem is composed of the medulla, pons, and midbrain. It conveys information between the cerebrum and the spinal cord, integrates information, and regulates vital functions. From it arises twelve pairs of cranial nerves: (I) olfactory, (II) optic, (III) Oculomotor, (IV) Trochlear, (V) trigeminal, (VI) abducens, (VII) facial, (VIII) vestibulocochlear, (IX) glossopharyngeal, (X) vagus, (XI) spinal accessory, and XII Hypoglossal as shown in Figure 2. The cranial nerves I, II, and VII are exclusively used for sensory input, the III, IV, VI, XI, and XI for motor control; the remain cranial nerves have both sensory and motor functions (Lundy-Ekman, 2013; Purves et al., 2018).

Figure 2 – Brain hemispheres and its main structures

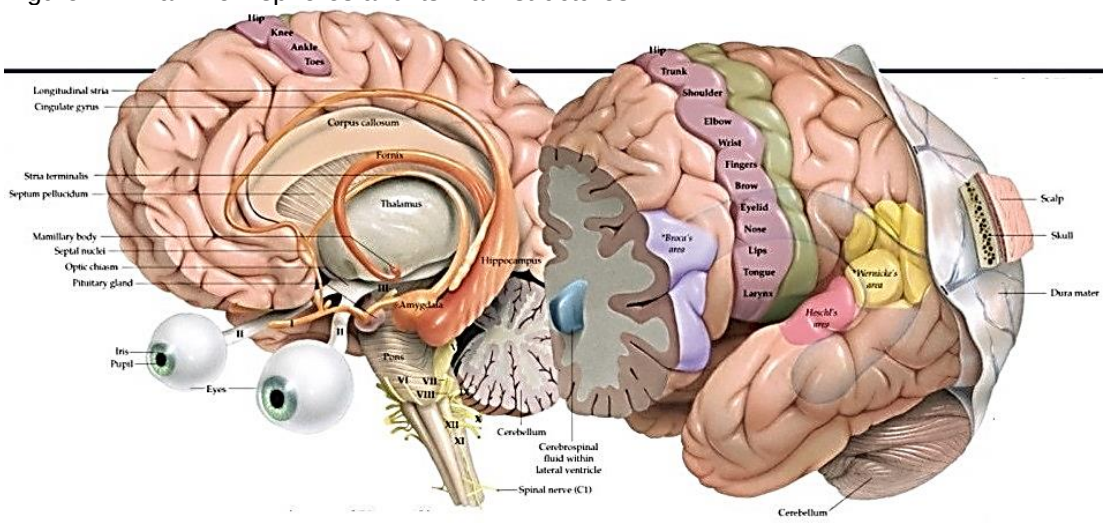

Right and left hemispheres with their main structures. In lilacs and yellow are Broca's and Wernicke's structures, associated with language, while the maroon marks the prefrontal gyrus, responsible for movement control, followed (in green) by the post-central gyrus, responsible for somatic sensation. Source: ANATOMICAL CHART COMPANY, [s.d.]

Figure 2 shows the cerebellum in the posterior part of the brain, it has two hemispheres, and its function is to coordinate movements. It is composed of a continuous layered sheet of cells folded into small convolutions called folia (from the Latin “leaves” for its appearance) (Lundy-Ekman, 2013; Purves et al., 2018).

The brain is divided into two hemispheres – right and left – each of them is subdivided into four or six lobes depending on the approach. The first approach considers lobes: frontal, parietal, temporal, and occipital (Figure 3A) (Purves et al., 2018). Some (Figure 3B) add the limbic (over the corpus callosum) and insular (buried within the lateral sulcus, revealed by separating the temporal and frontal lobes) (Lundy-Ekman, 2013).

Figure 3 – Brain hemispheres division

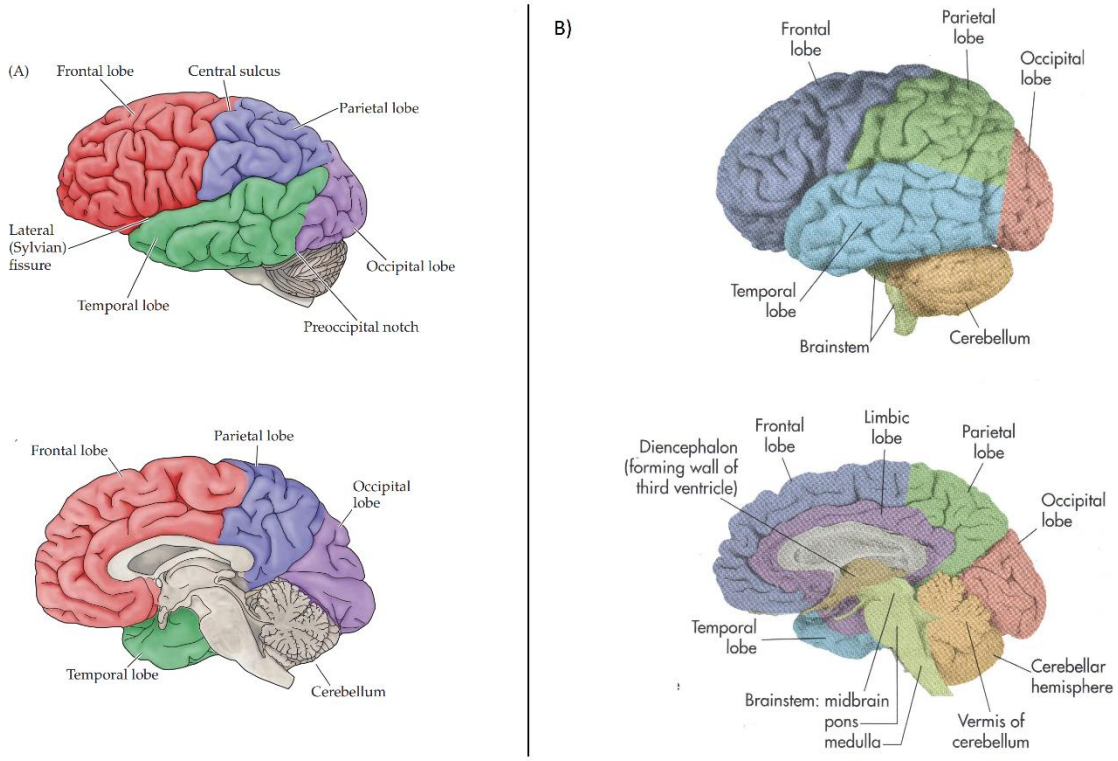

Medial (top) and lateral (bottom) views of the brain’s left hemisphere. Depending on the view, they are divided into four (A) or six lobes (b).
Source: adapted from (A) Purves et al. (2018) and (B) Lundy-Ekman (2013)

The surface of the hemispheres is the cerebral cortex is composed of gray matter; inside the cortex is the white matter, which contains axons that connect the cerebral cortex with central nervous system areas. The *corpus callosum* is a commissure that connects most areas of the cerebral cortex (Lundy-Ekman, 2013; Purves et al., 2018).

The cerebral cortex is characterized by gyri that are crests of folded cortical tissue, and by sulci – grooves or spaces that divide gyri from one another. Relevant for anatomy localization are those sulci that show the division of the lobes. Figure 3A shows the central sulcus that divides the frontal and parietal lobe; the lateral (Sylvian) fissure between the frontal and temporal lobes; and between the frontal and limbic lobes is the cingulate sulcus. Figure 2 also shows the precentral (purple) and postcentral (green) gyrus, that are relevant for their role in motor control and sensation, respectively, of the contralateral side of the body (Lundy-Ekman, 2013; Pliszka, 2004; Purves et al., 2018).

2.2 BRAIN FUNCTIONS

The brain is intrinsically organized in a series of networks (Bagshaw & Khalsa, 2013; Nani, Seri, & Cavanna, 2013) that are a subset of cortical and subcortical regions that functions together in an interconnected manner with a task or at rest (Hyder et al., 2011).

Those networks comprise several brain functions like consciousness, sensation, and perception (somatosensory, pain, vision, auditory, vestibular, and chemical); movement; cognition; attention; memory; emotion; speech and language; and thinking, planning, and deciding (Purves et al., 2018). Specific sessions will better explain consciousness and perception.

The sensation is the ability to transduce, encode, and perceive information generated by stimuli arising from both the external and internal environment. For the tactile sensation to happen, very specialized nerve cells (receptors) convert the energy associated with the stimuli into neural signals that convey its information to the spinal cord and brain (afferent sensory signals). Those signals activate central neurons representing the qualitative and quantitative aspects of the stimulus and its location in space (Purves et al., 2018; Ranade, Syeda, & Patapoutian, 2015).

Signals that originate from neural circuits lead to voluntary and involuntary *movement* in the prefrontal gyrus (mainly) and spinal cord and produce spatial and temporal well-organized patterns of muscular contractions. The brainstem and spinal cord circuitry are responsible for simple reflex movements. The circuits in the forebrain and cerebellum organize complex, intentional motor acts (Latash, 2012; Purves et al., 2018; Shumway-Cook, 2007).

The association cortices carry out the *cognitive* function that uses most of the brain. These regions of the cortex associate information from projections from the primary and secondary sensory and motor cortices, the hippocampus, the thalamus, and the brainstem. They project to the hippocampus, basal ganglia, cerebellum, thalamus, and other cortical areas (Luria, 1981; Purves et al., 2018).

The behaviorism states that rather than to pay *attention* as a noun, attention should be used as a verb, since it is considered a behavior, and the person can direct for what would bring a reward (Ríco, Goulart, Hamasaki, & Tomanari, 2012). Neuroscientists found that, even if one directs their attention to something, there is still some perception of the other stimuli that are happening around. It is believed to have a dedicated attentional system that monitors brain activity and makes decisions about the allocation of neural resources (not without disagreement), so it focuses on endogenous (voluntary) or exogenous (involuntary) attention (Nani et al., 2013; Purves et al., 2018).

Memory is the ability to store and retrieve information. It is an essential ability to imagination and learning; for that, humans use many biological strategies and the anatomical substrate. Two different systems are associated with memory: declarative memory – that can be expressed by language and can be made available to the conscious mind; and procedural memory – for skills – primarily nonverbal. Declarative memory acquisition and consolidation are attributed to the hippocampus and associated midline diencephalic and medial temporal lobe structures, while its storing is associated with cerebral cortices. Procedural memory acquisition and consolidation depend on the premotor cortex, basal ganglia, and cerebellum; its store relies on the strength and number of the synaptic connections in the cerebral cortices that mediate associations between stimuli and the behavioral responses to them, which include perceptions, thoughts, and emotions as well as motor actions (Dudai, Karni, & Born, 2015; Purves et al., 2018).

The subjective feelings, also called *emotions*, help to regulate behavior. It has visceral motor effects and stereotyped somatic motor response such as the movement of the facial muscles and the complex of skeletal muscles underlying posture – when one is afraid, tends to feel stomachache, dilate the pupil, to contract the facial muscles – especially the forehead, as well as the body to prepare to scape or to hide (motor response). In the past, the limbic system was the only region considered responsible for emotions. Now, it is also associated with the broader cortical and subcortical

regions, including the amygdala and cortical areas in the orbital and medial aspects of the frontal lobe that are also associated with the regulation of goal-directed behavior, decision making, social behavior, and moral judgments (Dixon, Thiruchselvam, Todd, & Christoff, 2017; Purves et al., 2018)

Speech and language are considered the basis of the development of high order brain function as thinking and consciousness and the transmission of the culture (Luria, 1981; Vigotski, 1998). The importance of Broca and Wernicke areas for motor speech and comprehensive language, respectively, was already addressed (Broca, 2011; Luria, 1981; Wernicke, 1969). The left hemisphere – in right-handed, and most left-handed – is associated with the processing of lexical, grammatical, and syntactic aspects of language, while the right hemisphere holds the affective content of the speech. There is evidence that the regions devoted to language are specialized for symbolic representation rather than for heard and spoken language, since congenitally deaf individuals use the same cortical areas when using sign language (Purves et al., 2018; Sacks, 2010).

Some of the most advanced functions of humans are *thinking, planning, and deciding*. The flexibility of the brain that comes from these functions gives humans the ability to behave in a sophisticated way. They are complex functions and can not be placed in a region of the brain, but preferably involves the functioning of several networks simultaneously as a whole (Luria, 1981; Purves et al., 2018).

2.2.1 Consciousness

The conscious processes are usually related to two different concepts: consciousness as an intransitive verb in the sense of awareness or vigilance as in the statement: “After one month of coma, she is now conscious.” It can also be used in a transitive form when it means that someone is processing a specific kind of information as in: "she suddenly became conscious of the sound of her mother coming home." That means that there are two main tasks when studying the consciousness: to study the objective level of arousal and the subjective contents of awareness (Michel et al., 2019; Nani et al., 2013).

At the beginning of the study of the brain, Luria (1981) associated the consciousness with the third functional unity, placing it in the anterior regions of the brain. This unity gives the capability to the human been to not only passively react, but

to intent, to plan their actions, to inspect its realization, and to regulate the behavior so that it occurs as intended, being able to correct any mistake that they may have committed. He inferred that each conscious activity is always a complex functional system, and it occurs by the combined functioning of the three cerebral unities, each with its contribution.

More recently, with the arrive of non-invasive brain imaging resources – that enabled to study not only the damaged brain as Luria did, but the healthy one as well – there are three main theories to explain consciousness: the integrated information theory, the global workspace theory, and the cognitive binding theory (Bonhomme, Boveroux, & Brichant, 2013).

Figure 4 – Default mode and task-related maps in healthy controls

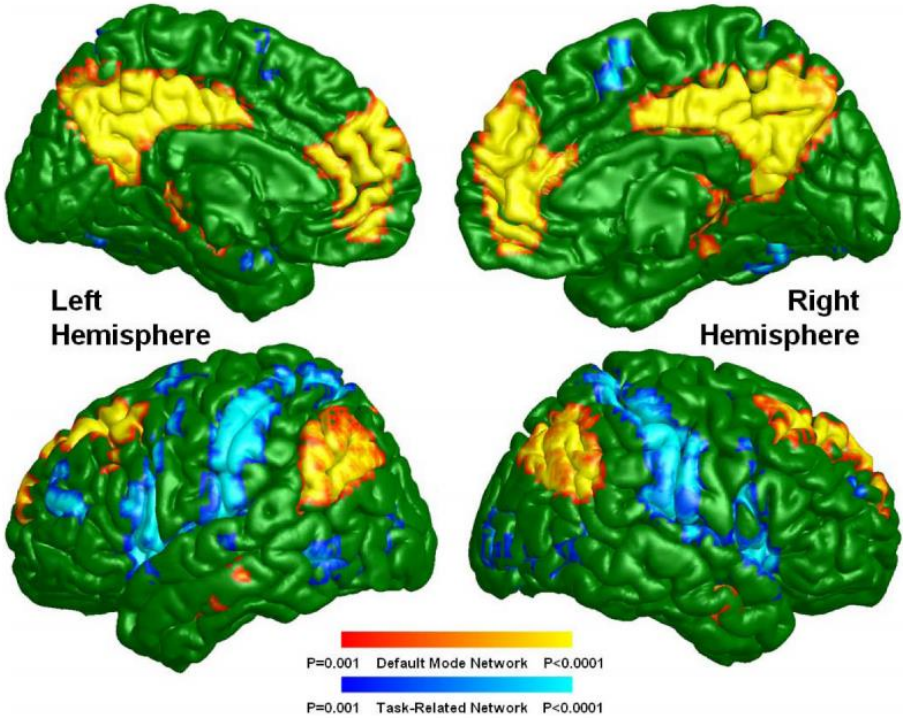

On a green background, the default mode network is highlighted in warm colors (red and yellow), and the task-related network is highlighted in cold colors (blue and light blue) depending on the p-value of the one-sample t-test.
Source: Shim et al. (2010)

Functional imaging in a resting state led to the development of the ***integrated information theory***. Those studies sought to find the primary mechanisms through which the consciousness would happen. There is a common understanding that rather than a single region, the conscious state occurs in a network called Default Mode Network (DMN), where there is a high level of spontaneous coupling of ongoing neuronal activity. Those regions are both functionally linked and structurally connected

by white matter pathways. DMN shows more activity during rest than when in cognitive tasks compared to other brain regions. This DMN integrates a broader repertoire of information generated by functionally specialized cortical areas, as seen in Figure 4 (Bonhomme et al., 2013; Mak et al., 2017; Nani et al., 2013; Tononi, Boly, Massimini, & Koch, 2016).

The DMN represents spontaneous fluctuations, making researchers believe that this activity might maintain functional systems in an active state to improve performance whenever someone undertakes a cognitive or motor task. These fluctuations could also represent internal neuronal dynamics (Nani et al., 2013).

An fMRI study that compared subjects doing a task and asking them to stop has proven that during the effort in a cognitive task, there is a deactivation of the DMN circuitry. At the same time, more significant activity in the DMN regions preceded performance errors, indicating that the subject was acting automatically, rather than making a cognitive effort (Q. Li et al., 2014).

The ***global workspace theory*** assumes that two different processes are often seen as one: consciousness and attention. Consciousness is "a global process capable of elaborating information in order to give a survey of what is going on inside and outside the body" (Nani et al., 2013, p. 9). Attention is the "ability of shifting between mental states in order to appreciate the sensory relevance or salience from one perception to another" (Nani et al., 2013, p. 9), and it can be voluntary or involuntary. Although those are different processes, they correlate within frontoparietal association networks.

For the global workspace theory, consciousness has five essential concepts:

a) a *supervisory system* that processes the information consciously. It requires attentional support and seems to be associated with subsystems in prefrontal and inferior parietal cortices;

b) a *serial processing system* that accesses information serially through the sensory or memory systems;

c) a *coherent structure of recurrent neural loops* that creates a unified perception by a bidirectional exchange of information between different neuronal assembling that elaborate different aspects of the same object (as color, sound, shape, smell…);

d) a *global neuronal workspace (GNW) architecture* that interlinks different parts of the brain broadcasting the information through the whole brain and involves

coalitions of cortical pyramidal neurons with long-range excitatory axons, which populate the prefrontal cingulate, and parietal areas;

e) a *complex system of topological properties* where crucial hub nodes might preserve consciousness (Furman & Blumenfeld, 2013; McGonigal & Bartolomei, 2013; Nani et al., 2013).

The ***cognitive binding theory*** states that synchronization across corticothalamic networks (gamma oscillation) is necessary for binding together information and percept the different features of a single object (Bonhomme et al., 2013; McGonigal & Bartolomei, 2013). With that in mind, consciousness depends on functional integration and preserved information capacity in the brain (Schnakers, Laureys, & Boly, 2013).

Studies with people with brain injury and epilepsy had associated several brain regions with conscious impairment as the upper brainstem and medial diencephalon; and the left extreme capsule adjacent to the anterior dorsal insula and claustrum, those regions may represent switches of synchrony in widespread regions of the subcortical arousal systems (Blumenfeld, 2014; W. Li et al., 2015).

It is essential to notice that this neural basis of consciousness might be variable even across the neurotypical members of a single species. It means that a neuronal correlate for a conscious state is not what causes it. Different ways usually explain this assumption: some would say that this relationship is one of identity, others of constitution or realization, or even that conscious states correlate with neuronal states (dualist perspective) (Bayne & Hohwy, 2013).

Finding a neural correlate of consciousness may be used as a tool for the ascription of consciousness; this may be used when the individual is not able to report their perception as in locked-in syndrome (Bayne & Hohwy, 2013; Michel et al., 2019; Schnakers et al., 2013).

2.2.2 Perception

“Perception may be defined as the cognitive process that lets us know what is out there, based on incoming sensory signals.” (Bruno, 2018, p. 1). It is – in a traditional view – the end of events that start with the stimulation of our senses, generating sensations. After processing, interpretation, and comparison with previous knowledge, it creates *percepts* that are the conscious experiences of objects and events in the

environment. It is the use of sensory information that can or not create a subjective experience (as in the case of the control of our balance) (Pleger & Villringer, 2013; Rogers, 2017)

2.2.2.1 Visual conscious perception

Visual awareness is the subjective sensation of seeing something (Searle, 2004). To understand how conscious perception occurs, the *Global Neuronal Workspace* model states that lowering a stimulus masking strength makes it increasingly visible. It was constructed based on the assumption that when one presents a mask right before a stimulus, it should be necessary a threshold time (>50ms) between them so the stimulus would be perceived (Del Cul et al., 2007a).

Through scalp EEG, they reported that subliminal processing (before consciousness) could occur in the occipitotemporal pathway (<250ms) in response to strong masking; and, when the mask is over the threshold, consciousness should occur after the subliminal processing (>270ms) with a neuronal correlate of a highly distributed fronto-parieto-temporal activation, when it is preceded by weak masking (Figure 5). What determines the suppression are the stimulus duration and onset asynchrony between target and mask (Del Cul et al., 2007a; Hesselmann, 2013).

Figure 5 – Subliminal and conscious processing according to the “global neuronal workspace” model

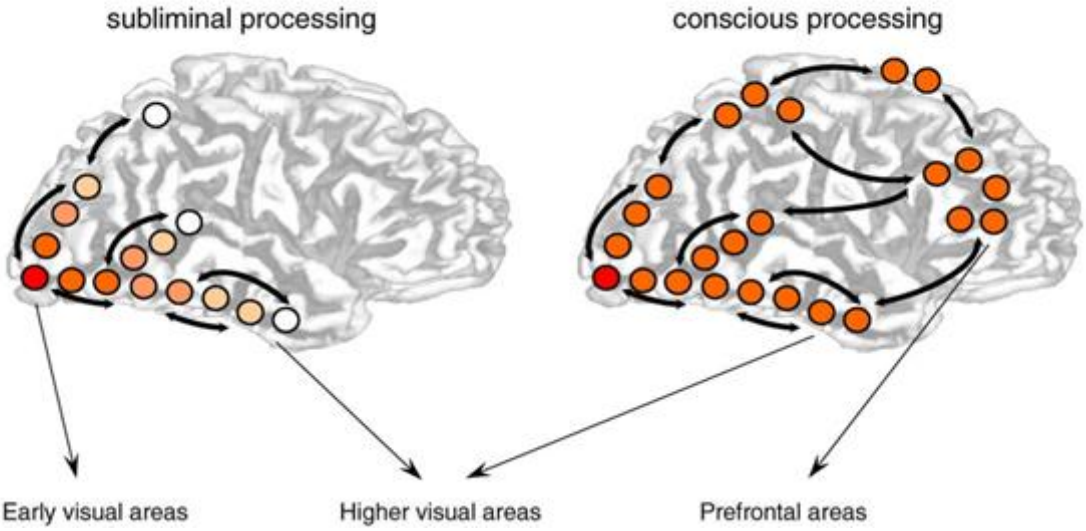

The “global neuronal workspace” explanation for visual perception states that subliminal processing (left) occurs in the occipitotemporal pathway (<250ms) in response to strong masking; consciousness (right) occurs after the subliminal processing (>270ms) with a neuronal correlate of a highly distributed fronto-parieto-temporal activation when it is preceded by weak masking.
Source: adapted from Del Cul et al. (2007a)

Wyart and Tallon-Baudry (2008) relate consciousness to attention: it is more likely/natural to perceive something to which one is attending. The researchers propose a neural correlate of visual awareness distinguishing top-down attention from awareness. They did that by using weak stimuli at the threshold of 50% of the perception. The stimuli were constant across trials in terms of contrast and duration but were consciously seen only in half of the trials. As seen in Figure 6, the subject would see a cross with a *cue* arrow (mask) on the right or left side, and attend to it; in the sequence, a fainting grating would appear (*stimulus*), under the arrow, in the opposite side or no stimulus at all (15% of the time). The subject should then report the direction of the grating (*Orientation?*) and if they have *seen* it, allowing the study of both visual awareness and spatial attention.

Figure 6 – Wyart and Tallon-Baudry Experimental Design

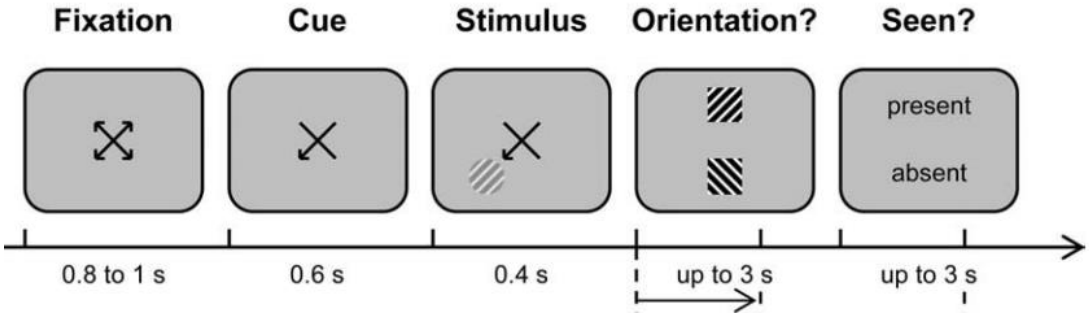

The task consists of a *Fixation* period of 0.8 to 1 s, followed by a *Cue* arrow presented for 0.6 s that may or not point to the direction that the *Stimulus* is presented (duration = 0.4 s 86% of the time). The subject should then report the *Orientation* of the grating and if they have *Seen* it.
Source: adapted from Wyart and Tallon-Baudry (2008)

While conducting this experiment, Wyart and Tallon-Baudry (2008) collected continuous magnetoencephalographic data. In this study, they proved that behaviorally visual awareness and spatial attention appeared mutually dependent, because the attended stimulus was more consciously seen (49.9 ±3.1%) when compared to the unattended one (40.4 ±3.0%); and because the subjects took more time to answer when the stimulus was on the unattended side.

They also proved that visual awareness does not reflect the orienting of spatial attention. Since, even while paying attention, one could not perceive some stimuli – shown by brain activation (Wyart & Tallon-Baudry, 2008). Since visual awareness and spatial attention could operate independently of each other at the neural level, the two should be considered distinct mental operations that support distinct brain functions.

These two paradigms (Del Cul et al., 2007a; Wyart & Tallon-Baudry, 2008) are examples of using masking to explore conscious visual perception. Figure 7 shows other ways to use a mask in order to evaluate perception.

In Figure 7A is shown the backward masking (as in Del Cul et al., 2007a), where the target is briefly presented before the mask. Figure 7B represents continuous flash suppression. In this form, one eye is presented with flashes of high-contrast random masks at 10 Hz in one eye, while the target stimulus is presented to the other. Figure 7A represents a bistable perception; this picture shows a vase (white) or two faces (black). The perception switches between the two, but the sensory input remains unchanged. Figure 7D illustrates attention-induced motion blindness: the presentation of random (open circles) and coherent (closed circles) motion 100-ms episodes; suppression of awareness of a coherent motion target if coherent motion episodes (distractors) precede a centrally presented red color cue signaling target (Hesselmann, 2013).

Figure 7 – Visual paradigms to evoke “transient blindness” in neurologically intact observers

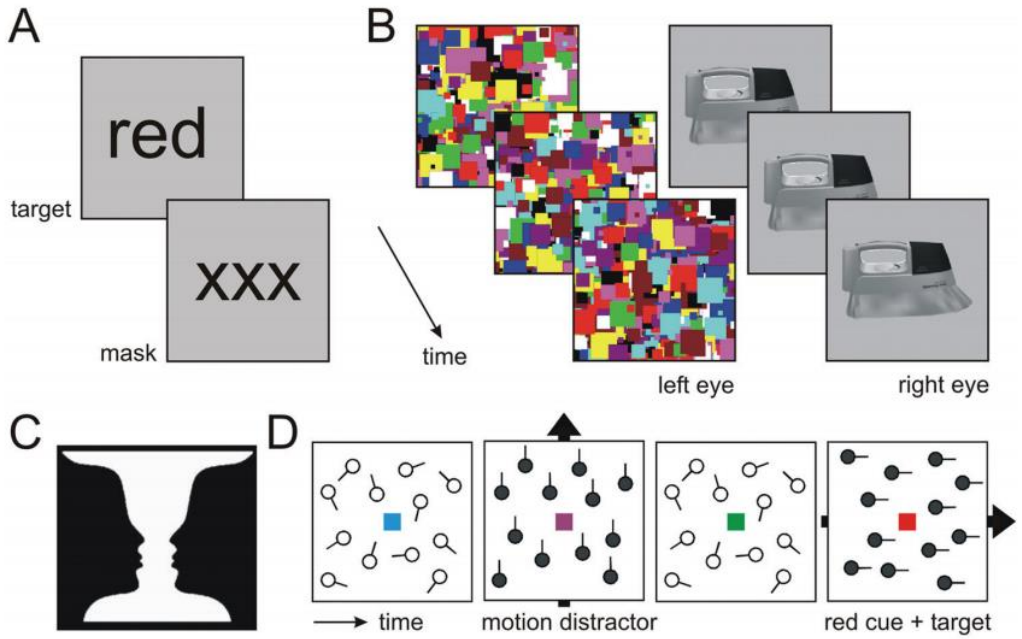

Representation of different masking processes to the study of conscious visual perception. Figure (A) shows the backward masking, where the target is briefly presented before the mask; (B) represents continuous flash suppression by presenting flashes of high-contrast random masks at 10 Hz in one eye, while the target stimulus is presented to the other; (C) displays a bistable perception with the perception switching between the two images, but the sensory input remains unchanged. Moreover, figure (D) illustrates attention-induced motion blindness: the presentation of random (open circles) and coherent (closed circles) motion 100-ms episodes; suppression of awareness of a coherent motion target if coherent motion episodes (distractors) precede a centrally presented red color cue signaling target.
Source: Hesselmann (2013)

However, using masks could lead to potentials confounds of variation since the mask can interfere with the brain response (Herman et al., 2019). To avoid that, the Blumenfeld Lab (Yale University) used a threshold task to analyze the conscious visual perception and established a new paradigm: The “Detect, Pulse, Switch, and Wave” model of conscious perception (Figure 8). In this study, Herman et al. (2019) used intracranial electroencephalography (icEEG) to evaluate how visual perception occurs during the first second of conscious perception. They chose icEEG due to its higher temporal resolution – in the order of milliseconds – than other methods and are less prone to external artifacts liability. They showed a picture of a black and white face in the participant’s 50% perception threshold and then analyzed through the K-means clustering algorithm the 1,000 ms before and after the receiving of the stimulus.

Figure 8 – Switch and wave of neuronal activity in the first second of conscious perception

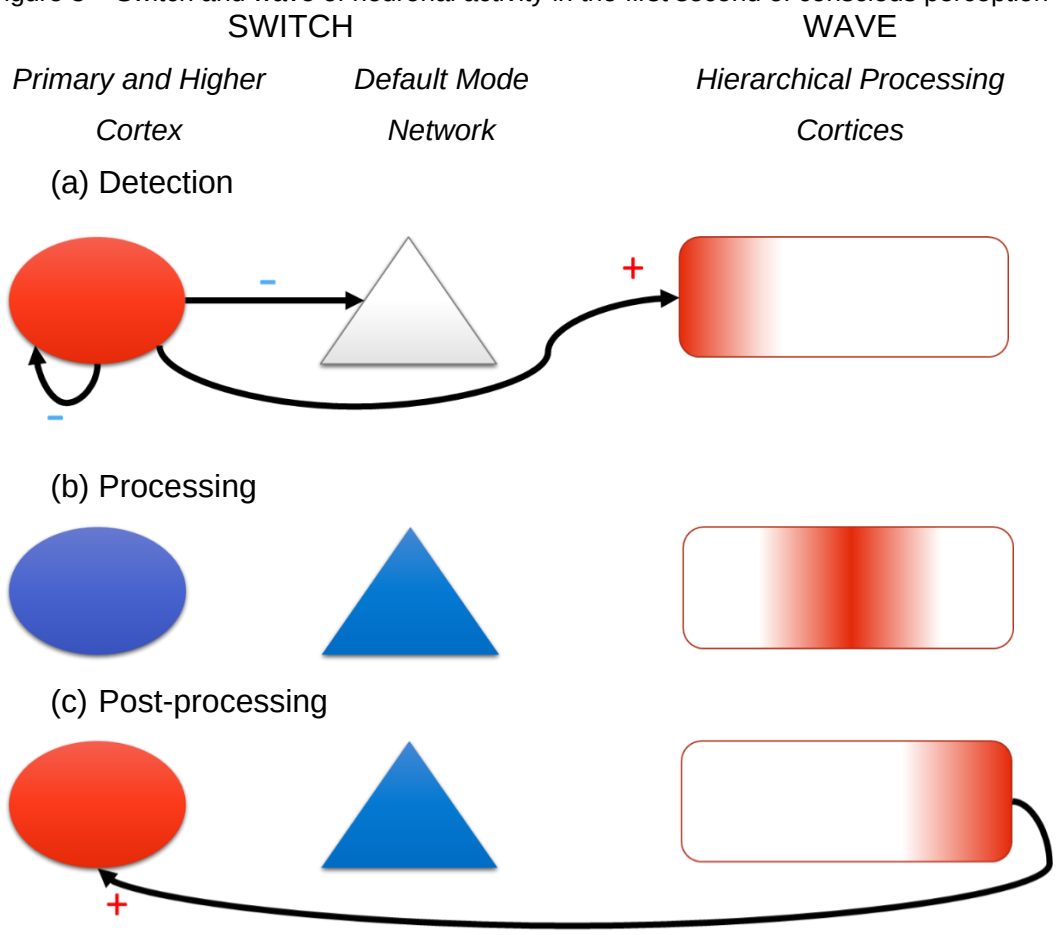

Brain activation during conscious perception. In this process, (a) the visual cortex perceives the image and elicits a forward-sweeping wave of activity through the cerebral cortex; (b) during the occurrence of this wave, a broadband gamma activation moves through the bilateral association cortex, switching networks at a rate of ≈ 150 mm/s; at this moment, both visual cortex and DMN are deactivated during the conscious stimulus processing; (c) when it finally reenters the visual cortex.
Source: adapted from (Herman et al., 2019)

With the data collected, they suggested that both perceived and non-perceived stimuli activate the visual cortex, but only the perceived one will activate the rest of the brain. Figure 8 shows brain activation during conscious perception. In this process, (a) the visual cortex perceives the image and elicits a forward-sweeping wave of activity through the cerebral cortex; (b) during the occurrence of this wave, a broadband gamma activation moves through the bilateral association cortex, switching networks at a rate of ≈ 150 mm/s; at this moment, both visual cortex and DMN are deactivated (C. S. Li, Yan, Bergquist, & Sinha, 2007) during the conscious stimulus processing; (c) when it finally reenters the visual cortex (Herman et al., 2019).

Visual and auditory perception paradigms corroborate this model of conscious perception. It is essential to highlight that the three studies had used different kinds of stimuli that are usually interpreted by different regions of the brain. The letters and numbers interpretation (C. S. Li et al., 2007) are associated with the left temporal lobe, the directions (Wyart & Tallon-Baudry, 2008) with the primary and secondary visual cortex; and face recognition (Herman et al., 2019) with the fusiform face area what may influence the results.

2.2.2.2 Auditory conscious perception

The hearing begins when sound waves vibrate the tympanic membrane. This membrane converts the pressure into mechanical energy, making the middle ear bones to move back and forth. The bones convert the mechanical into hydraulic energy that stimulates the sensory hair cells in the cochlea and generates nerve impulses. This process transforms sound stimuli into patterns of neural activity that are integrated with information from other sensory systems and brain regions. It sends information to regions linked with movement, attention, and arousal to guide behaviors that include orienting to auditory stimuli, engaging in intraspecies communication, and distinguishing self-generated sounds from other sounds in the environment (Bhatnagar, 2002; Purves et al., 2018).

The hearable sound for humans is usually classified by frequency and intensity. Frequency is the speed of vibration or the number of complete cycles that a particle executes; it is expressed in cycles per second or hertz (Hz). It is known as the tone of a sound; humans with normal hearing can hear a frequency range from 20 Hz to 20 kHz. The intensity is the amplitude of the sound waves and is measured in decibels; it

is popularly called loudness or hearing level. Figure 9 illustrates the hearing and pain thresholds for different frequencies and intensities (Bhatnagar, 2002).

Figure 9 – Thresholds of hearing sensitivity for various frequencies

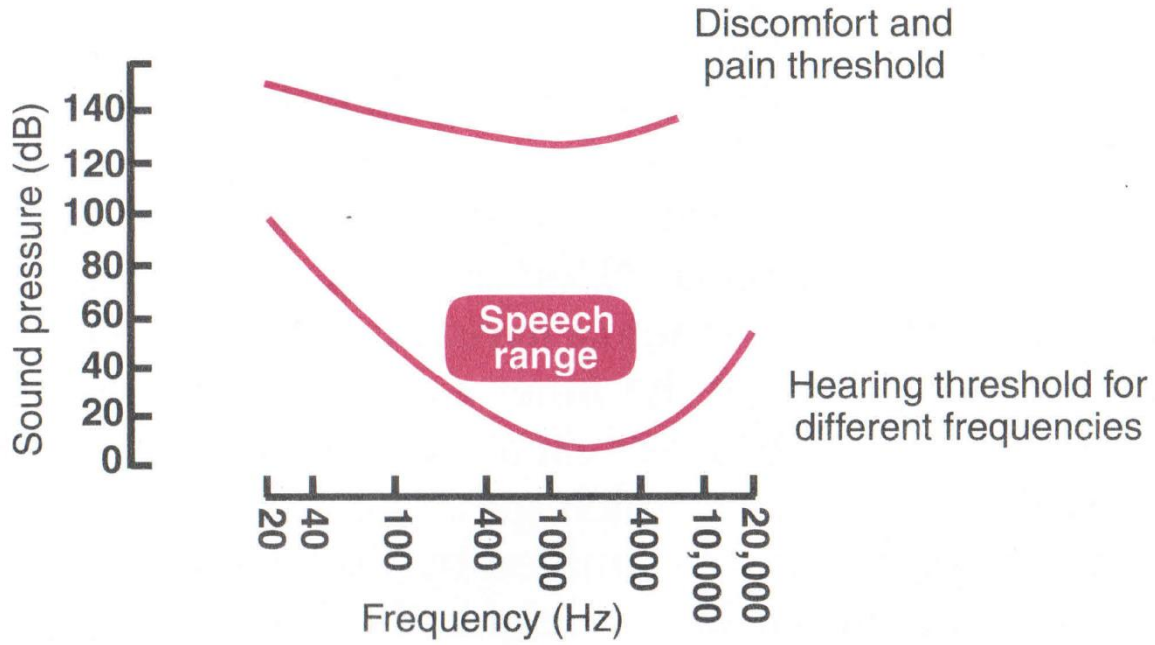

Higher and lower limits of human hearing. The top line defines where hearing becomes uncomfortable or painful. The shaded area is the usual speech range.
Source: Bhatnagar (2002)

Auditory conscious perception is associated with positive activation in the thalamus, auditory cortex, insular cortex, and contralateral supplementary and primary motor areas (in red in Figure 10), and negative activation in visual areas and ipsilateral motor areas (in blue in Figure 10) (Walz et al., 2015). One way to evaluate the process of auditory conscious perception is through the oddball paradigm. In this paradigm, the participant should focus their attention on task-relevant stimuli. If a violation of the prediction is detected, it generates an error signal, calling attention. This attention is involuntarily directed to the new sound even if it is not relevant for the task at hand (Eckstein et al., 2017; Wetzel, Buttelmann, Schieler, & Widmann, 2016). Unexpected auditory stimuli may cause pupil dilatation response (PDR) both in adults and in infants, although only adults would have pupil dilatation with frequency deviants (Wetzel et al., 2016).

Figure 10 – Traditional fMRI Results on auditory trials for left stimulus

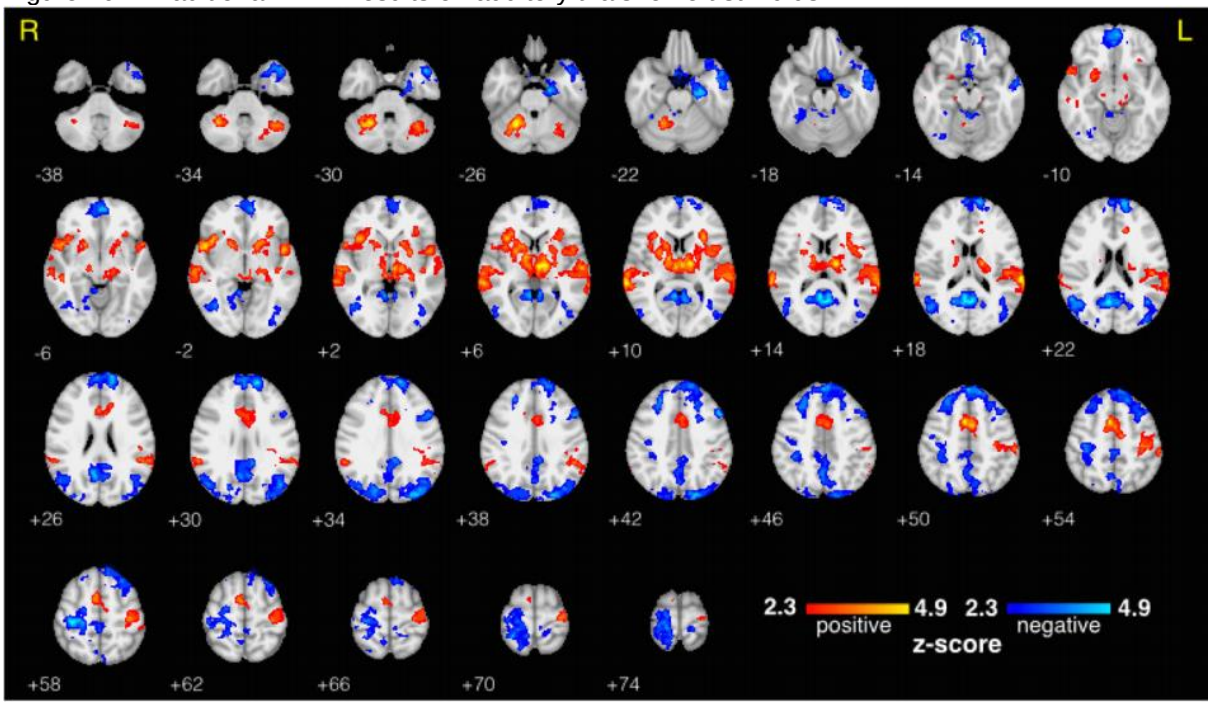

Group level average fMRI BOLD response to auditory target stimuli (including all trials regardless of alpha activity), thresholded at $z > 2.3$, and cluster corrected at $p < 0.05$. Statistical maps are displayed on an MNI (Montreal Neurological Institution and Hospital) template brain using radiological coordinates, and z-coordinate is displayed to the lower left of each axial slice.
Source: Walz et al. (2015)

2.2.2.3 Somatosensory conscious perception

The somatosensory conscious perception begins in its peripheral mechanisms that encompass its neurons and receptors that can be proprioceptors (4 types), nociceptors (3 types), thermoreceptors (2 types), or mechanoreceptors (4 types). Each mechanoreceptor has its characteristics and function. As shown in Table 2 and Figure 11), the mechanoreceptors' sensory feedback helps us to better cope with our environment, helping us in our ability to move, handle tools, and others (Hendry & Hsiao, 2013; Siegel, 2019).

The Pacinian Corpuscles (Figure 11) are concentric lamellae of flattened cells supported by collagenous tissue. A myelinated nerve enters the corpuscle, with the open nerve terminal occupying the center of the corpuscle. They have a low threshold and rapidly adapt, making them sensitive to rapid indentation of the skin caused by high-frequency vibrations (Siegel, 2019).

Table 2 – Primary afferent fibers and their roles

Afferent Type	**Slowly adapting (SA) 1**	**Rapidly adapting (RA)**	**Pacinian corpuscle (PC)**	**SA2**
Receptor	**Merkel**	**Meissner**	**Pacinian**	**Ruffini**
Location	Tip of epidermal sweat ridges	Dermal Papillae (close to the skin surface)	Dermis and deeper tissues	Dermis
Axon diameter	7-11µm	6-12 µm	6-12 µm	6-12 µm
Conduction velocity	40-65m/s	35-70m/s	35-70m/s	35-70m/s
Sensory function	Form and texture perception	Motion detection, grip control	Perception of distant events through transmitted vibration, tool use	Tangential force, hand shape, motion direction
Effective stimulus	Edges, points, corners, curvature	Skin motion	Vibration	Skin stretch
Response to sustained indentation	Sustained with slow adaptation	None	None	Sustained with slow adaptation
Frequency range	0-100Hz	1-300Hz	5-1,000Hz	0-?Hz
Peak sensitivity	5Hz	50Hz	200Hz	0.5Hz
Threshold for rapid indentation or vibration (best)	8 µm	2 µm	0.01 µm	40 µm
Threshold (mean)	30µm	6µm	0.08µ	300µm
Receptive field area (measured with rapid 0.5 mm indentation)	9mm^2	22 mm^2	Entire finger or hand	60 mm^2
Innervation density (finger pad)	100/cm^2	150/cm^2	20/cm^2	10/cm^2
Spacial acuity	0.5mm	3mm	10+mm	7+mm

Source: (Hendry & Hsiao, 2013, p. 553)

Primary afferent neurons collect the information from the somatosensory receptors that terminate on second-order neurons on the medulla. From there, second-order neurons send their axons across the midline to the thalamus, mainly the ventral posterior complex – lateral from the body (VPL) and medial from the face (VPM) – that innervates the somatosensory cortex (SI) or from VPI (inferior) that innervates SII (Hendry & Hsiao, 2013).

SI is divided into areas organized in serial and parallel processing: 3a, 3b, 1, and 2 (rostral to caudal). The thalamic neurons use parallel processing, typically sending cutaneous input to areas 3b, 1, and 2, and from deep receptors to area 3a and 2. These areas also work serially by 3b, sending information to areas 1 and 2. Area 2

receives inputs from area 1 and indirect input from the thalamus, 3a, and 3b (Hendry & Hsiao, 2013).

Figure 11 – Receptors mediating tactile senses

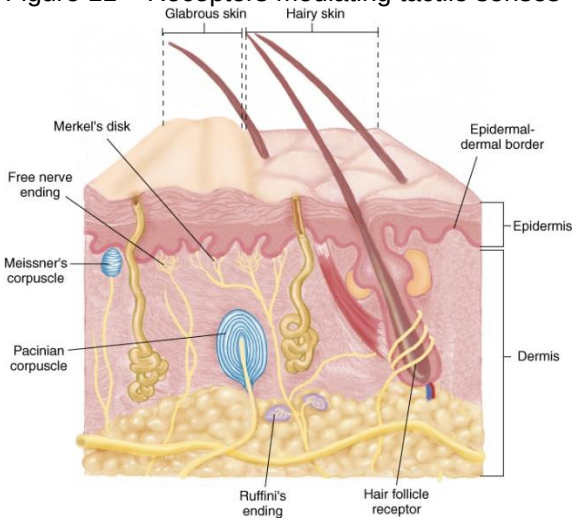

Skin slice showing the localization of mechanoreceptors. It shows the Meissner's corpuscles, and Merkel's disks more superficially, responsible for form and texture perception, and motion detection, respectively. The Pacinian corpuscle is more profound on the dermis, responsible for vibration perception and the Ruffini's endings that perceive tangential force, hand shape, motion direction.
Source: Siegel (2019)

The information, in a ventral path, goes from SI to (in order): SII, caudal insula, temporal lobe, and premotor and prefrontal cortical areas. Through its dorsal path, it goes to superior parietal lobules (Hendry & Hsiao, 2013; Siegel, 2019).

Although we know anatomically the paths of our nervous system through which the somatosensory information travels, the physiology that marks its perception is still to be determined. Studies with scalp electroencephalograms (EEG) have shown that their event-related potentials (ERPs) can be found as early as 50 ms after stimuli onset. Using a masking task, Schubert et al. (2006) have found that P100 (a positive peak at ~100 ms) in contralateral parietal areas related to the hand receiving the stimuli, and N140 (a positive peak at ~100 ms) in contralateral frontal areas related to the hand receiving the stimuli, affected the detection of tactile stimuli (Figure 12).

Other authors have also found P100, N140, P200, and P300 to be present when stimuli are perceived using different tasks modalities: oddball paradigms (Allison, McCarthy, & Wood, 1992; Kida et al., 2006; Yamaguchi & Knight, 1991), paradigms that use multiple, concomitant, sensory inputs – as visual and tactile – (Gallace & Spence, 2008; Juravle, Heed, Spence, & Roder, 2016; Ku et al., 2007; Montoya & Sitges, 2006), studies with subjective rating of the strength of stimuli (Auksztulewicz &

Blankenburg, 2013), and form of discrimination (Ballesteros, Munoz, Sebastian, Garcia, & Reales, 2009; Genna et al., 2018; Muñoz et al., 2014; Tang et al., 2020). There is also evidence – using fMRI – that stimulation of fingers evokes activity in the contralateral SI and bilateral SII) (Ruben et al., 2001).

Figure 12 – Grand averaged somatosensory ERPs

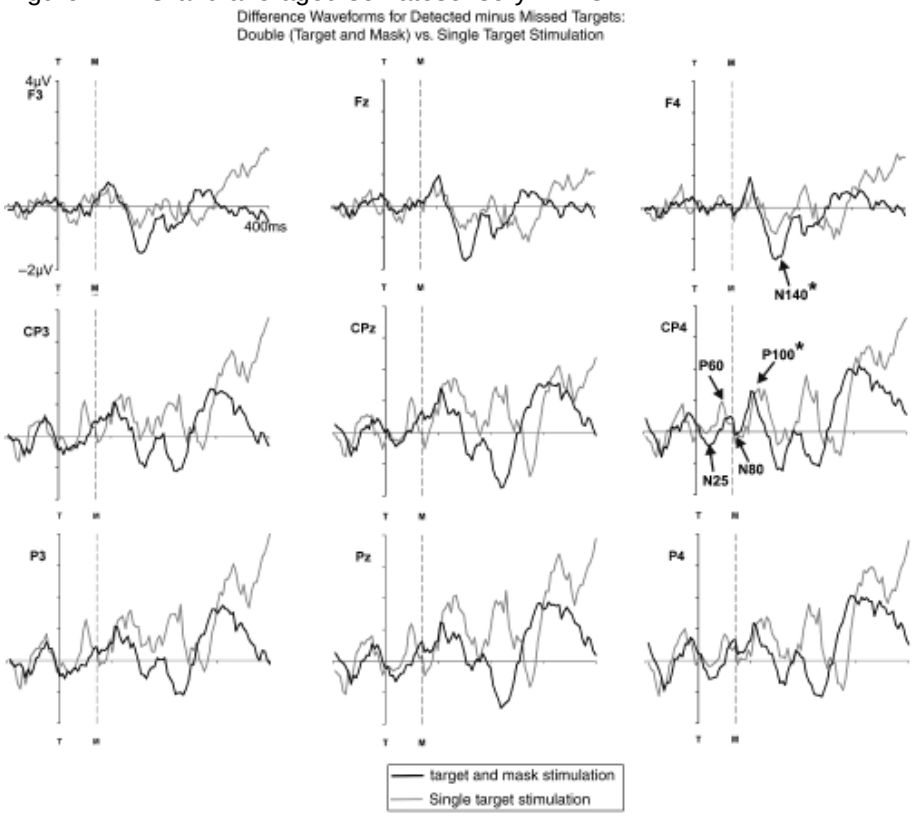

Grand-averaged somatosensory ERPs, showing the different waveforms for missed target trials subtracted from detected trials. It is separated for double stimulation and single target stimulation only in the 400 ms following the onset of the target stimulus. T denotes the onset of the target and M onset of the mask. A star denotes the peaks with a main effect of the factor Detection.
Source: Schubert et al. (2006, p. 36)

However, according to (Herman et al., 2019), those studies have a main confounder since they have other stimuli present, leading researchers to wonder if the signals acquired were due to the stimulus or the masking used. To solve this, a threshold task (not found in literature) would be necessary, where the stimuli are kept the same, and only the perception of it is changed.

2.3 BRAIN DATA ACQUISITION

One of the goals of neuroscience studies is to determine how neuronal populations process information within networks; with this, neuroscientists aim that imaging neuroscience becomes a part of routine clinical management to provide tools

to access the integrity necessary for conscious states (Bagshaw & Khalsa, 2013; Hyder et al., 2011).

2.3.1 Electroencephalography

The electroencephalography (EEG) “is a graphic representation of the [electrical] potential differences between two separated points on the scalp surface that represent brain-transmitted electrical potentials […] of the cortex bellow” (Bhatnagar, 2002, p. 380). As a functional measure of the nervous system, it is usually accompanied by anatomical tests like CT and MRI. It is particularly important when the neurological disorders are not accompanied by detectable brain morphological alteration. The EEG is dependable, inexpensive, and useful for exploring brain electrophysiology (Emerson & Pedley, 2011; Feyissa & Tatum, 2019).

EEG shows the extracellular currents that result from several cortical neurons synaptic potentials. It acquires the information through the cortex but can be influenced by the brainstem and thalamus. It reflects processes that are important for brain information processing and is composed of multiple rhythms, auto-organized, and hierarchically structured (Emerson & Pedley, 2011; Feyissa & Tatum, 2019).

Figure 13 – EEG electrode placing

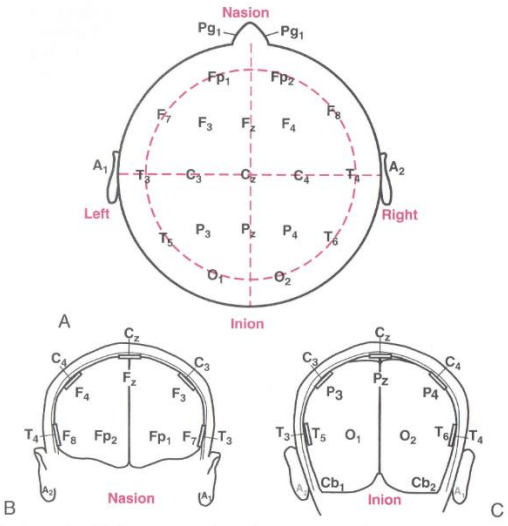

Map of typical electrodes placement on an (A) superior, (B) frontal, and (C) posterior view. The letters refer to the lobe and numbers to the position (exception “z” that indicates midline), being odd numbers placed on the left and even on the right hemisphere. F refers to frontal; Fp, prefrontal; C, central; P, parietal; T, temporal; and A, auricular.
Source: (BHATNAGAR, 2002)

Electrodes can be placed with different arrangements; one of the classic electrodes' placement is in Figure 13. They are metal electrodes with 5-10 mm in diameter, and it records spontaneous cortical surface activity generated from the fluctuating voltage differences between the apical and basal portion of cortical dendrites (Bhatnagar, 2002).

Adult regular EEG activity, when awakened, has alpha rhythm – a pattern of 8 to 12 Hz at parietal and occipital regions, especially when the subject is relaxed and with eyes closed, it is attenuated with eyes open, or alertness. The beta activity (13-25 Hz) is generally found in the frontal and central regions; a high beta voltage activity may suggest the use of sedatives. Theta activity (4-7 Hz) can be found in children (Emerson & Pedley, 2011). Broadband gamma (40-115 Hz) has been proven to have a lower threshold of changes during behavioral tasks (Fries, Reynolds, Rorie, & Desimone, 2001; Lu & Hu, 2019; Tallon-Baudry & Bertrand, 1999), and higher frequency increases from the baseline while doing spectral changes across subjects. Higher frequencies – over 115 Hz – have more artifact influence at 120 Hz because it is a harmonic of the electrical power network frequency of 60 Hz. It is an excellent diagnostic tool to examine altered consciousness (Baldauf & Desimone, 2014; Bhatnagar, 2002; Melloni et al., 2007).

The gamma frequency is also associated with conscious visual perception. When using subliminal tests (as in Figure 5 and Figure 14), unconscious processes may trigger local coordination of neural activity and propagation along sensory processing pathways.

Simultaneously, conscious perception would activate global coordination, widely distributed neural activity by long-distance synchronization that can be perceived by gamma frequency modulation (Baldauf & Desimone, 2014; Del Cul et al., 2007a; Melloni et al., 2007).

EEG has been proved to help in the understanding of conscious perception (Del Cul et al., 2007a; Herman et al., 2019; Hesselmann, 2013; Melloni et al., 2007) (DEL CUL; BAILLET; DEHAENE, 2007; HERMAN et al., 2017; HESSELMANN, 2013; MELLONI et al., 2007), and through a perception-related EEG, to even improve diagnostic techniques for Alzheimer (BARZEGARAN et al., 2016).

Figure 14 – Scalp maps of event related potentials elicited by visible and invisible words

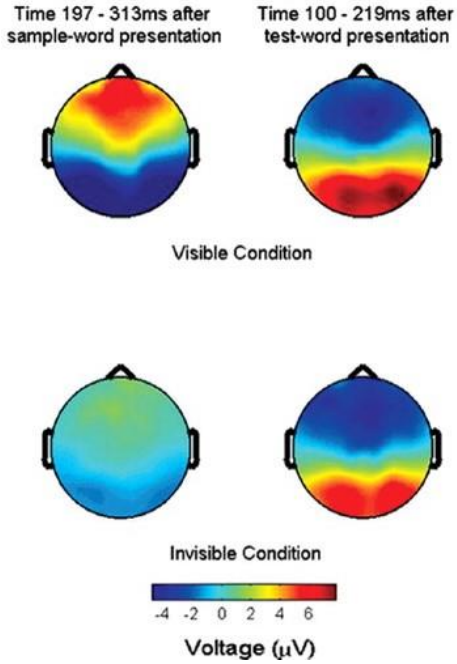

Voltage scalp map for two windows indicated for visible and invisible conditions. The first difference started at 130 ms after the sample-word presentation, as a P300a-like component. Then, a P1-like component was observed ~200 ms after the test-word presentation, for both conditions
Source: adapted from Melloni et al. (2007)

2.3.1.1 Event-Related Potentials

Event-related potentials (ERPs) are averaged electrical potentials gathered through EEG measurements and related to an event (usually a stimulus). It tries to determine the reaction of the brain to a particular event or stimulus. It is believed that the early brain responses are evoked by the stimulus presentation and its basic sensory processing, while later responses are likely to reflect the cortical processing of psychological activities as memorization and preparation for a report. ERP is one of the most popular measure in human cognitive neuroscience (Donchin & Coles, 1988; Lu & Hu, 2019; Niedermeyer, Da Silva, Niedermeyer, & Lopes Da Silva, 2004; M. A. Pitts, Padwal, Fennelly, Martínez, & Hillyard, 2014; Polich, 2007; Sauseng et al., 2007; Yamaguchi & Knight, 1991).

Two main theories explain ERPs generation: an evoked model or a phase reset model. The evoked model (Figure 15b) believes that ERPs are an additional activity, independent of the ongoing background (Figure 15a), while the phase reset model (Figure 15c) states that ERPs' generation comes from the reorganization of phases of the ongoing EEG rhythmic activity. A third group defends that is a conjunction of both

things (Fell et al., 2004; Jervis, Nichols, Johnson, Allen, & Hudson, 1983; Lu & Hu, 2019; Niedermeyer et al., 2004; Sauseng et al., 2007).

Figure 15 – Evoked and reset phase model

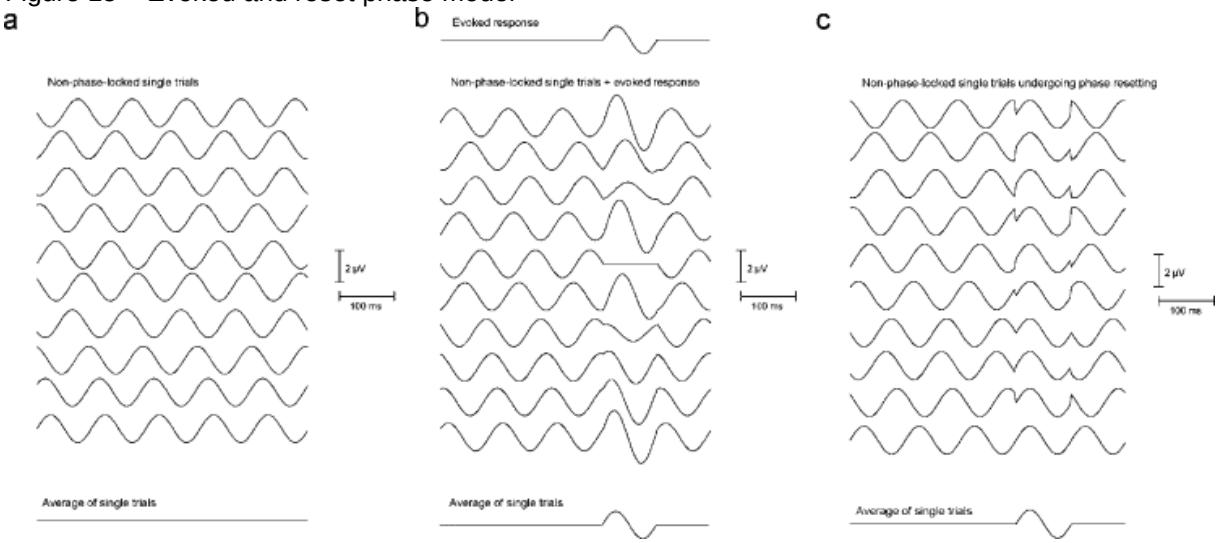

General idea of evoked and phase reset model. (a) When several unrelated single trials that are not phase-locked to a stimulus are averaged, a flat line will ideally be the result. (b) The evoked model assumes that in every single trial, a constant evoked response is added onto the ongoing EEG. The background EEG is considered as noise utterly unrelated to the ERP. When the single trials composed of the background EEG and an additive evoked response are averaged, the ERP, which accurately reflects the original evoked response, will result. (c) The phase reset model suggests that the ERP is generated by a phase resetting of oscillatory background EEG. Without any additive evoked response, an ERP will arise when single trials are averaged
Source: Sauseng et al. (2007, p. 1436).

There is evidence that both views (evoked and reset phase models) are correct and should be studied to reveal specific insights into the mechanisms underlying different cognitive functions (Fell et al., 2004).

Since the magnitudes of ERPs (on the order of microvolts) are often tens of times smaller than the magnitude of the background EEG activity, it is necessary to use different processing methods for enhancing the signal-to-noise ratio (SNR), with the most common technique being calculating its average (Lu & Hu, 2019).

2.3.2 Eye-metrics

Eye metrics are the measurement and evaluation of eye and eyelid dynamics. They provide an ideal and powerful objective measure of ongoing cognitive processes and information requirements during behavior. They are non-invasive and complementary measures of cognition that have high temporal resolution and well understood neural foundations providing an ideal neuroscience model to investigate

the association between brain mechanisms and behavior (Eckstein et al., 2017; Luna, Velanova, & Geier, 2008; Tatler, Kirtley, Macdonald, Mitchell, & Savage, 2014).

2.3.2.1 Pupillometry

Pupillometry measures variations in the diameter of the pupillary aperture of the eye in response to psychophysical or psychological stimuli (Granholm & Steinhauer, 2004; Laeng, Sirois, & Gredebäck, 2012). Pupil size is changed by two antagonistic muscles: the dilator pupillae and the sphincter pupillae. The sphincter muscle receives input from brain systems involved in pupillary light reflex, and both muscles receive inputs from brain systems involved in cognitive and autonomic functions, been influenced by it (Eckstein et al., 2017).

Pupil dilatation is directly related to conditions of increased attention or cognitive load, or of emotional or cognitive arousal. Pupillometry is proven to be related to perception, language processing, memory and decision making, emotion and cognition, and cognitive development (Sirois & Brisson, 2014).

One of the explanations for the link between pupil dilation and psychological and physiological stimuli is that the dilatation can be attributed to the activation of the sympathetic system during autonomic arousal and mental activity, being modulated by the noradrenergic *locus coeruleus* (LC). The LC is essential for the regulation of physiological arousal and cognitive functioning. It produces the neurotransmitter norepinephrine and has direct inhibitory projections to the parasympathetic Edinger-Westphal nucleus; that is where the pupil's constricting fibers originate, therefore also inhibiting its constriction and indirectly enabling pupil's dilatation. LC also stimulates the sympathetic system, including the fibers that innervate the pupil to dilate it (Aminihajibashi, Hagen, Laeng, & Espeseth, 2020; Eckstein et al., 2017; Sirois & Brisson, 2014).

The process of pupil measurement that once was time-consuming is today relatively easy to carry out and non-invasive, being able to resolve better than 0.025 mm in diameter on individual measurements at rates of 25 to 2,000 Hz (Eckstein et al., 2017; Granholm & Steinhauer, 2004).

Visual and auditory stimuli may cause pupil dilatation response both in adults and in infants (Aston-Jones & Cohen, 2005; Eckstein et al., 2017; Einhauser et al., 2010; Kang & Wheatley, 2015; Laeng & Endestad, 2012; Piquado et al., 2010; Wetzel

et al., 2016). Moreover, it appears to be affected by arousal, rather than attention itself, since its reaction to a cue was not a predictor of better performance on a visual task (Aminihajibashi et al., 2020). Pupillary light reflex can be artificially created by showing pictures containing the Sun, revealing the top-down effects of perception in the pupil dilatation. Its properties, like delay, speed, and length of a change in pupil diameter index various aspects of attention and memory (Sirois & Brisson, 2014).

Pupil study is crucial since it may benefit the evaluation of “special populations who may not be able or willing to provide a typical behavioral answer (complex motor or verbal responses) to certain research questions, such as pre-verbal infants, nonverbal adults, or children with ASD” (autistic spectrum disorder) (Sirois & Brisson, 2014, p. 687). The close relationship between task-evoked pupil dilatation and its underlying neural mechanisms enables the use of this method with participants of any age; and knowledge about this relationship allows to relate results about the neural system and cognitive studies, allowing them to interpret results of cognitive studies in terms of underlying neurophysiological processes (Eckstein et al., 2017; Medathati, Desai, & Hillis, 2020).

2.3.2.2 Microsaccades

Saccades (Figure 16a) are rapid eye movements that allow us to shift between fixations; they can reflect voluntary or involuntary shifts in attention (as when looking at a target vs. reflexively looking at a stimulus) (Eckstein et al., 2017). Microsaccades (Figure 16b) are small movements (<1º) that occur at 80% of our waking hours when our eyes are fixating on something; they are essential for seeing. Visual neurons can accommodate. The most accepted hypothesis is that the microsaccades' goal is to inhibit this accommodation by prodding visual neurons into action and counteracting neural adaptation hence preventing stationary objects from fading. This hypothesis gets its support from the fact that if microsaccades are not present during gaze fixation, a static scene fades from view (Figure 16c (Martinez-Conde & Macknik, 2011; Martinez-Conde, Macknik, Troncoso, & Hubel, 2009).

Figure 16 – Fixational eye movements and visual fading

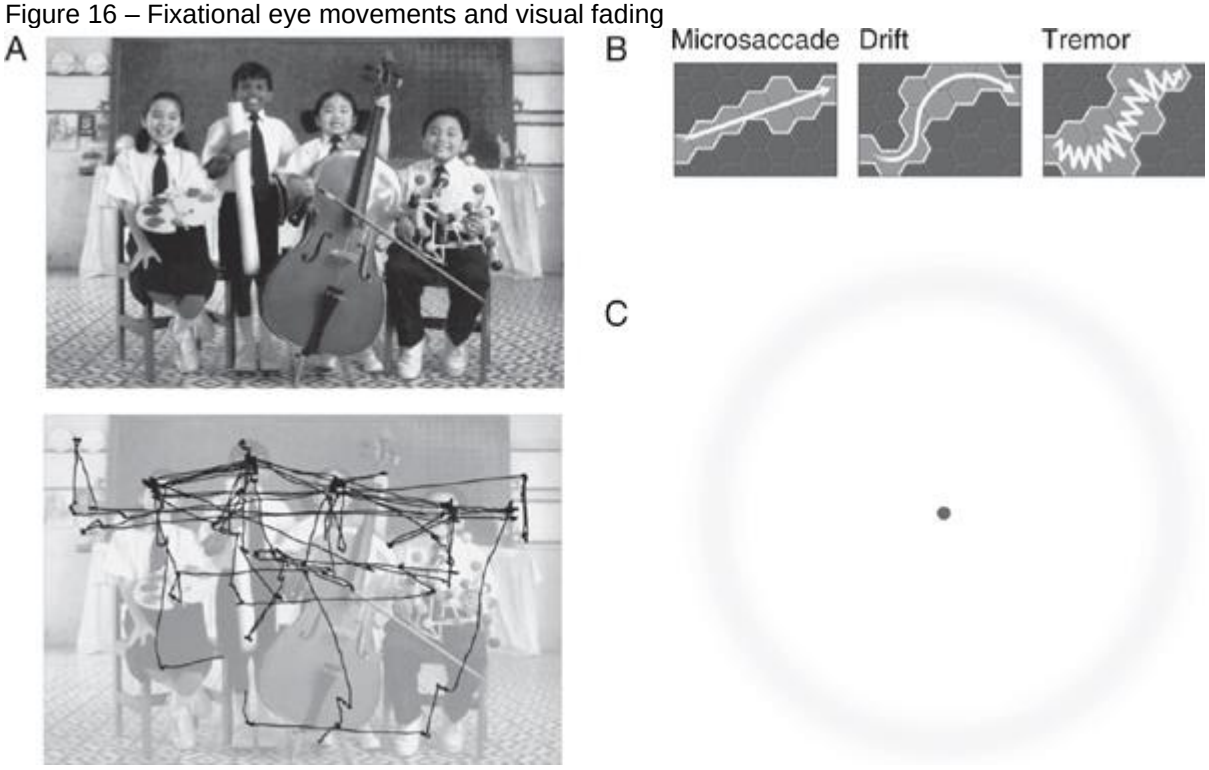

In (A), an observer views a picture (top) while eye positions are monitored (bottom). The eyes jump, seem to fixate or rest momentarily, producing a small dot on the trace, then jump to a new region of interest. The large jumps in eye position illustrated here are called saccades. However, even during fixation, or 'rest' times, eyes are never still, but continuously produce fixational eye movements: drifts, tremor, and microsaccades. In (B), a cartoon representation of fixational eye movements in humans and primates. Microsaccades (straight and fast movements), drifts (curvy slow movements), and tremor (oscillations superimposed on drifts) transport the visual image across the retinal photoreceptor mosaic. In (C), Troxler fading. In 1804 Swiss philosopher Ignaz Paul Vital Troxler discovered that deliberately fixating on something causes surrounding stationary images to fade away. To elicit this experience, stare at the central dot while paying attention to the surrounding pale ring. The ring soon vanishes, and the central dot appears set against a white background. If you move your eyes, it pops back into view. Source: Martinez-Conde and Macknik (2011, p. 2)

Although the microsaccades rate is one of the biggest measurements in the research field of visual perception, other perception modalities also can be better understood with the use of this tool. In visual studies, two phenomena relate to stimulus onset: a microsaccade inhibition and a rebound effect. The microsaccade inhibition occurs ~150 ms after stimulus onset as it reaches a minimum rate. The rebound effect peaks at ~350 ms after stimulus onset (Holmqvist et al., 2011).

2.3.2.3 Blink Rate

From ocular health to non-verbal communication, blinking serves several different functions. Eyeblink rate is the frequency at which the eyelids open and close, and it is a non-invasive, indirect measure of dopamine activity in the central nervous

system. There are three types of blinks: voluntary, reflexive (as a response to environmental stimuli), and spontaneous (not-volitional to distribute the tear film uniformly over the eye). It has been used to study cognitive control and learning (Eckstein et al., 2017).

3 METHODOLOGY

This thesis reports two experiments: the first is a tactile threshold conscious perception task, with data acquired through hdEEG and an eye-metrics system, and the second is an auditory task (Christison-Lagay & Micek, 2017, unpublished) with the acquisition of eye-metrics.

3.1 EXPERIMENT 1

3.1.1 Participants

Twenty-six adult participants were recruited to perform a behavioral task while undergoing high-density scalp electroencephalography (hdEEG) (8 participants), or hdEEG concurrent with eye-metric monitoring (16 participants). Two participants were excluded from data analysis due to poor behavioral performance (they answer with the correct finger for when reporting that they perceived for less than 60% of the time); an additional four were excluded from eye metric analysis and one from hdEEG analysis due to inadequate data collection.

All the eye metric data was collected with concomitant hdEGG. Data analysis of neurophysiological signals acquired with a 256-electrode net (see 3.1.3) was completed for 23 participants (10 male; 6 left-handed); analysis of eye metrics was completed for 10 participants (4 male; 3 left-handed) (see Table 3). All experimental procedures were approved by the Yale University institutional review board HIC#1107008859 (Appendix 1).

3.1.2 Task Design

The behavioral task tested tactile conscious perception using a vibration delivered to the pulp of one of the four non-thumb fingers (Figure 17B). Vibrating tactors were secured to each participant’s fingers using adjustable foam straps and a custom-made positioning template. Straps were color-coded to correspond to their counterpart button on a four-button response box controlled by the hand contralateral to the hand receiving stimuli.

Table 3 – Tactile task's participant demographic information

Participant	Gender	Age	Stimulated hand	Handedness	Included data modality
1	F	26	Left	Left	Tactile hdEEG
2	M	21	Left	Right	Tactile hdEEG
3	F	33	Right	Right	Tactile hdEEG
4	M	25	Left	Right	Tactile hdEEG
5	M	22	Right	Right	Tactile hdEEG
6	F	22	Left	Right	Tactile hdEEG
7	M	43	Right	Right	Tactile hdEEG
8	M	25	Right	Left	Tactile hdEEG
9	F	42	Right	Left	Tactile hdEEG
10	M	32	Right	Left	Tactile hdEEG
11	F	35	Right	Right	Tactile hdEEG
12	F	28	Right	Right	Tactile hdEEG
13	M	31	Right	Right	Tactile hdEEG
14	F	30	Left	Right	Tactile hdEEG
15	M	23	Right	Left	Tactile Eye metrics + hdEEG
16	F	33	Right	Left	Tactile Eye metrics + hdEEG
17	M	32	Left	Right	Tactile Eye metrics + hdEEG
18	F	43	Right	Right	Tactile Eye metrics + hdEEG
19	F	30	Right	Right	Tactile Eye metrics + hdEEG
20	M	22	Right	Right	Tactile Eye metrics + hdEEG
21	F	27	Left	Right	Tactile Eye metrics + hdEEG
22	F	29	Right	Right	Tactile Eye metrics + hdEEG
23	F	29	Left	Right	Tactile Eye metrics + hdEEG
24	M	30	Left	Left	Tactile Eye metrics

After setting up the equipment (see 3.4 for more information on the equipment, including software version), the task was run from MATLAB's (The Mathworks Inc., Natick MA, United States) **Command Window**. To ensure that all the equipment and connections were correctly working, the researcher would do an instrument reset (*instrreset*) and run the script *run_tactile_task_v2_3*. A window would pop up, prompting the subject ID that should be composed of the deidentified alphanumeric code correspondent (000AA – it was imperative that the **subject ID,** when using **EyeLink** – the eye metrics acquisition system**,** should be of **5 characters or less**).

Figure 17 – Tactile threshold task and experimental set-up.

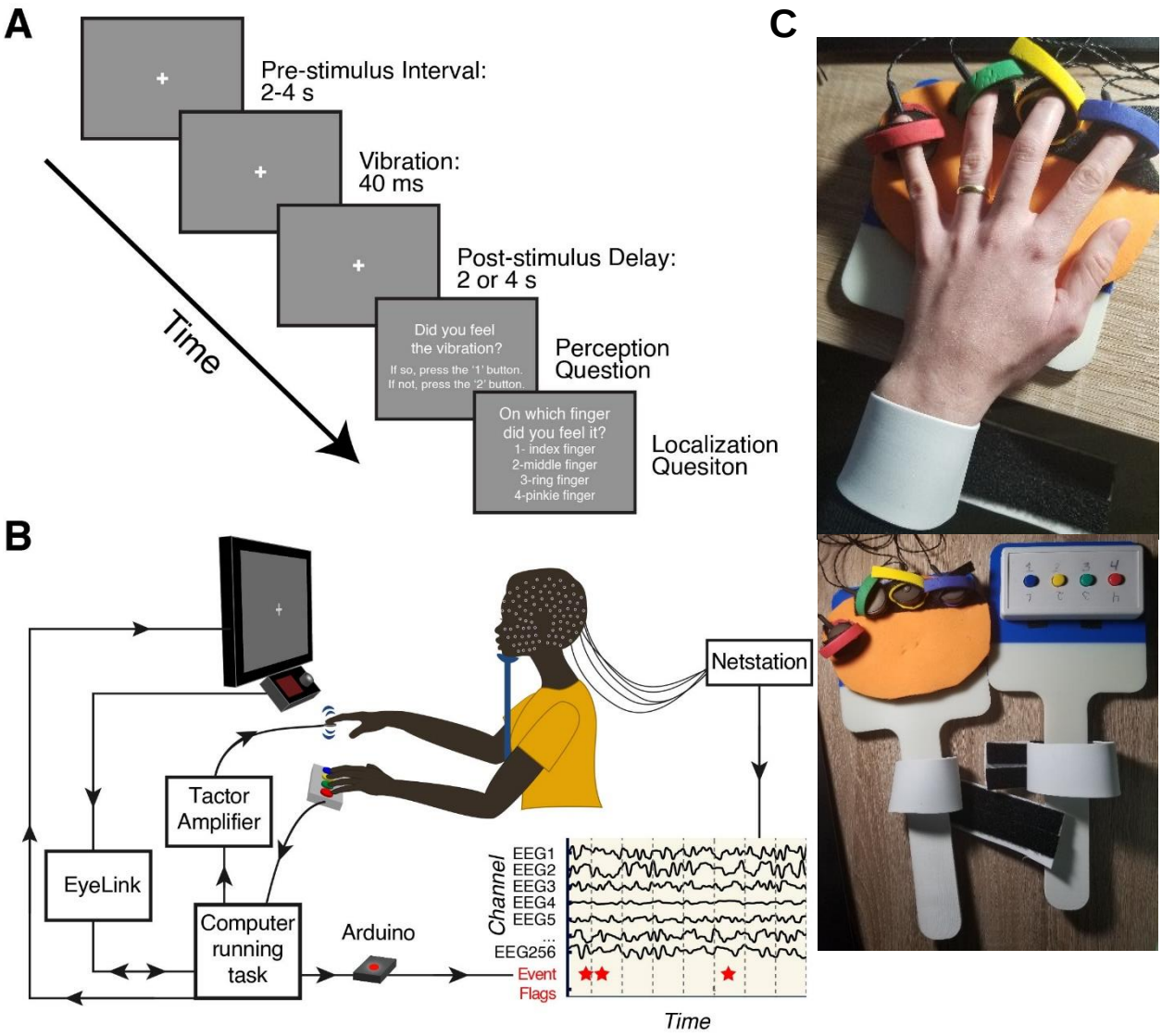

In (A), threshold tactile task for a single trial. Trials began with a randomly jittered pre-stimulus duration of 2-4 s of a gray screen with a fixation cross, which was followed by a 40 ms 200 Hz sinewave vibration presented to one of a participant's fingers (index, middle, ring, or pink) at the participant's tactile threshold. After a post-stimulus delay of 2 or 4 s, participants were prompted (onscreen) to answer two forced-choice questions regarding 1) whether they felt a stimulus, and 2) to which finger it was delivered. Participants answered with their non-stimulated hand using a response box. The next trial began immediately following the button press for the second question; there were 50 trials per run. In (B), experimental setup. Participants were positioned in a chinrest (to stabilize head position), facing an external monitor (which showed a fixation cross or task-related questions) and an infrared (IR) camera to record eye metrics, managed by the EyeLink system that received signals from the computer running the task. The external monitor was attached to a laptop that ran the tactile task. Signals for the stimuli (sinewaves generated by the laptop) were sent to the tactor amplifier and then to vibrating tactors placed on the participant's fingers. The participant's free hand was used to control a response box that was connected to the laptop. Signals from the IR camera were sent to a dedicated pupillometry computer. Task, behavioral, and eye metric data were synchronized via an Ethernet connection. Task, behavioral, and EEG data were synchronized by TTL pulses, initiated by the laptop, and generated through an Arduino UNO, recorded directly through the EEG amplifier. (C) shows hand positioning and paddles settings.

After filling in the subject ID, the software posed the following questions:

1. Are you using pupillometry? (yes/no)
2. Which button should mean yes? (1 for yes, 2 for no/2 for yes, 1 for no)
3. Which hand will receive the vibration? (right hand/ left hand)
4. Do you want to feel the practice stimuli? (Play practice stimuli/Do not play practice stimuli)

   It is highly recommended to respond in the affirmative, to ensure that all the tactors are properly working.

5. Use Arduino? (yes/no)
6. Use NetStation scalp EEG? (yes/no)

   This question should only be answered yes when using the NetStation scalp. Unlike our standard Arduino set up in which different durations of pulses are sent to the same pin, this sends TTL pulses to different pins.

7. Use External screen? (yes/no)

   Because the amplifier is linked through an HDMI cable, the computer assumes that it is an external screen. If you are using the MacBook to show the task, select No; otherwise, select Yes. This setting will get the external screen to display the task via a VGA/Thunderbolt connection.

After setting-up, MATLAB would connect with the EyeLink system, and EyeLink calibration would be conducted. After that, the following instructions were read:

> Thank you for agreeing to participate in our task! Today, you'll be participating in the sensory awareness behavioral task; and specifically, the tactile identification task. I am now going to describe some instructions briefly for the task.
> **How to hold the button box:**
> You will be responding during the computer game using a 4-button button box. Please keep the button box under your **right hand**. Please place your right index finger on the blue button (#1), your right middle finger on the yellow button (#2), your right ring finger on the green button (#3), and your right little finger or pinky on the red button (#4). **Your fingers should be in these positions at all times.**
> The computer game has three parts: **(1) practice, (2) calibration,** and **(3) runs.** Directions are going to appear on the screen before each part of the task, but I'm quickly going to go over what you should be doing now:
> **Part 1: Practice**
> In the practice, you'll get a chance to feel the vibrations you'll be feeling throughout this experiment. In the actual experiment, one of your four fingers will be stimulated at a time. In other words, you will not receive simultaneous vibrations in two or more of your fingers.
> During the practice, you'll feel each target buzz 2 times. It should be easy to feel these vibrations and you should be able to tell us the finger that received the vibration.
> **Part 2: Runs**
> When you're done with the practice, a new screen will come up, telling you that you're going to move on to the run phase. The runs are organized into trials. Each trial lasts several seconds. During the trial, there will be a white cross on a noisy background **- please stay fixated on the white cross for the whole trial**. For each trial, one of the target fingers (index, middle, ring, or pinky) may or may not get a vibration—and if it does, it will be a very faint sensation. If you think you felt the vibration in one of the fingers, don't press a button immediately! At the end of the trial, you'll be asked about

> what you felt with 2 questions. The first question is whether you felt a vibration (if you did feel it, press the blue button (#1); and if you didn't feel anything, press the yellow button (#2)). The second question asks about the finger in which you felt the vibration. A kind of funny part of our experiment is that you'll be asked this question even if you said you didn't feel a vibration. So, if you feel the vibration in one of your fingers, press the button corresponding to the correct finger (#1 for index, #2 for middle, #3 for ring, and #4 for pinky finger). If you *didn't* feel anything, answer randomly.
> In the runs, you wait until you're asked the questions, so you should remember if you felt a vibration, and where it was (in what finger you felt it). Before each section, a set of directions will come up to remind you what you're supposed to be doing; and there are instructions on what the buttons mean during the trials too.
> Remember to always use your **right hand** to hold the button box.
> **Breaks**
> And finally—sometimes this task gets a little boring or tiring. At the end of the calibrations or the runs, you'll be prompted to take a break if you want to… We encourage you to take a break if you're feeling fatigued.

A computer screen, with a central white fixation cross on a gray background, was placed in front of the participant. The distance from the central fixation cross to the bridge of the participant's nose was standardized to 55 cm when eye metrics were measured (85 cm when eye metrics were not measured); the size of the displayed screen was adjusted to keep the apparent size and viewing angle (19^{o}) consistent across conditions.

To familiarize the participants with the stimuli, they underwent a pre-test training. In this training, participants received suprathreshold stimuli to each finger in turn and should identify which finger had received stimulation. Following training, participants completed four runs of 50 trials (200 trials total). For each trial (Figure 17A), participants were asked to fixate on a white cross positioned centrally on a gray background on the computer screen while they waited for the deliverance of vibration to one of their fingers. From the instructions, the participants knew that they may or may not feel a vibration on every trial. Trials began with a random 2-4 s period in which the participant fixated on the white cross. Following this period, 86% of the trials had a vibration; 14% did not have it (blank trials).

Following the vibration (or blank), there was an additional 2 or 4 s delay before the first behavioral report question appeared on the screen. Participants were asked two self-paced questions, presented successively on the computer screen. The first question (perception question) was: "Did you feel the vibration?" which offered two options: 1 for yes, 2 for no; or 2 for yes, 1 for no. The 'yes' button was counterbalanced across participants, but remained constant for the duration of the study for any given participant. Following the perception question, participants were presented with the question (localization question): "On which finger did you feel it?" with the numbers one

to four followed by their correspondent fingers (1-index, 2-middle, 3-ring, 4-pinky). The screen would show this question regardless of their answer to the first question; if they reported not feeling the vibration, they were instructed to answer the second question randomly. Participants reported their answers to these questions using a response box under the hand contralateral to the hand receiving stimulation (Figure 17B). To aid in answering the second question, both the color and finger identity of the button box corresponded to the hand receiving stimulation (Figure 17C, e.g., if they felt the vibration on the ring finger – which had a green foam strap – of the right hand, they should press the ring finger – green button – of their left hand).

3.1.3 Experimental Design

Tactile stimuli consisted of a 200 Hz sinewave pulse (peak sensitivity for Pacinian Corpuscles, (Hendry & Hsiao, 2013; McGlone & Reilly, 2010; Siegel, 2019)) presented for 40ms. The Psychtoolbox Minimum Expected Entropy Staircase method shown in Appendix 2 (Saunders & Backus, 2006) titrated the amplitude of the vibration in a trial-by-trial manner (Fig. S2) to approximate the participant's 50% perceptual threshold. The task was written in Matlab (The Mathworks Inc., Natick MA, United States) using the Psychophysics Toolbox ('Psychtoolbox') extensions (Brainard, 1997; Cornelissen, Peters, & Palmer, 2002; Kleiner, Brainard, & Pelli, 2007; Pelli, 1997). Stimuli were generated in Matlab, amplified (Marantz NR1609 AV Receiver), and transduced by vibrating tactors (C-2 tactor, Engineering Acoustics, Inc.) placed on the participants' fingers (Figure 17B).

The code was based on Christison-Lagay and Micek (2017, unpublished) auditory task v1_18. At first, it followed the same calibration process, where different amplitudes were delivered, and the participant was supposed to report when felt. The stimuli perception report was fit to a Weibull distribution curve, identifying where the threshold is at 50%. This process was unsuccessful since the tactile perception is more fluid than auditory and visual, not fitting to a Weibull distribution and also changing with accommodation during testing.

We searched for a faster and more efficient way of getting to the 50% threshold, which would also be able to update itself in case of a change in the threshold due to tactor displacement, sensory accommodation, or other variables.

What we found was the PsychStairCase function from MATLAB's Psychtoolbox (Appendix 2). It works with the principle of Minimum Expected Entropy. The staircase gives suggestions for which probe value to test next, choosing the probe that will provide the most information (based on the principle of minimum entropy = maximally unambiguous probability distribution). The algorithm would choose the next probe from a set of possible probe values provided initially, and their use is evaluated based on the expected amount of information gain given a space of PSE and slope values to test over. This section will describe the code and its functionalities. Each topic will describe one script.

1. *run_tactile_task*
    a. Cleans the instruments.
    b. Reports if the button box is plugged.
    c. Calls *tactile_pipeline_localization_v2_3*.
2. *tactile_pipeline_localization_v2_3*
    a. Calls the following .m files:
        1. *digital_write*
        2. *variable_setup_localization_v2_3*
        3. *setup_screenstuff_localization_v2_3*
        4. *setup_keyboards_localization_v2_3*
        5. *setup_touch_localization_v2_3*
        6. *setup_trialstuff_localization_v2_3*
        7. *setup_staircase_localization*
        8. *practice_localization_v2_3*
        9. *setup_Eyelink_v2_3*
        10. *task_tactile_localization_v2_3*
    b. Asks questions about the study subject.
    c. Saves general file about main subject information, and a session file (subjectId_sessionnumber.mat = 000AA_1.mat).
    d. Runs up to 15 runs.
3. *digital_write*:
    a. Configure the Arduino.
4. *variable_setup_localization_v2_3*
    a. Defines basic parameters.
5. *setup_screenstuff_localization_v2_3*
    a. Starts Psychtoolbox;
    b. Gets screens numbers and defines the first screen as the one to be used if you are not using an external screen and screen two if you are using it. It differs from other codes because it is not the last screen, since this is usually the HDMI/amplifier one. In case the external screen is not working, try to change this variable (screenNumber);
    c. Determine the variables like colors, fonts, and cross dimensions.
6. *setup_keyboards_localization_v2_3*
    a. Defines the response box as the keyboard;
    b. Listens only to determined keys to avoid clicking the wrong button.
7. *setup_touch_localization_v2_3*
    a. Starts Psychtoolbox sounds;

b. Connects to the amplifier and get its characteristics;
c. Defines stimulus parameters:
    1. *T:* duration: **40ms**.
    2. *f:* vibration sinewave frequency: **200Hz**.
    3. *prelength_audio_choices*: time before stimuli: **2 or 4s**.
    4. *totallength_choices*: time after stimuli: **2-4s**.
    5. *panhandle = PsychPortAudio('Open', 2, 1, 1, fs, nrchannels)*: open Psych-Audio port, with the following arguments:
        1. 2: external output.
        2. 1: sound playback only.
        3. 1: default level of latency.
        4. Frequency in samples per second (44,100Hz)
        5. Number of channels (8).
    6. *sound#:* creates the 4 sounds to be played. Inserting tone1 to the channel and a variable called silence to the other ones. The sounds are:
        1. channel 1/front left;
        2. channel 2/front right;
        3. channel 5/surround left;
        4. channel 6/surround right;

8. *setup_trialstuff_localization_v2_3*
    a. Randomizes the trials, creating at least eight trials per finger, also adds 14% of blank trials (7 per run).
9. *setup_staircase_localization_v2_3*
    a. Sets the parameters for the minimum entropy method.
    b. *probeset:* sets possible amplitude values between 0.003 and 0.5 with a 0.001 increase;
    c. *stair1-4:* start four different stairs for each finger;
    d. *stair#.toggle_use_resp_subset_prop(8,.9):* uses a subset of all data for choosing the next amplitude, with a minimum of 8 previous trials and a maximum of 90% of them.
    e. *stair#.set_first_value(0.07)*: sets the first amplitude to be played to 0.07. Notice that with staircase methods, if you start with a value the person feels, the threshold tends to be higher than if you start with a value that the person does not feel.
    f. *stair#.loadhistory(…):* if it is the second session, this variable loads the history of the two last felt vibrations and the two not felt ones to seed the new stair. We found that when changing the hand position, the threshold significantly changes most of the time. Because of that, when we are doing two separate sessions, we load just those four points of history to make it faster to find the new threshold without compromising it too much if the difference is big.
10. *practice_localization_v2_3*
    a. Sends a clearly felt vibration to each finger twice at 0.65 amplitude
11. *setup_Eyelink_v2_3*
    a. sets up Eyelink configurations when using it.
    b. *edffile:* creates .edf file, notice that the file should be at most eight characters since the file name is composed by the subject

ID_sessionnumber, the subject ID, when using Eyelink, should be of **5 characters or less**.

c. Does a 9 points eye calibration.
d. Sets the EDF file contents using file_sample_data and file_event_filter

12. *task_tactile_localization_v2_3*
    a. Call function *eyelink_startrecording_v2_3*
    b. Sends TTL pulses when events happen:
        1. "HIGH" – 100 ms pulse, for question periods – pin 11
        2. " MED" – 25 ms pulse, for button presses – pin 12
        3. " FIX" – 200 ms pulse, for the run start– pin 13
        4. " QUE" – 150 ms pulse, for stimulus presentation – pin 10
        5. " TRI" – 300 ms pulse, for a trial start – pin 13
    c. Sends information messages to Eyelink with the events.
    d. *a:* trial 1-50
    e. *stair#.get_next_probe():* gets the next amplitude as *p#.*
    f. *sound_ID*: defines which tactor will be activated based on the randomized definition on setup_trialstuff_localization_v2_3.
    g. *tone1:* defines the sound to be played.
    h. *stair#.process_resp(r#):* stores the response in the staircase = 1 for correct and 0 for incorrect.
    i. *allanswers_run:* table with all the trials information:
        1. adjusted answer to question 1: 1 = y 2 = n, regardless of if button one or two was used as yes.
        2. reaction time to answer
        3. answer to 2nd question
        4. reaction time to answer
        5. stimulus amplitude used
        6. length in samples of pre-stim (divide by sr [sampling rate = 44100, column 7] to have the value in s)
        7. sampling rate (fixed at 44,100 Hz)
        8. stimuli frequency (fixed at 200 Hz)
        9. time after the beginning of the stimulation in samples (divide by the sampling rate (44,100) and subtract the duration of the stimuli (.040 s) to get the value in s)
        10. length of touch presentation (fixed at 40 ms)
        11. session (each time you have to restart the task, i.e., different days or if something has to be fixed)
        12. total number of runs across all sessions
        13. raw answer 1 (it is the real button pressed for yes, if it is 2 for yes, then it will be different from question 1)
        14. raw answer 2
        15. button for yes
        16. button for no
        17. total time size of trial in samples (divide by sampling rate to get the value in s)
        18. which finger was stimulated
        19. when the run started in s relating to the beginning of the session
        20. when the trial started in s relating to the beginning of the session

21. when the vibration started in s relating to the beginning of the session
22. when question 1 was presented in s relating to the beginning of the session
23. when question 1 was answered in s relating to the beginning of the session
24. when question 2 was presented in s relating to the beginning of the session
25. when question 2 was answered in s relating to the beginning of the session
    1. answer to 1st question: 1 = y
    2. reaction time to answer
    3. answer to 2nd question
    4. reaction time to answer
    5. amplitude used
    6. size of pre-stim
    7. sampling rate
    8. frequency
    9. time after the touch
    10. time of touch presentation
    11. session
    12. total of runs
    13. raw answer 1
    14. raw answer 2
    15. button for yes
    16. button for no
    17. total time size of the trial
    18. which finger was stimulated
    19. when the run started
    20. when the trial started
    21. when the sound started
    22. when question 1 was presented
    23. when question 1 was answered
    24. when question 2 was presented
    25. when question 2 was answered.

13. *eyelink_start_recording_v2_3*
    a. Starts Eyelink

When eye metrics were measured, participants viewed a fixation cross on a visual display placed directly above a mounted EyeLink® 1000 Plus pupillometer and infrared illuminator (SR-research). By using consistent lighting sources within a windowless testing room, we controlled the luminance across testing sessions. Binocular eye-tracking data was collected in head-stabilized mode at 1,000 Hz; head stabilization was achieved using a chinrest. Before initiating the behavioral task, participants performed an automated eye-gaze calibration procedure to ensure accurate tracking of eye position.

Non-invasive high-density EEG was recorded from the scalp using a 256-channel net Figure 18. Electrodes were placed using saline electrode gel (SIGNAGEL – Parker Laboratory) to enhance conductivity between the head and electrodes. After gelling the electrodes, the impedance was measured and was considered acceptable if it was <70 kΩ in more than 90% of the electrodes. Signals were amplified through two 128 channel EEG amplifiers (Electrical Geodesics, Inc. Eugene, Oregon), and recorded and digitized via a Net Station System (1,000 Hz sampling rate, a high-pass filter of 0.1 Hz, a low-pass filter 400 Hz). During recording, channels were Cz-referenced.

Figure 18 – 256 electrodes net positioning – superior view

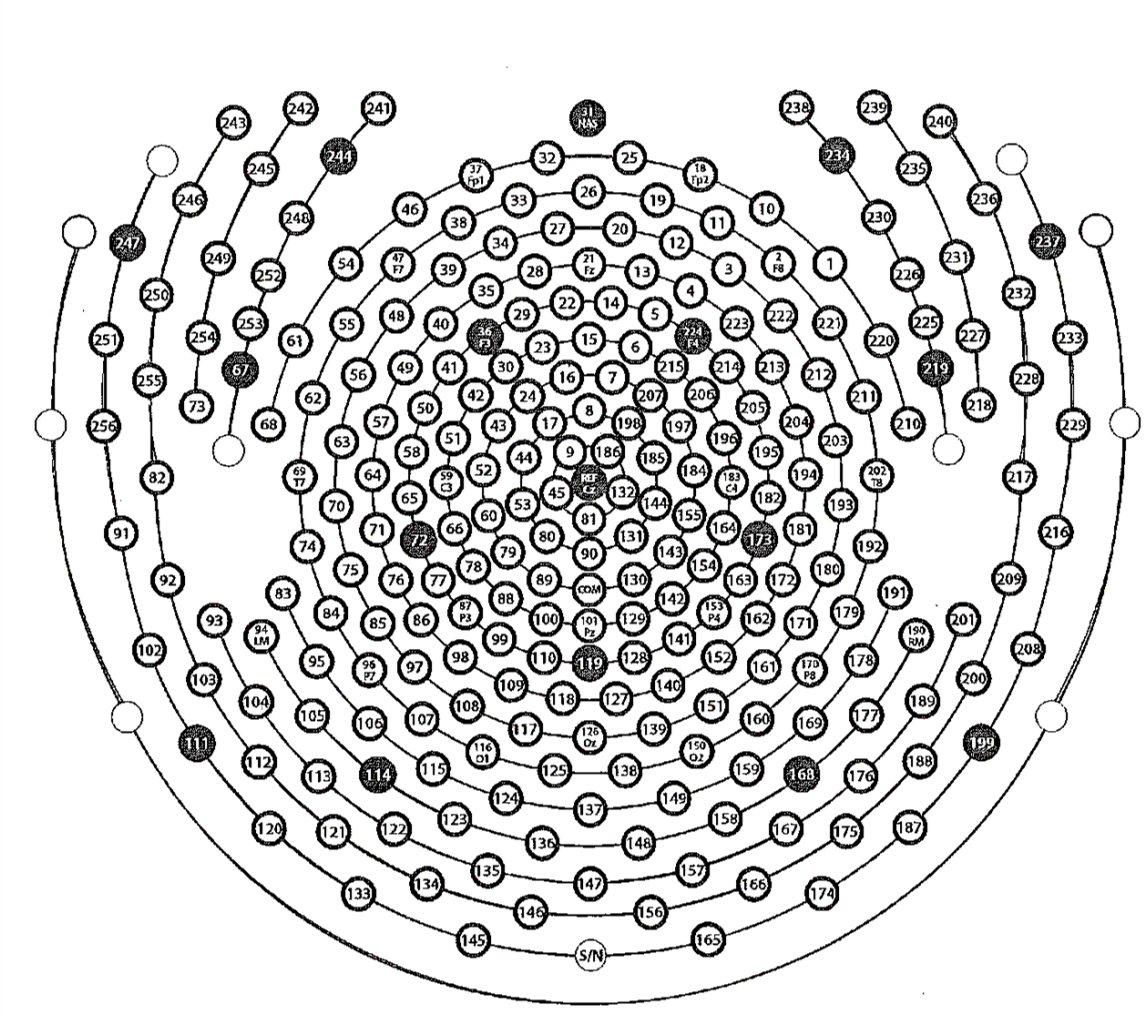

Superior map of the electrodes' placement that was used during the study. The numbers had an equivalent map on the screen to check for impedances. Standard electrodes positions are also assigned to their location (see Figure 13).
Source: Luu and Ferree (2000, p. 12)

Task, behavioral, and pupillometry data were synchronized using digital timing information sent over Ethernet. TTL pulses were directly inputted to the EEG amplifier and recorded as event flags on the EEG recording on Net Station, ensuring precise synchronization between task, behavioral, and EEG data. TTL pulses were initiated by the laptop (Macbook Pro) running the task and generated by an Arduino Uno (R3; Smart Projects) connected to the digital input port of the EEG amplifier via a DB9 cable. Responses were recorded using a four-button response box connected to the laptop via USB and sampled by the computer at 1,000 Hz. A checklist of the steps for experimenting is available in Appendix 3.

3.2 EXPERIMENT 2

3.2.1 Participants

Twenty-five adult participants were recruited to perform an auditory behavioral task while undergoing eye-metric monitoring (14 male, four left-handed, mean age = 28.24 y ± 11.51, Table 4).

3.2.2 Task design

The behavioral task (developed by Christison-Lagay and Micek, 2017, unpublished) tested auditory conscious perception using three sounds (whistle, laser – a swiping sound, or waterdrop) calibrated to the participant's 50% perception threshold.

After setting up the equipment (see Item 3.4 for more information on the equipment), the task was run from MATLAB's **Command Window**. To ensure that all the equipment and connections are correctly working, the researcher would do an instrument reset (*instrreset*) and run the script *run_auditory_task_v1_18*. A window would pop up, prompting the subject ID that should be composed of the deidentified alphanumeric code correspondent (000AA – it was imperative that the **subject ID,** when using **Eyelink,** should be of **5 characters or less**).

Table 4 – Auditory eye-metrics' participant demographic information

Participant	Gender	Age	Handedness	Included data modality
1	M	57	Left	Auditory eye-metrics
2	F	52	Right	Auditory eye-metrics
3	F	29	Right	Auditory eye-metrics
4	M	19	Right	Auditory eye-metrics
5	M	29	Right	Auditory eye-metrics
6	F	23	Left	Auditory eye-metrics
7	F	19	Right	Auditory eye-metrics
8	M	63	Right	Auditory eye-metrics
9	F	31	Right	Auditory eye-metrics
10	F	27	Right	Auditory eye-metrics
11	M	18	Right	Auditory eye-metrics
12	F	25	Right	Auditory eye-metrics
13	M	24	Right	Auditory eye-metrics
14	M	24	Right	Auditory eye-metrics
15	M	21	Left	Auditory eye-metrics
16	M	29	Right	Auditory eye-metrics
17	M	24	Right	Auditory eye-metrics
18	F	25	Right	Auditory eye-metrics
19	F	20	Right	Auditory eye-metrics
20	M	24	Right	Auditory eye-metrics
21	M	22	Right	Auditory eye-metrics
22	M	20	Left	Auditory eye-metrics
23	F	30	Right	Auditory eye-metrics
24	F	31	Right	Auditory eye-metrics
25	M	29	Right	Auditory eye-metrics

After filling in the subject ID, the software posed the following questions:

1. Are you using pupillometry? (yes/no)
2. Which button should mean yes? (1 for yes, 2 for no/2 for yes, 1 for no)
3. Do you want to feel the practice stimuli? (Play practice stimuli/Do not play practice stimuli)
4. Use Arduino? (yes/no)

After setting-up, MATLAB would connect with the EyeLink system, and EyeLink calibration would be conducted. After that, the following instructions were read:

> Thank you for agreeing to participate in our task! Today, you'll be participating in the sensory awareness behavioral task; and specifically, the auditory identification task. I am now going to describe briefly some instructions for the task.
> How to hold the button box:
> You will be responding during the computer game using a 4-button button box. Please keep the button box under your right hand. Please place your right index figure on the

blue button (#1), your right middle finger on the yellow button (#2), your right ring finger on the green (#3), and your right little finger or pinky on the red button (#4). Your fingers should be in this position at all times.
The computer game has three parts: (1) practice, (2) calibration, and (3) runs. Directions are going to appear on the screen before each part of the task, but I'm quickly going to go over what you should be doing now:
Part 1: Practice
In the practice, you'll get a chance to hear the sounds you'll be listening to for this experiment. There are four sounds you'll hear:
The first is the background noise that will be playing for most of the experiment. This sounds kind of like static—like you might hear over the radio if you've tuned it to a wrong station.
The other three sounds are target sounds, and your job in the experiment is to listen very carefully for them and tell us when you hear them, and which one of them you've heard. They are a whistle, a sound like a laser, or a water drop. During the practice, you'll hear each target sound three times. They should be easy to hear and to tell apart.
Part 2: Calibration
After you've heard the sounds you'll be listening for; we'll begin the actual experiment with the calibration phase.
In the calibration, you will see a white cross on a noise background—this will look a little like what a TV turned to a non-station looks like. Please try to fixate on the cross at all times. Over the laptop's speakers, the static-y background sound will start to play. While that background sound is going on, we will sometimes play the target sounds (the whistle, the laser, or the water drop). They will be very quick; sometimes, they'll be pretty loud and easy to hear, and other times, they will be very quiet. But whenever you hear one of the target sounds, press the yellow button (#2; middle finger) as quickly as possible.
Part 3: Runs
When you're done with the calibration, a new screen will come up, telling you that you're going to move on to the run phase.
The runs are organized into trials. Each trial lasts several seconds. During the trial, there will be a white cross on a noisy background—please stay fixated on the white cross for the whole trial. For each trial, you will listen to the background noise, and one of the target sounds (the whistle, the laser, or the water drop) may or may not be played—and if they do play, they will be very soft. If you hear one of these sounds, don't press a button immediately! At the end of the trial, you'll be asked about what you heard with 2 questions. The first question is whether you heard a sound (if you did hear a sound, press the yellow button (#2); and if you didn't hear anything, press the blue button (#1)). The second question asks about what sound you heard. A kind of funny part of our experiment is that you'll be asked this question even if you said you didn't hear a sound. So, if you heard one of the sounds, press the button corresponding to the correct sound (#1 for the whistle, #2 for the laser, and #3 for the water drop). If you didn't hear any sound, answer randomly.

So, in short: in the calibration phase, you press the button whenever you hear the sound. In the runs, you wait until you're asked the questions, so you should remember if you heard a sound and what it was. Before each section, a set of directions will come up to remind you what you're supposed to be doing; and there are instructions on what the buttons mean during the trials too.
Remember to always use your right hand to hold the button box.
Breaks
And finally—sometimes this task gets a little boring or tiring. At the end of the calibrations or the runs, you'll be prompted to take a break if you want to… We encourage you to take a break if you're feeling fatigued.

A computer screen, with a central white fixation cross on a white noise background, was placed in front of the participant. The distance from the central

fixation cross to the bridge of the participant's nose was standardized to 55 cm when eye metrics were measured; the laptop was placed 85 cm away for sound deliverance; the size of the displayed screen was adjusted to keep the apparent size and viewing angle (19^{o}).

During the three steps, apart from when the questions were presented, there was a white noise background being played. To familiarize the participants with the stimuli, they underwent a pre-test training. In this training, participants heard twice each of the stimuli (whistle, laser, or waterdrop) fully audible. Following training, the threshold was obtained via a calibration run when the participants were prompted to press a button immediately after hearing one of the three sounds. The results of the calibration run were fitted into a Weibull distribution curve that would set the specific amplitude on which the sound should be played to meet the participant's 50% threshold.

Participants completed six runs of 50 trials (300 trials total). For each trial, participants were asked to fixate on a white cross positioned centrally on a white noise background on the computer screen while they waited for the sounds. From the instructions, the participants knew that they may or may not hear it on every trial. Trials began with a random 3-5 s period in which the participant fixated on the white cross. Following this period, 86% of the trials had a sound (75 ms); 14% did not have it (blank trials).

Following the sound (or blank), there was an additional 3, 4, or 5 s delay before the first behavioral report question appeared on the screen. Participants were asked two self-paced questions, presented successively on the computer screen. The first question (perception question) was: "Did you hear a sound?" which offered two options: 1 for yes, 2 for no; or 2 for yes, 1 for no. The 'yes' button was counterbalanced across participants, but remained constant for the duration of the study for any given participant. Following the perception question, participants were presented with the question (identification question): "Which sound was it?" with the numbers one to four followed by their correspondent fingers (1-whistle, 2-laser, 3-waterdrop). The screen would show this question regardless of their answer to the first question; if they reported not hearing a sound, they were instructed to answer the second question randomly. Participants reported their answers to these questions using a response box.

3.2.3 Experimental design

Tactile stimuli consisted of three different sounds presented for 75 ms. Based on the calibration run, each sound had its amplitude titrated to the participant's 50% perceptual threshold (following the same method as Herman et al., 2019). The task was written in Matlab using the Psychophysics Toolbox ('Psychtoolbox') extensions (Brainard, 1997; Cornelissen et al., 2002; Kleiner et al., 2007; Pelli, 1997). Stimuli were generated in Matlab and delivered through the computer's sound system. The code was written by Christison-Lagay and Micek (2017, unpublished).

The participant viewed a fixation cross and background noise on a visual display placed directly above a mounted EyeLink 1000 pupillometer and infrared illuminator. By using consistent lighting sources within a windowless testing room, we controlled the Luminance across testing sessions. Binocular eye-tracking data was collected in head-stabilized mode at 1,000 Hz; head stabilization was achieved using a chinrest. Before initiating the behavioral task, participants performed an automated eye-gaze calibration procedure to ensure accurate tracking of eye position.

Task, behavioral, and pupillometry data were synchronized using digital timing information sent over Ethernet. Responses were recorded using a four-button response box connected to the laptop via USB and sampled by the computer at 1,000 Hz.

3.3 DATA ANALYSIS FOR BOTH TASKS

3.3.1 Behavioral analysis

For both tasks, trials were considered for analysis if they were classified as confirmed perceived or confirmed not perceived. Trials in which vibration was present, detected, and then localized to the correct finger were considered "confirmed perceived"; trials in which vibration was present, not detected, and then incorrectly localized were considered "confirmed not perceived".

Because the tactile perceptual threshold changed across the course of a single behavioral session, we used a continually adjusting staircase method to approximate the instantaneous perceptual threshold. This method results in several perception threshold trials. Nonetheless, some trials' amplitudes are supra- and subthreshold. To select the threshold trials, we used a Euclidean distance analysis. For each participant,

on a finger-by-finger basis, trials categorized as confirmed perceived and confirmed not perceived were selected. The order of perceived trials was randomized; the shuffled order of perceived trials was then used to match each perceived trial's amplitude to the not-perceived trial with the closest amplitude. If the amplitude difference between the perceived and not-perceived trials fell within 0.03 (arbitrary units [au]; amplitudes could adjust by 0.001 au), the pairing was included, and both trials were removed from their respective pools; if it fell outside of those boundaries, that perceived trial was discarded, and the not-perceived trial was replaced into the not-perceived pool. The matching continued until all perceived trials were either paired with a unique not-perceived trial or discarded. The total number of trials included was tallied, and the sum of differences between each unique pairing was calculated. After replicating this procedure 100,000 times, the replications with the largest number of trials were selected for analysis. If two or more replications yielded the same number of included trials, the replication with the smallest sum of amplitude differences was selected; if this was also identical, a replication was chosen randomly from the equivalent replications. For simplicity, we will hereafter refer to this selected subset of trials as perceived and not perceived, with the understanding that all analyzed trials have been validated regarding both localization accuracy and proximity to the participant's perceptual threshold.

3.3.2 *Event-Related Potential (ERP) analysis*

After extraction from the NetStation system, the EEG data were analyzed using Matlab and EEGLAB (v14_1_2b) (Delorme & Makeig, 2004). For each participant, a high-pass 0.1 Hz filter and the CleanLine procedure (Mullen, 2012) were run to exclude 60 Hz and 120 Hz (±2 Hz) frequency. CleanLine adaptively estimates and removes sinusoidal artifacts from scalp channels using a frequency-domain (multi-taper) regression technique with a Thompson F-statistics for identifying significant sinusoidal artifacts.

To reject channels with high-frequency noise (e.g., from muscle or movement artifact), a high-pass 30 Hz filter was applied on at the channel level across the entirety of the session (window size: 4 s, 2 s overlap). The resulting windowed data were then z-scored (per channel), flagging for later exclusion channels that exceeded a z-score

of greater than 2 for more than 25% of windows – the high pass-filter was only applied for flagging the data. The EEG data continued the same as in the previous step.

Epochs were identified and cut from -2,000 ms to +2,000 ms, centered on the vibration onset. All further analyses were conducted independently for trials belonging to perceived or not perceived trials (see 3.3.1).

For each trial condition, channels with high-frequency power spectrum were excluded (since it represents channels that did not had a good acquisition and did not represent brain activity, but noise), and their positions were re-populated using a spherical interpolation method. The resulting data were re-referenced to the mastoid signals' average (electrodes 94 and 190 – see Figure 18).

All epochs were collated and passed through a semi-automatized principal component analysis (PCA) and Independent Component Analysis (ICA) decomposition rejection procedure, in which the ten principle components that explained the most variance of the data were identified. Then, among these components, ten independent components were found. Trained study personal removed independent components that corresponded to signatures for a blink, eye-movement, and heartbeat artifacts. Doing ICA decomposition procedures have been proved to be more sensitive to small non-brain artifact than the use of ICA directly to the scalp channel data (Delorme, Sejnowski, & Makeig, 2007).

Finally, a 25 Hz low-pass filter was applied, and the average of perceived and not perceived epochs was acquired. The resulting signals were baselined by subtracting the mean of the interval from 1,000 to 500 ms pre-stimulus.

The brain maps of participants that received the vibrations on their left hand were mirrored to control for effects of lateralization, with the electrodes assuming the position of their contralateral equivalents (Table 5). The means and standard errors of the means (SEM) were calculated across participants.

The results were also resampled at 200 Hz, re-baselined by subtracting the average of the 2,000 to 5 ms pre-stimulus period, and went through false discovery rate (FDR) procedures to control for multiple comparisons using the mass univariate analysis (MUA) and EEGLAB’s ERPLab toolboxes (Benjamini & Hochberg, 1995; Groppe, Urbach, & Kutas, 2011; Lopez-Calderon & Luck, 2014).

Table 5 – Original (O) and New (N) electrodes mapping

O	1	2	3	4	5	6	7	8	9	10	11	12	13	14	15	16
N	54	47	39	35	29	23	16	8	186	46	38	34	28	22	15	7
O	17	18	19	20	21	22	23	24	25	26	27	28	29	30	31	32
N	198	37	33	27	21	14	6	207	32	26	20	13	5	215	31	25
O	33	34	35	36	37	38	39	40	41	42	43	44	45	46	47	48
N	19	12	4	224	18	11	3	223	214	206	197	185	132	10	2	222
O	49	50	51	52	53	54	55	56	57	58	59	60	61	62	63	64
N	213	205	196	184	144	1	221	212	204	195	183	155	220	211	203	194
O	65	66	67	68	69	70	71	72	73	74	75	76	77	78	79	80
N	182	164	219	210	202	193	181	173	218	192	180	172	163	154	143	131
O	81	82	83	84	85	86	87	88	89	90	91	92	93	95	96	97
N	81	217	191	179	171	162	153	142	130	90	216	209	201	178	170	161
O	98	99	100	101	102	103	104	105	106	107	108	109	110	111	112	113
N	152	141	129	101	208	200	189	177	169	160	151	140	128	199	188	176
O	114	115	116	117	118	119	120	121	122	123	124	125	126	127	128	129
N	168	159	150	139	127	119	187	175	167	158	149	138	126	118	110	100
O	130	131	132	133	134	135	136	137	138	139	140	141	142	143	144	145
N	89	80	45	174	166	157	148	137	125	117	109	99	88	79	53	165
O	146	147	148	149	150	151	152	153	154	155	156	157	158	159	160	161
N	156	147	136	124	116	108	98	87	78	60	146	135	123	115	107	97
O	162	163	164	165	166	167	168	169	170	171	172	173	174	175	176	177
N	86	77	66	145	134	122	114	106	96	85	76	72	133	121	113	105
O	178	179	180	181	182	183	184	185	186	187	188	189	191	192	193	194
N	95	84	75	71	65	59	52	44	9	120	112	104	83	74	70	64
O	195	196	197	198	199	200	201	202	203	204	205	206	207	208	209	210
N	58	51	43	17	111	103	93	69	63	57	50	42	24	102	92	68
O	211	212	213	214	215	215	217	218	219	220	221	222	223	224	225	226
N	62	56	49	41	30	91	82	73	67	61	55	48	40	36	253	252
O	227	228	229	230	231	232	233	234	235	236	237	238	239	240	241	242
N	254	255	256	248	249	250	251	244	245	246	247	241	242	243	238	239
O	243	244	245	246	247	248	249	250	251	252	253	254	255	256		
N	240	234	235	236	237	230	231	232	233	226	225	227	228	229		

3.3.3 *Eye metrics analyses*

Custom software written in Matlab analyzed the Eye-metric data. First, to prepare eye-metric data for analysis, artifact rejection was conducted to remove invalid portions of data for a given data type (e.g., removing blinks and associated rapid signal spikes from pupil diameter measures; removing noise or large eye movements from

microsaccade measures). The Matlab algorithm called Stublinks detected Blinks and artifacts (Greg J. Siegle, Steinhauer, Stenger, Konecky, & Carter, 2003). Data segments were flagged if no pupil was detected (due to blink or loss of signal); or if signal spikes were detected (e.g., those associated with the opening or closing of the eyelid during a blink, or those differing more than 4mm from a trial's median diameter). Segments of flagged data that lasted from 100-400 ms were labeled as blinks based on their duration (Schiffman, 2000) and used to generate the blink time-course data; other flagged segments were marked as artifacts. No marked segments were included in pupil diameter analyses.

Eye metrics (pupil diameter, blink rate, microsaccade rate) were analyzed as a function of trial type (e.g., perceived or not perceived) on a per participant basis and then averaged across participants. For each metric, a time window from 1,000 ms before the vibration to 2,500 ms following vibration onset was extracted and analyzed.

To calculate the mean pupil diameter time-course, we first baseline-corrected the data to control changes in steady-state (e.g., not event-related) pupil diameter across runs, or differences across participants. The baselining was made by subtracting the median pupil diameter from the 1,000 ms preceding the onset of the vibration on a trial by trial basis. The mean of the resulting baseline-corrected time-courses was calculated within-trial condition (e.g., perceived or not perceived) within each participant; the grand mean across participants was then calculated.

Blink rate, using the detected blinks, corresponds to the proportion of trials that had a blink occurring at a given time point (e.g., if 20 out of 100 trials had a blink occurring during time *t*, the blink rate at time *t* would be 0.2). The blink rate was calculated for each sample; without binning or baselining.

Saccades were extracted from the eye-tracking data, and the ones smaller than one degree (microsaccades) were identified using the algorithm described by Engbert and Kliegl (2003). The Microsaccade rate was calculated by identifying the number of saccades initiated inside 500 ms windows (successive windows overlapped by 250 ms). On a trial basis, the number of microsaccades initiated within a given window was tallied; this was then converted to the rate of microsaccades per second (e.g., if three microsaccades were initiated, the rate within that window would be six microsaccades/second or 6 Hz). Mean microsaccade rates were calculated across trials for each participant; these means were then used to calculate a grand mean of microsaccade rate across participants.

To calculate when pupil diameter, blink rate, and microsaccade rate significantly differ as a function of perception, we performed a bootstrap analysis. First, the grand mean of the not perceived trials was subtracted from the perceived trials for each eye metric. For each bootstrap, trials were randomly selected (with replacement) from the original dataset and given a randomly shuffled perceived or not perceived trial label. These relabeled trials were analyzed in the same manner as the original data. The resulting group-averaged time-courses from bootstrapped trials assigned to the “not perceived” group was subtracted from that of bootstrapped trials assigned to the “perceived” group. This procedure was repeated 10,000 times. The grand mean of the 10,000 bootstrapped, subtracted time-courses was then calculated. Timepoints (or bins) in the original data were considered to significantly differentiate between perceived and not perceived conditions if there was a less than 5% chance of the observation occurring in the bootstrapped data.

The two grand means (from tactile and auditory tasks) were averaged, and the perceived and not-perceived data from both modalities were put together to undergo the bootstrapping analysis.

3.4 FUNDING SOURCE

This work was supported by the Betsy and Jonathan Blattmachr Family; by the Loughridge Williams Foundation; Coordenação de Aperfeiçoamento de Pessoal de Nível Superior (CAPES) [grant numbers 88887.147295/2017-00, and 88881.186875/2018-01]; and Fundação Araucária and CAPES [grant number 88887.185226/2018-00].

3.5 RESOURCES

Experiment 1 was conducted at the Yale Child Study Center (230 S Frontage Rd, New Haven, CT 06520). Experiment 2 was conducted at the Yale Magnetic Resonance Research Center (at The Anlyan Center for Medical Research & Education, 300 Cedar Street, New Haven, CT 06520-8043)

The equipment used for the tactile task is shown in Figure 19 and described here.

Figure 19 – Tactile data collection set-up

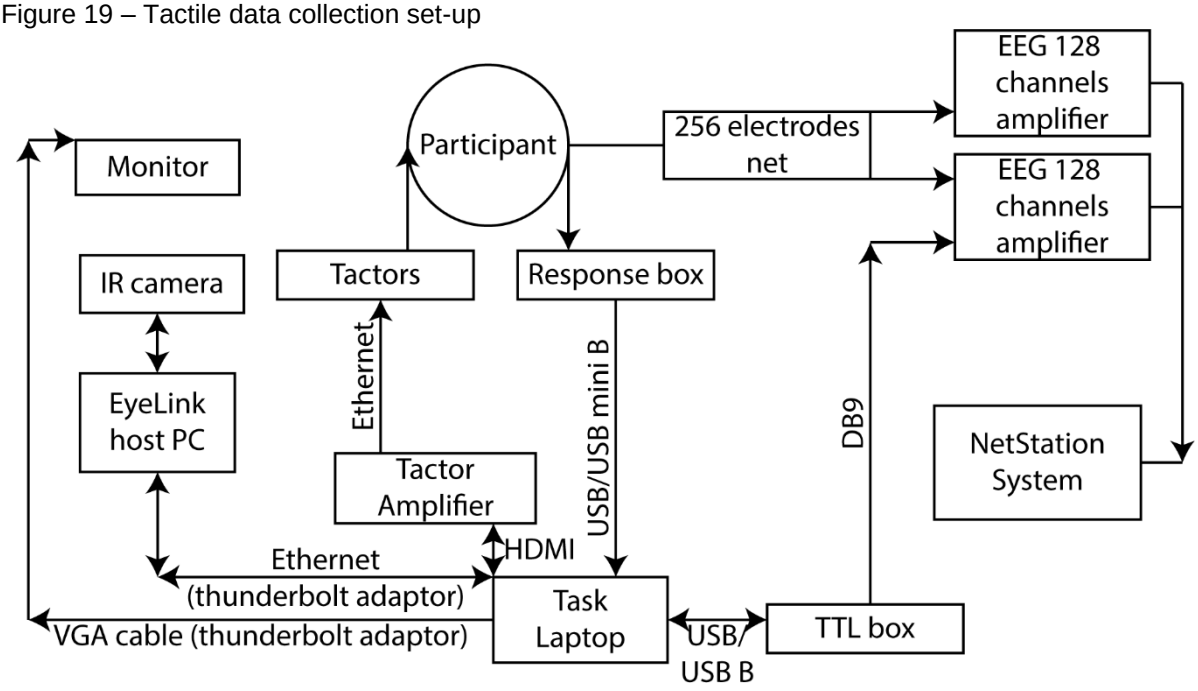

Each square represents a device, and the arrows are the cables representing their communication direction. The task laptop commands the other systems; it receives information confirming that the TTL box is connected and sends flags to it so that the data can be synchronized between the systems. Those flags are sent to one of the two 128 channels amplifiers connected to the 256 electrodes net (Figure 18), acquiring the neurons' electrical signals. The participant uses a response box with four color-coded buttons to one of their hands, and the other hand's non-thumb fingers are receiving vibration from tactors. Those tactors are activated via an audio amplifier, and for convenience, we used an ethernet cable to facilitate that connection. The amplifier is controlled by the task laptop and sends calibration information and the final file to it via an ethernet cable; it captures the eye's image and its reflection through an infrared camera (IR). Finally, the task is shown by a monitor accoupled to the IR camera (but not connected to it) that receives the images through a VGA cable (using a thunderbolt adaptor).

- For behavioral testing:
  - Cart for moving equipment (https://www.amazon.com/gp/product/B07Q6ZQT6L/ref=ppx_yo_dt_b_search_asin_title?ie=UTF8&psc=1 or similar) – *experiment 1.*
  - Amplifier: Marantz NR1609 AV Receiver https://www.amazon.com/gp/product/B07CVGRMX2/ref=ppx_yo_dt_b_search_asin_title?ie=UTF8&psc=1 (Important: if a new amplifier needs to be purchased, it needs to be an amplifier with actual "real" separate eight channels; many are "virtual" 8 channels, which carry information from other channels) – *experiment 1.*
  - HDMI cable, 1.5 m minimum – *experiment 1*.
  - MacBook with Matlab and Psychtoolbox installed – *experiment 1 and 2*:
    - macOS Sierra 10.12.6. (Newer versions are NOT compatible)
    - MATLAB r2017b. (Newer versions are compatible)
    - Psychtoolbox 3.0.15 (and its plugins). (Newer versions are compatible)
  - 4 model C2 tactors https://www.eaiinfo.com/product/c2/ – *experiment 1*

        - Representative contact as of Fall 2019: Brian Altenbernd <bAltenbernd@eaiinfo.com>.
    - Button box (Trainer 4 Button Inline - https://www.curdes.com/mainforp/electrical-trainers/otr-1x4-l.html) – *experiment 1 and 2.*
    - USB/USB mini B cable, standard length – *experiment 1 and 2*.
- For high-density scalp electroencephalography (hdEEG) – *experiment 1*:
    - Behavioral testing equipment.
    - Multi-pin Arduino with DB9 cable.
    - USB/USB B cable, standard length.
    - EEG nets.
    - Conductive gel.
    - Distilled water (for cleaning the nets).
    - Combs (for later use by the participant).
    - Makeup wipes (for participants to remove eye makeup before testing to not interfere with pupillometry).
- For pupillometry – *experiment 1 and 2*:
    - Behavioral testing equipment.
    - EyeLink® 1000 plus: For eye-tracking and pupillometry, the laboratory has an EyeLink 1000 Plus system from SR Research (Ontario, Canada) consisting of a dedicated host PC and a mounted camera with an infrared illuminator, stored on a rolling cart for maximum portability. The display, camera, and illuminator are all held in place by the EyeLink LCD hydraulic arm-mount, attached to the cart to allow for the entire eye-tracking apparatus to be easily positioned in front of the subject and moved
    - VGA/Thunderbolt adaptor.
    - Ethernet/Thunderbolt adaptor.
    - Chinrest.

3.6 SCHEDULE

For this study, the schedule in Table 6 was followed. I was able to participate in seminars and weekly meetings with other researchers of Dr. Hal Blumenfeld group.

Table 6 – Activities schedule

Year	**2016**	**2017**			**2018**			**2019**			**2020**	
Trimester/activity	**3**	**1**	**2**	**3**	**1**	**2**	**3**	**1**	**2**	**3**	**1**	**2**
Systematic literature review	X	X	X	X	X	X	X	X	X	X	X	X
French as the second foreign language	X											
Preparation for and approval on TOEFL test (107/120)				X								
Development and approval of a paper for PAHCE congress about the intellectual evaluation of non-verbal children			X	X								
Oral presentation on PAHCE about the intellectual evaluation of non-verbal children					X							
Oral presentation on PAHCE about assistive technologies in Brazil					X							
Development of evaluation plan for ETMweb software and submission to Ethics committee			X	X								
Approval by the Ethics committee					X							
Development of a plan for the international sandwich and doctoral dissertation thesis				X	X	X						
Development of an evaluation plan for ABACADA educational method for the ethics committee						X	X					
Development of virtual keyboard for Brazilian Portuguese				X	X	X						
Development and submission of a paper about the keyboard to CTBA Congress						X						
Publish of the paper as a book chapter about assistive technology							X					
Class: Rehabilitation engineering		X										
Class: Mathematics for bioscientists					X							
The exchange at Yale University							X	X	X	X	X	X
Weekly discussions about the research development with Dr. Blumenfeld							X	X	X	X	X	X
Lab meetings							X	X	X	X	X	X
Participation in seminars and conferences							X	X	X	X	X	X
Protocol creation							X	X	X			
Subjects recruitment									X	X		
Subjects examination									X	X		
Participation in GRC conference on Thalamocortical Interactions												
Data Statistical analysis										X	X	X
Results compilation, conclusions, and publication												X
Preparation of paper 1												X
Preparation of paper 2												X
Writing of the thesis									X	X	X	X

Source: the author, 2020

4 RESULTS

4.1 BEHAVIORAL RESULTS

4.1.1 Experiment 1

Participants reported feeling a vibration in 58.85% (±1.36%) of trials in which there was a vibration present; this remained relatively consistent across the two post-stimulus delays (2 s: 60.69% (±1.49%); 4 s: 56.96% (±1.61%); only two participants had significant differences in their percentage perceived as a function of post-stimulus delay (chi-square<.05)). Participants reported feeling a vibration on only 7.58% (±1.29%) of the blank trials (Figure 20A). On average, 86.11% (±0.97%) of the trials reported as perceived were also reported in the correct location (Figure 20B); 73.29% (±1.00%) of trials that were reported as not perceived were reported on the wrong finger (chance is 75%). After the Euclidean distance analysis (see Behavioral analysis), an average of 57.33 (±1.80) trials per condition were considered per participant.

Figure 20 – Tactile behavioral results.

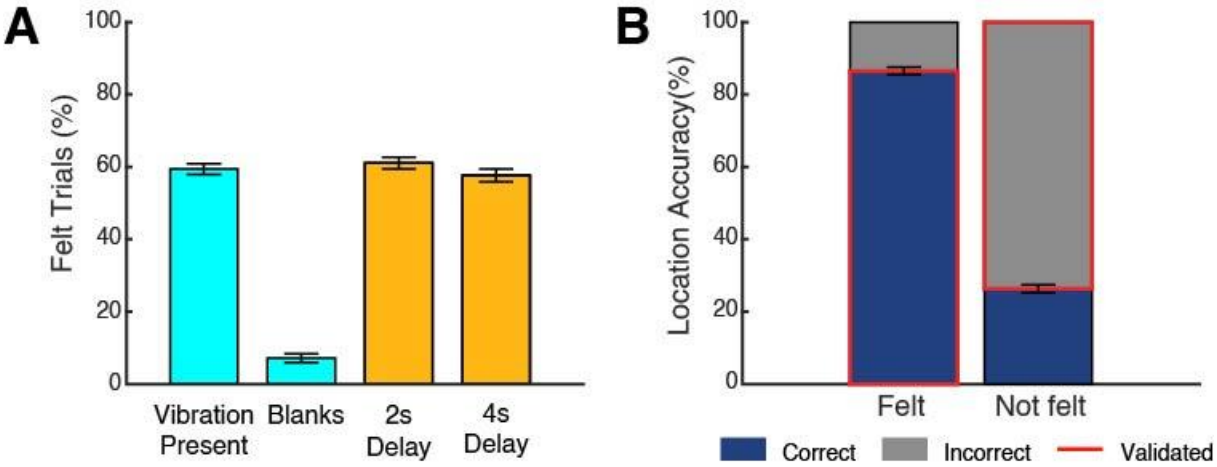

(A) Responses to perception question. In trials in which a vibration was present, 58.85% were reported as felt; in trials in which no vibration was played, only 7.58% were reported as felt. Report of vibration was approximately the same for 2 or 4 s post-stimulus delays. Error bars are SEM. (B) Responses to localization question. When vibrations were reported as felt, participants correctly reported which finger received a vibration for 86.11% of trials; when they reported they did not feel a vibration (in trials when there was a vibration present), they misreported the finger for 73.2% of trials (chance=75%). Correctly identified trials are shown in blue; incorrectly identified trials are in gray. Data considered for analysis are highlighted in red. Error bars are SEM.

4.1.2 Experiment 2

As seen in Figure 21, participants indicated that they heard a target in 57.53% (±2.32%) of trials; the false alarm rate was 6.76% (±1.46%). When participants indicated they heard a target, they had an accuracy rate of 92.17% (±1.25%). When they indicated not hearing the target, they correctly identified it in 37.81% (±2.36%) of trials (chance is 33.3%).

Figure 21 – Auditory behavioral results

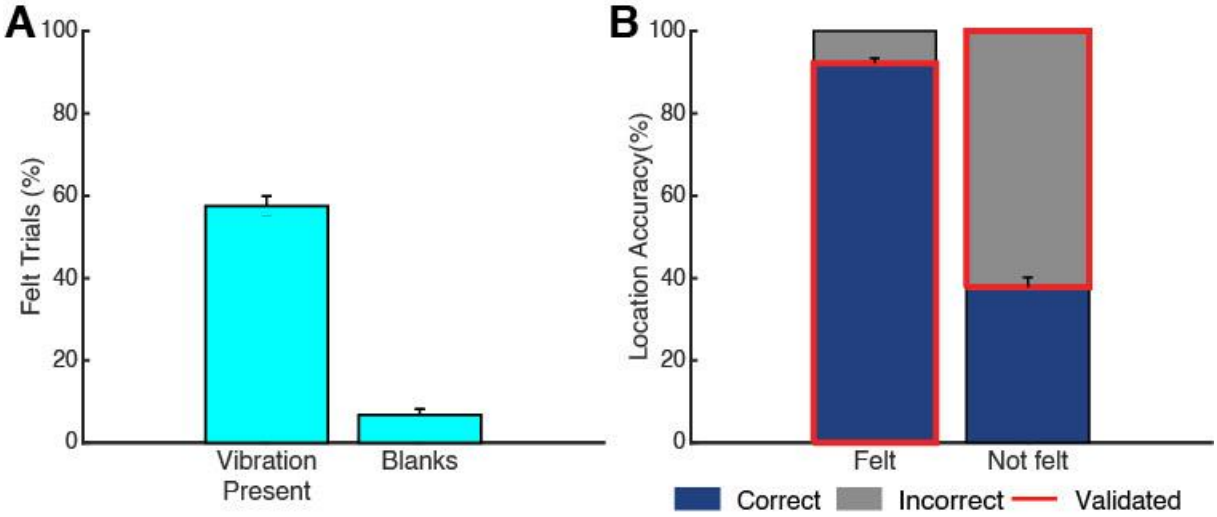

(A) Responses to perception question. In trials in which a sound was present, 57.53% were reported as heard; in trials in which no sound was played, only 6.76% were reported as heard. Error bars are SEM. (B) Responses to localization question. When sounds were reported as heard, participants correctly reported the sound's identity 92.17% of trials; when they reported they did not hear a sound (in trials when there was a sound present), they misreported the sound 62.19 % of trials (chance=66.67%). Correctly identified trials are shown in blue; incorrectly identified trials are in gray. Data considered for analysis are highlighted in red. Error bars are SEM.

4.2 EEG FILTERING PROCESS

The high-pass filter was able to filter values under 0.1 Hz, and the CleanLine procedure got rid of the 60 Hz and 120 Hz frequency, as can be seen in Figure 22.

Figure 22 – EEG before and after applying the high-pass filter and the CleanLine procedure

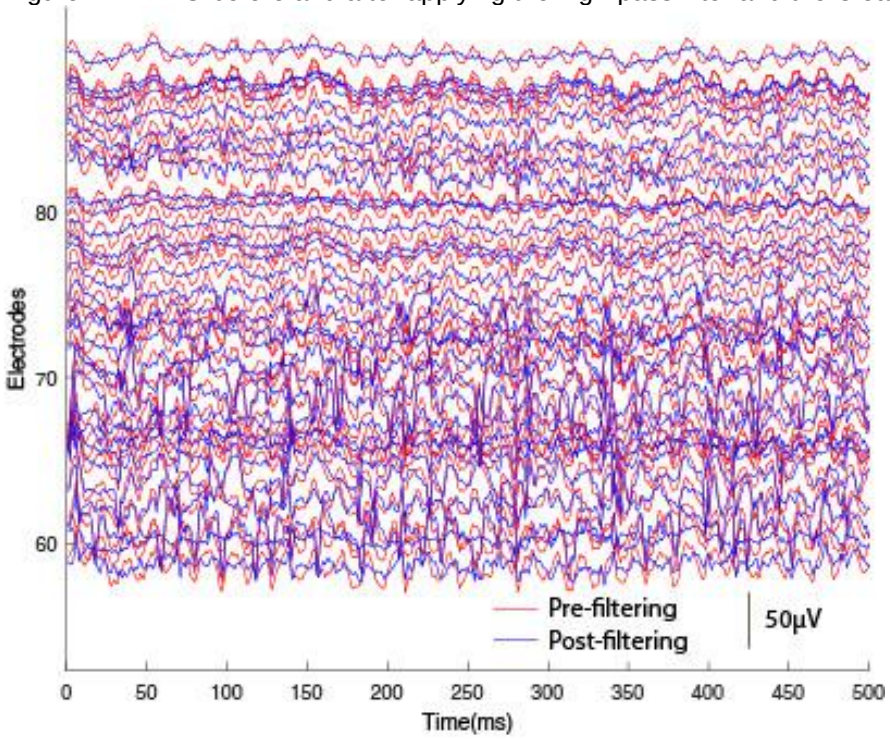

In red, the EEG timeline for 30 electrodes (60-79, see Figure 18Twenty-six adult participants were recruited to perform a behavioral task while undergoing high-density scalp electroencephalography (hdEEG) (8 participants), or hdEEG concurrent with eye-metric monitoring (16 participants). Two participants were excluded from data analysis due to poor behavioral performance (they answer with the correct finger for when reporting that they perceived for less than 60% of the time); an additional four were excluded from eye metric analysis and one from hdEEG analysis due to inadequate data collection.

for their localization). There is a 60 Hz noise. After filtering, in blue, the noise is not prominent anymore.

The high-pass 30 Hz filter identified an average of 8.1304 (±6.3697) channels per participant that were later excluded since they represent artifacts as muscles (Figure 23).

Figure 23 – 30 Hz channels flagged for deletion

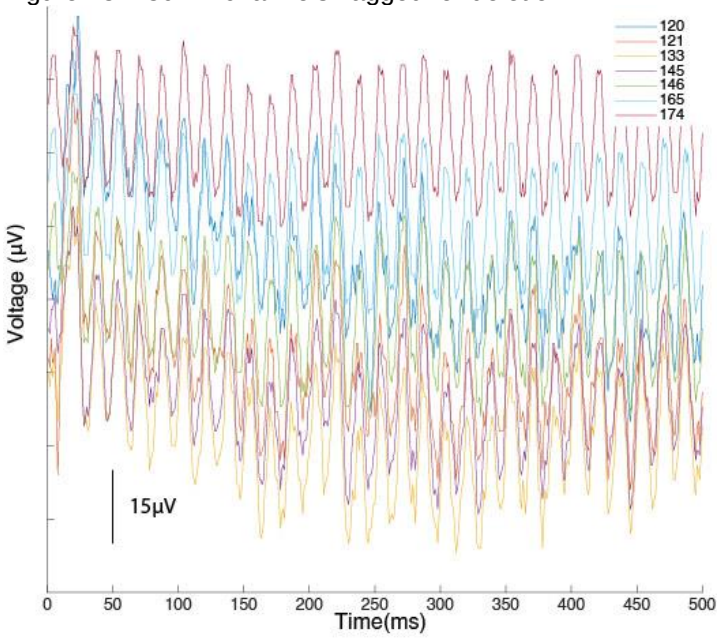

Seven channels marked for deletion because of their 30 Hz frequency. Those channels are from the same subject as Figure 22. The electrodes location corresponds to Twenty-six adult participants were recruited to perform a behavioral task while undergoing high-density scalp electroencephalography (hdEEG) (8 participants), or hdEEG concurrent with eye-metric monitoring (16 participants). Two participants were excluded from data analysis due to poor behavioral performance (they answer with the correct finger for when reporting that they perceived for less than 60% of the time); an additional four were excluded from eye metric analysis and one from hdEEG analysis due to inadequate data collection.

After cutting the epochs and deleting the channels with 30 Hz noise, the result of the spherical interpolation of the noisy channels can be seen in Figure 24. It is clear how the 30 Hz frequency is not there anymore, and how the updated channels are harmonious with their neighbors.

Figure 24 – 30 Hz electrodes after deletion and interpolation

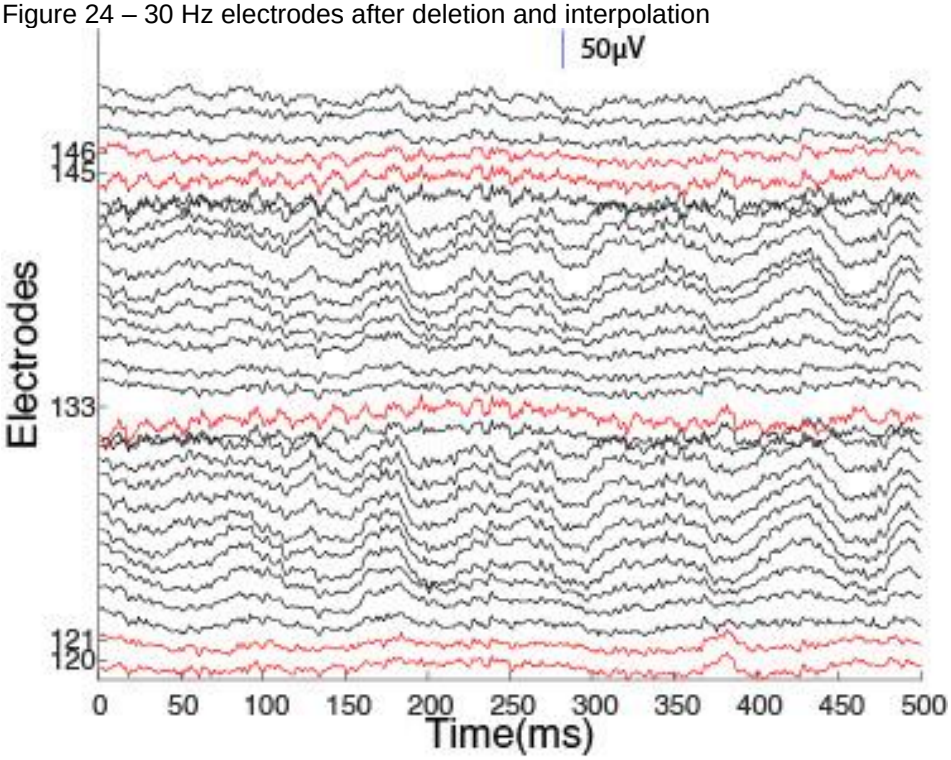

Thirty selected electrodes (120-149) from the same participant from previous figures, in black are electrodes that were not deleted, in red are the newly interpolated electrodes. See Twenty-six adult participants were recruited to perform a behavioral task while undergoing high-density scalp electroencephalography (hdEEG) (8 participants), or hdEEG concurrent with eye-metric monitoring (16 participants). Two participants were excluded from data analysis due to poor behavioral performance (they answer with the correct finger for when reporting that they perceived for less than 60% of the time); an additional four were excluded from eye metric analysis and one from hdEEG analysis due to inadequate data collection.

for electrodes position.

All the perceived and not perceived data were analyzed through PCA and ICA. The components found and the ones that were deleted are shown in Figure 25. The most common component was eyeblinks, that was present for all participants.

Figure 25 – Examples of components identified by ICA method

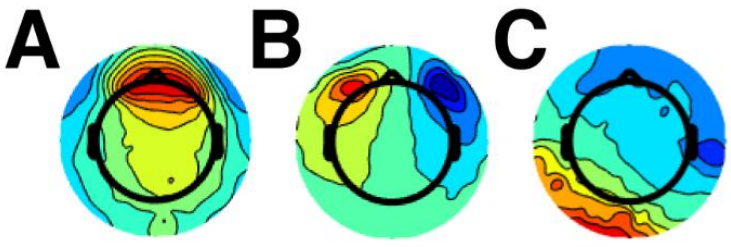

Topographic views of components analyzed. (A) represents a blink, (B) eye movements, and (C) heartbeat.

Figure 26 shows how the EEG looks like after the removal of artifacts after the ICA method.

Figure 26 – ICA deletion results

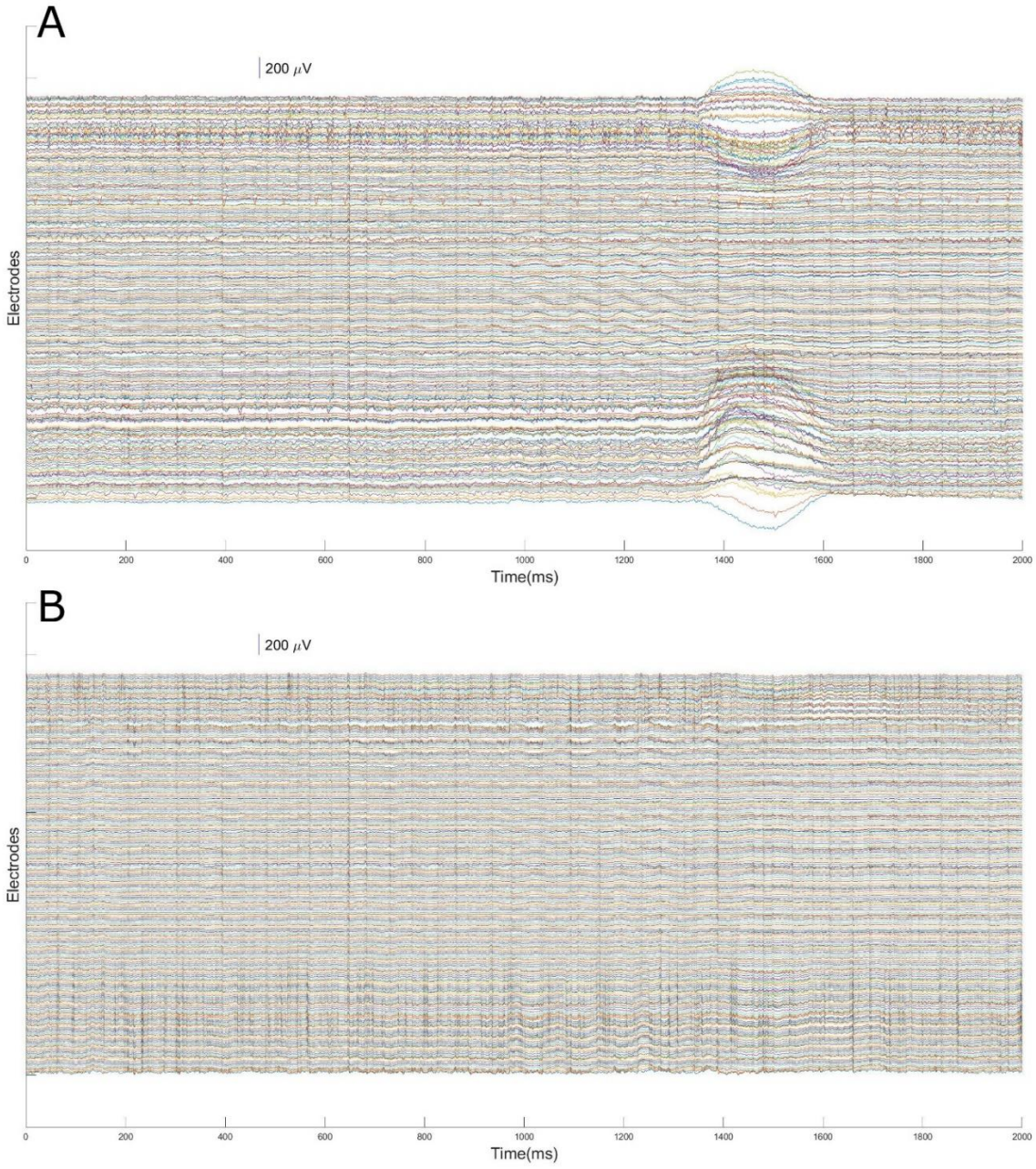

A) shows the 254 electrodes with a blink artifact at ~1,400ms, B) shows the same timeframe, now after deletion of the blink component through the ICA method

Figure 27 shows the result of the last step in processing the data. After that, the participants that received the stimuli to the left hand had their brain maps inverted with the electrodes assuming the position of their contralateral equivalent, as shown in Table 5.

Figure 27 – Data before and after 25 Hz low-pass filter

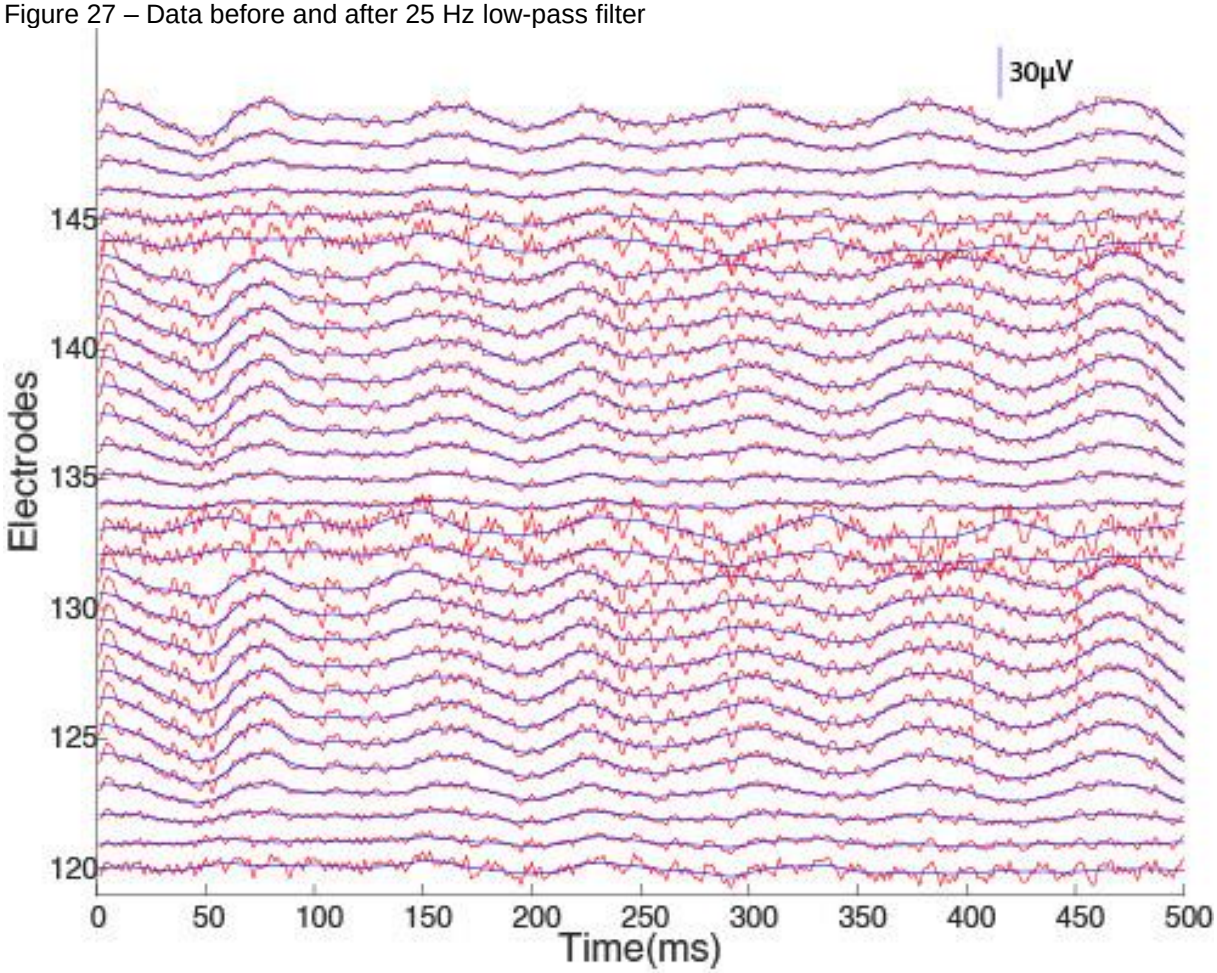

Timeline of 30 electrodes (120-154) where, in red, is the data before the 25 Hz low-pass filter, and in blue after filtering.

4.3 EVOKED POTENTIALS

FDR analyses were applied to early (0-250 ms post-stimulus) and late (250 ms post-stimulus and later) time windows to identify areas of significance (null hypothesis: voltage = 0 µV, $q<0.05$) in the grand average ERPs. For perceived trials, a significant P60 was found for contralateral (relative to hand being stimulated) parietal and occipital areas, a P100 in ipsilateral parietal areas, and P200 in bilateral occipital areas as well as contralateral parietal areas. For the not perceived condition, a significant ($q<0.05$) P100 was found bilaterally in parietal and occipital areas. A prominent N140 was observed contralaterally in frontal areas, but it only reached significance when comparing the difference between perceived and not perceived trials. Additionally, we observed earlier peaks of the P100 in not perceived trials than in perceived trials (~40

ms earlier); but there was no significant difference in magnitude of the peaks in electrodes that showed responses to both conditions (Figure 28A,

Figure 29A, also see https://youtu.be/x-x_Xkg_6Ew). Significant lateralization and the N140 were not found when data was not mirrored (i.e., when the stimulated hand was not controlled for; see Figure 30).

Figure 28 – Electrical potential difference (μV) topographic maps.

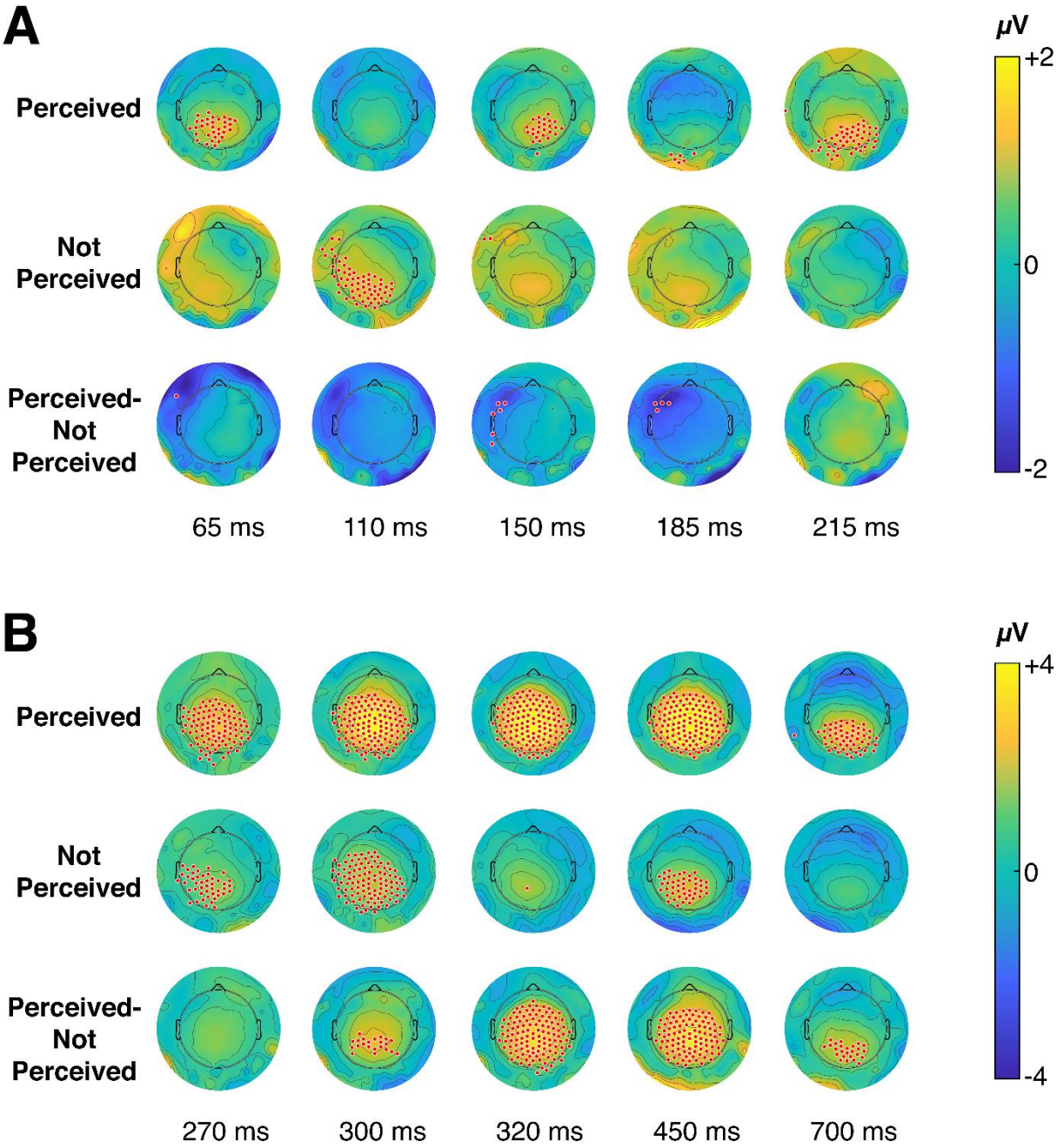

The electrical potential difference (μV) topographic maps for (**A**) early ERPs (0-215 ms post vibration), and (**B**) late ERPs (270-700 ms post vibration). Electrodes that achieve significance using an FDR analysis (null hypothesis: voltage=0 μV, $q<0.05$) are highlighted in red. Times are relative to vibration onset, and were chosen to highlight specific signals of interest.

Figure 29 – Electrical potential difference time courses.

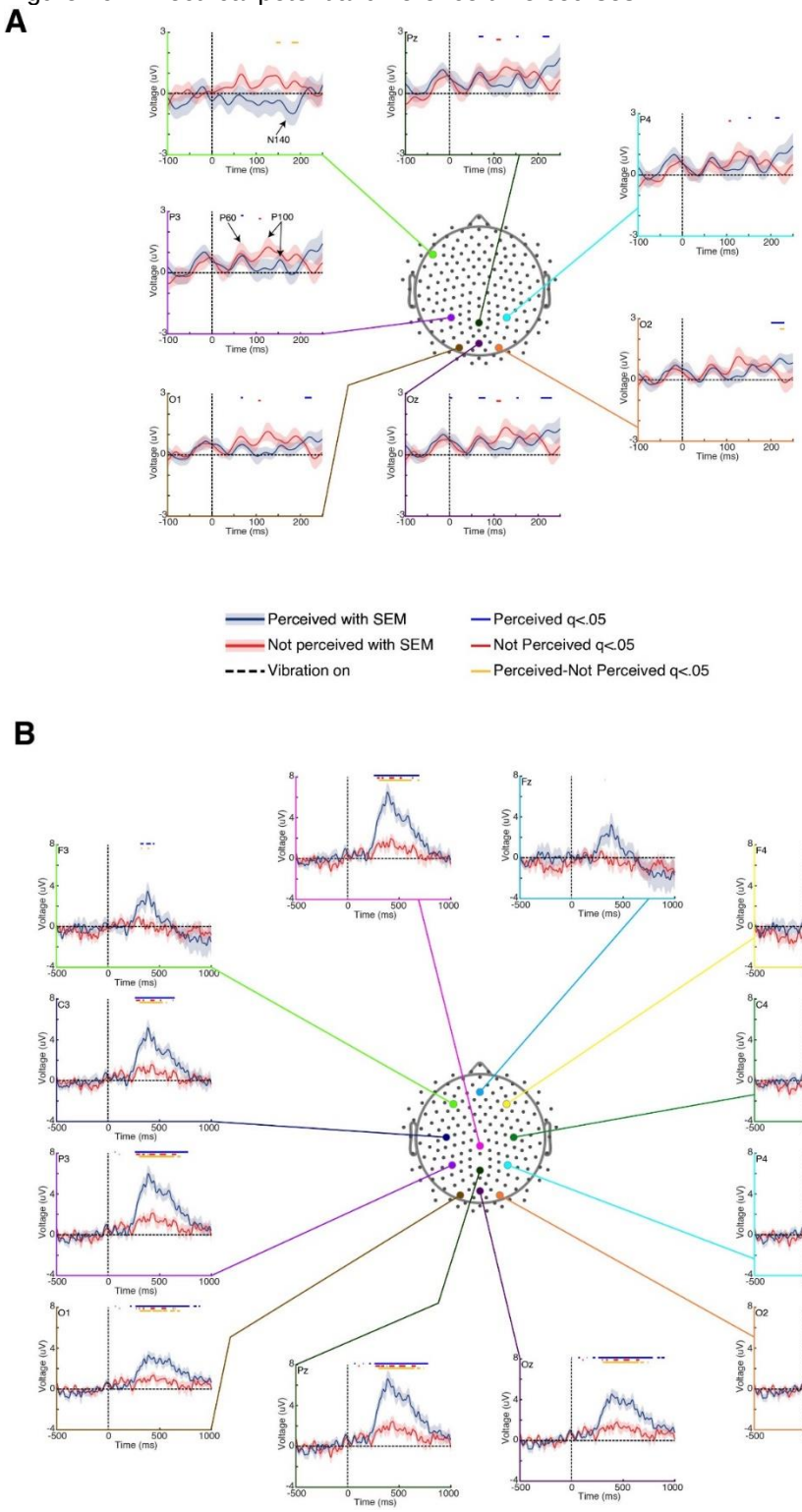

Electrical potential difference time courses of select electrodes (**A**) highlighting early changes post-vibration (-100 ms - +250 ms post-vibration onset), and (**B**) extended response (-500 ms - +1,000 ms post-vibration onset). Electrode positions are indicated via a color-matched point on the central head cartoon; axes, arrow to the electrode's position, and electrode are color-matched. Blue traces show time courses of perceived trials; red traces show time courses of not perceived trials. Shaded error bars show respective SEMs. Red, blue, and yellow lines at the top of each plot indicate windows that reached significance using FDR methods (null hypothesis: voltage=0 μV, q<0.05). Blue corresponds to significant windows in perceived data, red for not perceived data, and yellow for the perceived-not perceived data. Times are relative to the onset of vibration, represented by the dotted line.

Figure 30 – Electrical potential difference topographic maps without mirroring

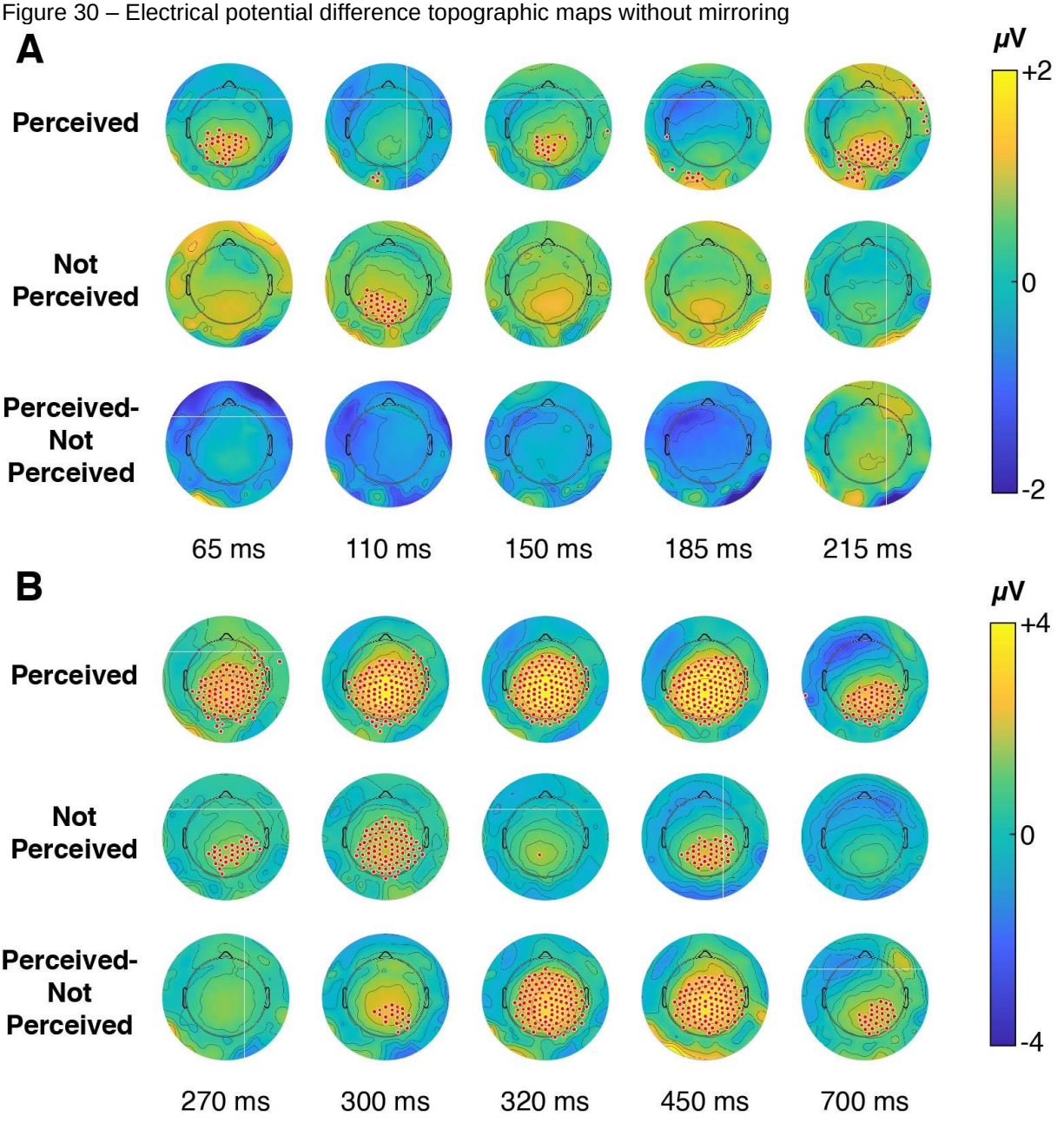

Electrical potential difference topographic maps without mirroring the maps for the participants who received the stimuli on the left hand for (**A**) early ERPs (0-215 ms post vibration), and (**B**) late ERPs (270-700 ms post vibration). Electrodes that achieve significance using an FDR analysis (null hypothesis: voltage=0 μV, $q<0.05$) are highlighted in red. Times are relative to vibration onset and were chosen to highlight specific signals of interest.

Significant P3b responses were found for both perceived and not perceived trials. For perceived trials, the P3b reached a peak at 370 ms post-vibration onset but showed significance above baseline from 255-780 ms post-vibration. Its onset is first observed in occipital and posterior parietal electrodes; the signal then spreads to central ipsilateral regions by ~270 ms post-vibration, and eventually reaches

contralateral, frontal regions by ~315 ms post-vibration. In contrast, the P3b for not perceived trials remains localized mostly to parietal and occipital regions, which spread and retract in six short waves (275-325 ms – peak: 305 ms; 330-360 ms – peak: 350 ms, 385-395 ms – peak: 390 ms; 405-455 ms – peak: 425; 500-575 ms – peak: 515 ms; 620-670 ms – peak: 630 ms) ((Figure 28B,

Figure 29B, S1).

4.4 EYE METRICS

For the tactile task, we found significant differences between perceived and not perceived conditions for pupil diameter, blink rate, and microsaccade rate. Pupil diameter increased markedly for perceived trials, peaking on average approximately 1,200 ms following a vibration. Pupil diameter was significantly different between perceived and not perceived trials from ~300 ms after vibration to the end of the analyzed epoch (2,500 ms post-vibration onset). Blink rate also increased following a vibration for perceived trials, reaching a peak rate of ~800 ms post-vibration. Blink rate differed significantly between perceived and not perceived trials for most of the period from ~500-2,300 ms post-vibration. While pupil diameter and blink rate showed an increase for perceived trials relative to not perceived trials, the microsaccade rate was suppressed in perceived trials relative to not perceived trials from ~250-750 ms post-vibration; but then significantly increased above not perceived microsaccade rate from 1250 ms post-vibration until the end of the analyzed epoch (

Figure 31A, B, and C).

For the auditory task, we also found significant differences between perceived and not perceived conditions for the three metrics. The significances are similar to the tactile ones, but there is also a significant difference for pupil diameter and microsaccades rates on the second before the stimuli onset (

Figure 31D, E, and F).

When the auditory and tactile tasks were added (

Figure 31G, H, and I), the pupil diameter increase persisted for perceived trials, as well as the differences presented on the Blink rate and microsaccade rate.

Figure 31 – Eye-Metrics' results

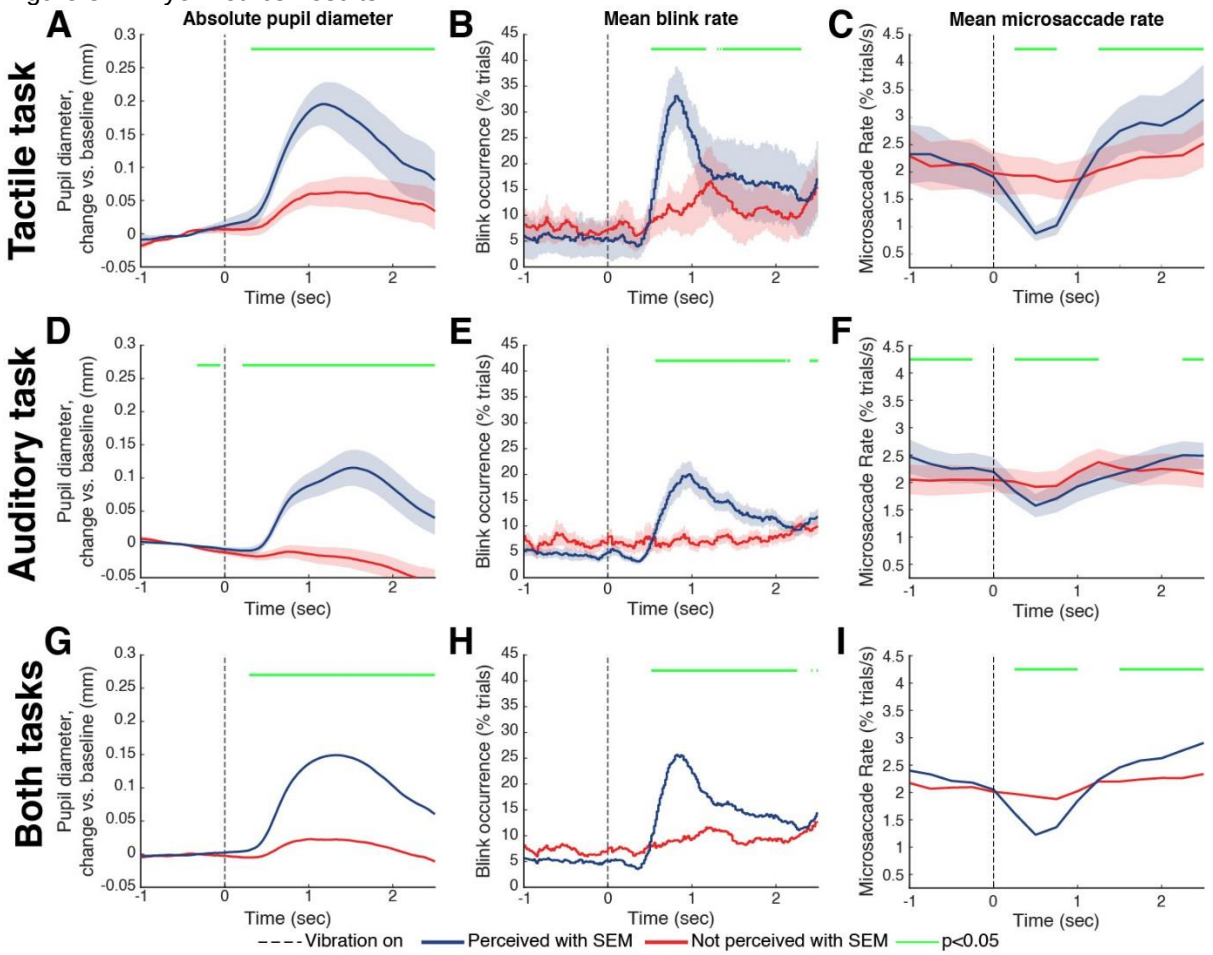

Time courses of (A, D, and G) average pupil diameter, (B, E, and H) mean percentage of trials where there is a blink occurrence; and (C, F, and I) mean microsaccade rate per second. Blue traces represent the grand mean of perceived trials; red traces represent the grand mean of not perceived trials. Shaded error bars show respective SEMs. The green line indicates times for which there is a significant difference between perceived and not perceived trials at the top of each plot. Times are relative to the onset of vibration, represented by the dotted line. A, B, and C refer to the tactile task (n = 10); D, E, and F are from the auditory task (n = 25); and G, H, and I are the combination of both tasks.

5 DISCUSSION

The design of the study was able, for the first time, to create a tactile threshold task. Having such a task allowed us to explore the conscious perception without the addition of masking stimuli, that is a stimulus itself. The use of masks or oddball paradigms can bring a confounder to the task, where it is not clear if the cause of the signal analyzed is the stimulus and the masking process. For this reason, threshold tasks have been widely used in the visual and auditory field (Eklund & Wiens, 2019; Herman et al., 2019; Wyart & Tallon-Baudry, 2008), and we were successful on bringing this modality also for the tactile field.

We chose standardized steps to do the EEG filtering and get the ERPs results. This steps proved to be efficient for having a clear signal, especially the choice of using the CleanLine protocol instead of a notch filter since the later can create a significant distortion of frequencies around the notch frequency, while the CleanLine procedure estimates and removes sinusoidal artifacts adaptively using a frequency domain regression technique with a Thompson F-statistics for identifying significant sinusoidal artifacts (Mitra, 2007; Mullen, 2012).

While doing the FDR procedure, we first had the EEG resampled for 10 Hz, but, since the fluctuations do not last long, there were not many significances found; although the permutation it was based on is very powerful, it means smaller signals were getting lost. So we resampled to 20 Hz. Although we found significances, it is essential to know that they are compared to the baseline period, and there are fluctuations within the signal that this method may not pick up on (Benjamini & Hochberg, 1995).

The ERP findings are not without precedent. Perhaps the best-documented perception-related ERPs are the components of the P300, in particular, the P3b. In the present study, we interpret the positivity present at approximately 300 ms post-vibration onset to be the P3b—a signal that has been variously attributed to the allocation of attentional resources (Donchin & Coles, 1988; Muñoz et al., 2014), awareness and conscious perception, or with a perceptual report or post-perceptual processing (Cohen, Ortego, Kyroudis, & Pitts, 2020; Dehaene & Changeux, 2011; Del Cul, Baillet, & Dehaene, 2007b; M. A. Pitts et al., 2014). Although it has historically been considered a marker of consciousness, multiple papers using different paradigms have more recently shown that the P3b is not present in the absence of perceptual

report or when a suprathreshold stimulus is not task-relevant (Cohen et al., 2020; Derda et al., 2019; Michael A Pitts et al., 2014; M. A. Pitts et al., 2014; Polich, 2007; Railo et al., 2011; Ye et al., 2019). Our task does require perceptual reports—even in the absence of a vibration or perception. It is interesting to note that we observe a P3b in both perceived and not perceived trials. However, the amplitude and spatial extent of the P3b is higher for perceived trials; indeed, the signal designated as the P3b for not perceived trials stays posterior and seems to oscillate multiple times before petering out. Polich (2007) suggested that the P300 (and its parts P3a and P3b) may represent the activity of a circuit involving perceptual, memory, and higher-level processing components. We propose that the fluctuations we observe in the not perceived trials may represent a signal that has been, for some reason, gated and is unable to propagate to frontal and association cortices fully, perhaps thus rendering it not perceived.

The other signals we observed also have precedence in perception literature. Previous studies have shown the P50, P100, and N140 concerning perceived or salient stimuli; these signals were more robust in the absence of masking or surrounding stimuli (Forschack, Nierhaus, Muller, & Villringer, 2020; Kida et al., 2006; Schubert et al., 2006). Schubert et al. (2006) suggest that the P100 marks the emergence of perception for a tactile stimulus. Because we find a P100 for both perceived and not perceived trials (with no significant difference in amplitude; though, notably, the latency of the peak P100 was approximately 40 ms later for perceived trials than for not perceived trials), our data is inconsistent with the attribution of the P100 as merely a marker of perceptual status. The fact that our data shows a P100 also in the not-perceived condition may be related to the fact that ours is the first task to not use any kind of masking – a well know confounder and signal addition – neither a background noise, making the stimuli deliverance cleaner, resulting in a more reliable expression of conscious perception.

The frontal N140 we observe when comparing the difference in signals between perceived and not perceived trials is consistent with the N140 relating to perceived stimuli; it reiterates what Forschack et al. (2020) say is a marker of perception, although their negative findings are more central than ours. The first positivity unique to perceived trials was the P200, observed in the parietal and occipital regions. Previous somatosensory tasks have associated the P200 with the need of complex cognitive functioning (Kida et al., 2006; Montoya & Sitges, 2006) or with nociperception or

evaluation of pain when using painful stimuli (Buchgreitz et al., 2008; Douros et al., 1994; Egsgaard et al., 2012; Truini et al., 2004). Our findings are consistent with the association of P200 with perception in an attention-demanding task. While previous works as Schubert et al. (2006) state that the first correlate to consciousness is the P100, we believe that N140 and P200 are the real first two indicators of conscious perception.

Although eye metrics – especially pupil diameter – are widely studied as a covert measure of visual and auditory perception (Aston-Jones & Cohen, 2005; Otero-Millan, Macknik, Serra, Leigh, & Martinez-Conde, 2011; Quirins et al., 2018; Zekveld, Koelewijn, & Kramer, 2018), studies are still scarce on the tactile field. The findings of this study corroborate with not-threshold tactile studies that have associate pupil dilation to perception (Lee & Margolis, 2016; Mückschel, Ziemssen, & Beste, 2020). We agree with van Hooijdonk et al. (2019) and Bertheaux et al. (2020) that pupil dilation occurs independently of emotional involvement. However, they have opposite opinions on the influence of emotions on pupil diameter – van Hooijdonk et al. (2019) found no relation between pupil diameter and affective touch, while Bertheaux et al. (2020) found that it was related to the pleasantness of the textures presented to the participant. Independently of the emotional factor that may be linked to tactile perception, through this study, it is evident that the arousal of the stimulus itself is enough to activate the sympathetic system, and therefore cause pupil dilation. The fact that the pupil dilation results were mainly replicated on the auditory task led us to belive that the pupil dynamics are linked to arousal states rather than a stimulus modality or being a reflex to a painful stimulus (Bala, Whitchurch, & Takahashi, 2020; Quirins et al., 2018).

We could not find studies associating blink rates to tactile stimuli, except for reflex-induced blinks (Giffin, Katsarava, Pfundstein, Ellrich, & Kaube, 2004; Hawk & Cook, 1997; Kountouris, Fritze, Blumm, Greulich, & Gehlen, 1984; Lipp, 2002; Rossi, Vignocchi, Rossi, & Muratorio, 1989). This novel way of approaching tactile conscious perception proved that blinks are not only a mechanism for protection of the eye, activated as a reflex response to an adverse stimulus, but also that it is a correlate to arousal and cognitive demand in both perceptual modalities (auditory and tactile). This has been previously hypothesized in studies of the visual perception that have shown that blink rate is inversely related to cognitive or attentional demand: blink rate decreases with increased attention and increases when attentional or cognitive

demands are removed (Fukuda & Matsunaga, 1983; Greg J Siegle, Ichikawa, & Steinhauer, 2008). The increase in blink rate that we found immediately following a perceived vibration is consistent with these findings; once a vibration has been felt, the participant has 'achieved' their goal and no longer needs to attend to the trial carefully, as a consequence of it, there is an increase on the blink rate.

Microsaccades have being associated with visual accommodation and a necessary physiologic response so that we can process the visual world (Otero-Millan et al., 2011). Here, we show that in addition to being affected by visual paradigms, changes in microsaccade rate can be elicited by tactile and auditory perception, notably by a decrease in microsaccades after perception. This decrease in rate is consistent with a recent study from Badde et al. (2020), who reported oculomotor freezing after cue acquisition. Although our study does not use cues, both Badde et al. (2020) and our current findings are consistent with decreased involuntary eye movement after a perceived sensory event, independent of that event's modality. The changes in microsaccade before the stimulus onset on the auditory task may be explained by the fact that there were sound and image backgrounds, which could serve as a clue to the upcoming stimulus and already modulate the microsaccades.

The modulation of microsaccade production by attention and cognition – like the one we found – might be (at least partially) related to the role of microsaccades in enhancing visibility and preventing fading during cognitive tasks. That is, cognitive processes such as attention could modulate microsaccade generation to dynamically enhance or suppress low-level visual information at various points in time. This possibility is thus far unexplored (Martinez-Conde & Macknik, 2011).

Overall, our current study uses a novel tactile threshold paradigm combined with high-density scalp EEG, pupillometry, and eye-tracking. We report, for the first time using a tactile-threshold task, that ERPs often associated with perceived stimuli in other sensory domains, such as the P50, P100, N140, P200, and P3b, are elicited by perceived tactile stimuli. We note that the P3b is also elicited in our not perceived trials, further complicating the already complicated story of what the P3b may represent.

The consistency of eye metrics in perceptual tasks across sensory modalities, now also encompassing tactile and auditory perception, lends further support to the idea that eye metrics are a covert measure of electrophysiological changes associated with cognitive engagement associated changes in physiological arousal levels. This similarity of eye-metric dynamics across sensory modality and paradigms suggests the

eye metrics represent a potentially powerful and robust tool for gauging perceptual and cognitive processing in the absence of an overt perceptual report.

5.1 STUDY LIMITATIONS

Although this study broadened the vision about how conscious perception is processed on the brain, and hdEEG has a better spatial resolution than other scalp EEG, it yet does not represent a perfect spatial resolution that would only be acquired by more invasive methods. Scalp EEG also does not have access to subcortical structures that also need more invasive methods or methods that do not have an excellent temporal resolution, like functional magnetic resonance, to be evaluated. The size of the sample for pupillometry was also a limitation and should be expanded in further studies.

5.2 NEXT STEPS

From the proposed methodology, the tests performed, the results obtained, and the limitations found during the development of this research, it is possible to propose further studies for the continuity of the research, solution to some problems faced, and advancement of science and technology in this area:

1. To get better spatial resolution over cortical areas that are activated during perception, we suggest the replication of the protocol during intracranial EEG;
2. To evaluate also subcortical structures not accessible through scalp EEG, behave during tactile perception, we suggest the application of the same protocol during Deep Brain Surgery;
3. With the available data, use other analysis methods as Bayesian approaches, and also considering the false positives as well, so we can broaden the understanding of tactile conscious perception;
4. To address the “report” problem, we propose using machine learning methods to create a classifier for perception based on eye-metrics. This approach has previously been used in our lab (Kronemer et al., unpublished) on a visual task, and was successful in classifying perception, with an accuracy (stimulus classified as perceived that were actually perceived) of 90% and retention

(compares how many were predicted perceived – whether or not it is actually perceived – with how many trials there were that were perceived) of 65%;

5. Since the eye metrics seem to represent a potentially powerful and robust tool for gauging perceptual and cognitive processing in the absence of an overt perceptual report, it leverages these metrics to develop no-report paradigms in future studies across sensory modalities. Such studies will allow the research of consciousness in a more “pure” way since it will not have cofounder facts as the activity of memorizing the stimulus and getting ready to answer a question;
6. Using eye-metrics, we suggest testing other sensory modalities (i.e., taste, smell, and vision) to ascertain if the same patterns repeat themselves and creating a thorough understanding of how perception relates to eye metrics.

6 CONCLUSION

This study represents the first instance of a tactile-threshold task to study Event-Related Potentials (ERPs) that differ due to perceptual status. With the threshold tactile task, we were able to identify correlates on EEG with conscious perception, especially the N140 and p200, as markers of perception. Moreover, we identified an increase in pupil diameter and blink rate and a decrease in microsaccade rate following stimulus presentation, confirming the fact that they can be used as indirect correlates of tactile perception and that the changes on eye-metrics are consistent throughout the two different modalities used here (auditory and tactile).

6.1 HIGHLIGHTS

Contributions to science:

1. In methods, a new tactile task for the threshold to evaluate conscious perception was proposed and tested;
2. In this research, we have obtained novel results about neural correlates of the tactile conscious perception. These findings will serve as a springboard to compare correlates of conscious perception across multiple sensory modalities, thus catapulting our understanding of this critical element of cognition;
3. The eye-metric findings further validate these types of measures as a reflection of physiological arousal and perception, rather than visual-specific processes. This allows for the development of paradigms that use eye metrics as a measure of perception, obviating the need for perceptual reports and thus allowing the future disambiguation of neural correlates of conscious perception from those of motor planning, working memory, and others;
4. This work represents the first perceptual threshold-based tactile paradigm that will be reported in the literature. This innovative task can now be used in other recording modalities, such as ongoing and upcoming work recording the activity from single neurons in subcortical structures and oscillations in cortical structures during DBS and intracranial recordings, respectively.

Contributions to technology:

1. We created a broad eye-metrics database that will allow the development of a machine-learning classifier of consciously perceived stimuli, which can be used in various future tasks.

Contributions to health:

1. Understanding brain activity underlying normal, healthy human conscious perception - such as described in this study - may facilitate new approaches and treatments for the millions of people worldwide with abnormal perception, altered conscious state, or an inability to communicate, such as those with epilepsy, locked-in syndrome, or schizophrenia.

REFERENCES

Allison, T., McCarthy, G., & Wood, C. C. (1992). The relationship between human long-latency somatosensory evoked potentials recorded from the cortical surface and from the scalp. *Electroencephalogr Clin Neurophysiol, 84*(4), 301-314. doi: 10.1016/0168-5597(92)90082-m

Aminihajibashi, S., Hagen, T., Laeng, B., & Espeseth, T. (2020). Pupillary and behavioral markers of alerting and orienting: An individual difference approach. *Brain Cogn, 143*, 105597. doi: 10.1016/j.bandc.2020.105597

Aston-Jones, G., & Cohen, J. D. (2005). Adaptive gain and the role of the locus coeruleus–norepinephrine system in optimal performance. *Journal of Comparative Neurology, 493*(1), 99-110.

Auksztulewicz, R., & Blankenburg, F. (2013). Subjective rating of weak tactile stimuli is parametrically encoded in event-related potentials. *J Neurosci, 33*(29), 11878-11887. doi: 10.1523/JNEUROSCI.4243-12.2013

Babiloni, C., Babiloni, F., Carducci, F., Cincotti, F., Rosciarelli, F., Rossini, P., . . . Chen, A. (2001). Mapping of early and late human somatosensory evoked brain potentials to phasic galvanic painful stimulation. *Hum Brain Mapp, 12*(3), 168-179. doi: 10.1002/1097-0193(200103)12:3<168::aid-hbm1013>3.0.co;2-o

Badde, S., Myers, C. F., Yuval-Greenberg, S., & Carrasco, M. (2020). Oculomotor freezing reflects tactile temporal expectation and aids tactile perception. *bioRxiv*, 2020.2004.2027.064899. doi: 10.1101/2020.04.27.064899

Bagshaw, A. P., & Khalsa, S. (2013). Functional Brain Imaging and Consciousness (pp. 37-48). Berlin, Heidelberg: Springer Berlin Heidelberg.

Bala, A. D. S., Whitchurch, E. A., & Takahashi, T. T. (2020). Human Auditory Detection and Discrimination Measured with the Pupil Dilation Response. *J Assoc Res Otolaryngol, 21*(1), 43-59. doi: 10.1007/s10162-019-00739-x

Baldauf, D., & Desimone, R. (2014). Neural mechanisms of object-based attention. *Science, 344*(6182), 424-427. doi: 10.1126/science.1247003

Ballesteros, S., Munoz, F., Sebastian, M., Garcia, B., & Reales, J. M. (2009). *ERP evidence of tactile texture processing: Effects of roughness and movement.* Paper presented at the World Haptics 2009-Third Joint EuroHaptics conference and Symposium on Haptic Interfaces for Virtual Environment and Teleoperator Systems.

Bayne, T., & Hohwy, J. (2013). Consciousness: Theoretical Approaches (pp. 23-35). Berlin, Heidelberg: Springer Berlin Heidelberg.

Benjamini, Y., & Hochberg, Y. (1995). Controlling the false discovery rate: a practical and powerful approach to multiple testing. *Journal of the Royal statistical society: series B (Methodological), 57*(1), 289-300 %@ 0035-9246.

Berrios, G. E. (2018). Historical epistemology of the body-mind interaction in psychiatry. *Dialogues Clin Neurosci, 20*(1), 5-13.

Bertheaux, C., Toscano, R., Fortunier, R., Roux, J. C., Charier, D., & Borg, C. (2020). Emotion Measurements Through the Touch of Materials Surfaces. *Front Hum Neurosci, 13*, 455. doi: 10.3389/fnhum.2019.00455

Bhatnagar, S. C. (2002). *Neuroscience: for the study of communicative disorders* (2nd ed.). Philadelphia: Lippincott Williams & Wilkins.

Blumenfeld, H. (2014). A master switch for consciousness? *Epilepsy Behav, 37*, 234-235. doi: 10.1016/j.yebeh.2014.07.008

Bonhomme, V., Boveroux, P., & Brichant, J. F. (2013). Anesthesia (pp. 183-203). Berlin, Heidelberg: Springer Berlin Heidelberg.

Brainard, D. H. (1997). The psychophysics toolbox. *Spatial vision, 10*(4), 433-436 %@ 0169-1015.

Broca, P. (2011). Remarks on the seat of spoken language, followed by a case of Aphasia (1861). *Neuropsychology Review, 21*(3), 227.

Bruno, N. (2018). Perception
a multisensory perspective. In F. Pavani (Ed.), (First edition. ed., pp. 1 online resource :). Oxford :: Oxford University Press.

Buchgreitz, L., Egsgaard, L. L., Jensen, R., Arendt-Nielsen, L., & Bendtsen, L. (2008). Abnormal pain processing in chronic tension-type headache: a high-density EEG brain mapping study. *Brain, 131*(Pt 12), 3232-3238. doi: 10.1093/brain/awn199

Christison-Lagay, K. L., Micek, C., Kronemer, S. I., Forman, M., Aksen, M., Abdel-Aty, A., . . . Blumenfeld, H. (2018). *Investigating auditory conscious perception with a threshold task and intracratial EEG*. Paper presented at the Neuroscience 2018, San Diego, CA. Abstract retrieved from https://www.abstractsonline.com/pp8/#!/4649/presentation/5352

Cohen, M. A., Ortego, K., Kyroudis, A., & Pitts, M. (2020). Distinguishing the Neural Correlates of Perceptual Awareness and Postperceptual Processing. *The Journal of Neuroscience, 40*(25), 4925-4935. doi: 10.1523/jneurosci.0120-20.2020

Colder, B. W., & Tanenbaum, L. (1999). Dissociation of fMRI activation and awareness in auditory perception task. *Brain Res Cogn Brain Res, 8*(3), 177-184. doi: 10.1016/s0926-6410(99)00015-4

Cornelissen, F. W., Peters, E. M., & Palmer, J. (2002). The Eyelink Toolbox: eye tracking with MATLAB and the Psychophysics Toolbox. *Behavior Research Methods, Instruments, & Computers, 34*(4), 613-617 %@ 0743-3808.

Dalmaso, M., Castelli, L., Scatturin, P., & Galfano, G. (2017). Working memory load modulates microsaccadic rate. *Journal of Vision, 17*(3), 6-6. doi: 10.1167/17.3.6

Dehaene, S., & Changeux, J.-P. (2011). Experimental and Theoretical Approaches to Conscious Processing. *Neuron, 70*(2), 200-227. doi: https://doi.org/10.1016/j.neuron.2011.03.018

Del Cul, A., Baillet, S., & Dehaene, S. (2007a). Brain dynamics underlying the nonlinear threshold for access to consciousness. *PLoS Biol, 5*(10), e260.

Del Cul, A., Baillet, S., & Dehaene, S. (2007b). Brain dynamics underlying the nonlinear threshold for access to consciousness. *PLoS biology, 5*(10).

Delorme, A., & Makeig, S. (2004). EEGLAB: an open source toolbox for analysis of single-trial EEG dynamics including independent component analysis. *J Neurosci Methods, 134*(1), 9-21. doi: 10.1016/j.jneumeth.2003.10.009

Delorme, A., Sejnowski, T., & Makeig, S. (2007). Enhanced detection of artifacts in EEG data using higher-order statistics and independent component analysis. *Neuroimage, 34*(4), 1443-1449. doi: 10.1016/j.neuroimage.2006.11.004

Derda, M., Koculak, M., Windey, B., Gociewicz, K., Wierzchoń, M., Cleeremans, A., & Binder, M. (2019). The role of levels of processing in disentangling the ERP signatures of conscious visual processing. *Consciousness and cognition, 73*, 102767.

Dixon, M. L., Thiruchselvam, R., Todd, R., & Christoff, K. (2017). Emotion and the prefrontal cortex: An integrative review. *Psychol Bull, 143*(10), 1033-1081. doi: 10.1037/bul0000096

Donchin, E., & Coles, M. G. (1988). Is the P300 component a manifestation of context updating? *Behavioral and brain sciences, 11*(3), 357-374.

Douros, C., Karrer, R., & Rosenfeld, J. P. (1994). The self-regulation of slow potential shifts and evoked potentials: interrelationships in response to somatosensory stimulation. *Int J Psychophysiol, 16*(1), 69-80. doi: 10.1016/0167-8760(94)90043-4

Dudai, Y., Karni, A., & Born, J. (2015). The Consolidation and Transformation of Memory. *Neuron, 88*(1), 20-32. doi: 10.1016/j.neuron.2015.09.004

Eccles, J. (1982). Sir Karl Popper. *Arch Psychiatr Nervenkr (1970), 232*(1), 1-3. doi: 10.1007/BF00343359

Eckstein, M. K., Guerra-Carrillo, B., Singley, A. T. M., & Bunge, S. A. (2017). Beyond eye gaze: What else can eyetracking reveal about cognition and cognitive development? *Developmental cognitive neuroscience, 25*, 69-91.

Egsgaard, L. L., Buchgreitz, L., Wang, L., Bendtsen, L., Jensen, R., & Arendt-Nielsen, L. (2012). Short-term cortical plasticity induced by conditioning pain modulation. *Exp Brain Res, 216*(1), 91-101. doi: 10.1007/s00221-011-2913-7

Eimer, M., Forster, B., & Van Velzen, J. (2003). Anterior and posterior attentional control systems use different spatial reference frames: ERP evidence from covert tactile-spatial orienting. *Psychophysiology, 40*(6), 924-933. doi: 10.1111/1469-8986.00110

Einhauser, W., Koch, C., & Carter, O. (2010). Pupil dilation betrays the timing of decisions. *Frontiers in Human Neuroscience, 4*(18). doi: 10.3389/fnhum.2010.00018

Eklund, R., & Wiens, S. (2019). Auditory awareness negativity is an electrophysiological correlate of awareness in an auditory threshold task. *Consciousness and cognition, 71*, 70-78.

Emerson, R. G., & Pedley, T. A. (2011). Eletroencefalografia e potenciais evocados. In L. P. Rowland & T. A. Pedley (Eds.), *Merritt: tratado de neurologia 2* (12 ed., Vol. 2). Rio de Janeiro: Guanabara Koogan.

Engbert, R., & Kliegl, R. (2003). Microsaccades uncover the orientation of covert attention. *Vision research, 43*(9), 1035-1045 %@ 0042-6989.

Fell, J., Dietl, T., Grunwald, T., Kurthen, M., Klaver, P., Trautner, P., . . . Fernandez, G. (2004). Neural bases of cognitive ERPs: more than phase reset. *J Cogn Neurosci, 16*(9), 1595-1604. doi: 10.1162/0898929042568514

Feyissa, A. M., & Tatum, W. O. (2019). Adult EEG. *Handb Clin Neurol, 160*, 103-124. doi: 10.1016/B978-0-444-64032-1.00007-2

Forschack, N., Nierhaus, T., Muller, M. M., & Villringer, A. (2020). Dissociable neural correlates of stimulation intensity and detection in somatosensation. *Neuroimage, 217*, 116908. doi: 10.1016/j.neuroimage.2020.116908

Fries, P., Reynolds, J. H., Rorie, A. E., & Desimone, R. (2001). Modulation of oscillatory neuronal synchronization by selective visual attention. *Science, 291*(5508), 1560-1563. doi: 10.1126/science.1055465

Fukuda, K., & Matsunaga, K. (1983). Changes in blink rate during signal discrimination tasks. *Japanese Psychological Research, 25*(3), 140-146.

Furman, M., & Blumenfeld, H. (2013). Temporal Lobe Seizures (pp. 51-62). Berlin, Heidelberg: Springer Berlin Heidelberg.

Gaillard, R., Dehaene, S., Adam, C., Clémenceau, S., Hasboun, D., Baulac, M., . . . Naccache, L. (2009). Converging intracranial markers of conscious access. *PLoS biology, 7*(3).

Gall, F. J. (1825). *Sur les fonctions du cerveau et sur celles de chacune de ses parties: avec des observations sur la possibilité de reconnnaitre les instincts, les penchans... des hommes et des animaux, par la configuration de leur cerveau*

et de leur tête. Organologie, ou exposition des instincts... et du siége de leurs organes (Vol. 5): Chez J.-B. Baillière.

Gallace, A., & Spence, C. (2008). The cognitive and neural correlates of "tactile consciousness": a multisensory perspective. *Conscious Cogn, 17*(1), 370-407. doi: 10.1016/j.concog.2007.01.005

Genna, C., Oddo, C., Fanciullacci, C., Chisari, C., Micera, S., & Artoni, F. (2018). Bilateral cortical representation of tactile roughness. *Brain Res, 1699*, 79-88. doi: 10.1016/j.brainres.2018.06.014

Giffin, N. J., Katsarava, Z., Pfundstein, A., Ellrich, J., & Kaube, H. (2004). The effect of multiple stimuli on the modulation of the 'nociceptive' blink reflex. *Pain, 108*(1-2), 124-128. doi: 10.1016/j.pain.2003.12.014

Granholm, E., & Steinhauer, S. R. (2004). Pupillometric measures of cognitive and emotional processes. *International Journal of Psychophysiology, 52*(1), 1-6. doi: 10.1016/j.ijpsycho.2003.12.001

Groppe, D. M., Urbach, T. P., & Kutas, M. (2011). Mass univariate analysis of event-related brain potentials/fields I: A critical tutorial review. *Psychophysiology, 48*(12), 1711-1725 %@ 0048-5772.

Hawk, L. W., & Cook, E. W., 3rd. (1997). Affective modulation of tactile startle. *Psychophysiology, 34*(1), 23-31. doi: 10.1111/j.1469-8986.1997.tb02412.x

Hendry, S., & Hsiao, S. (2013). Chapter 24 - The Somatosensory System. In L. R. Squire, D. Berg, F. E. Bloom, S. du Lac, A. Ghosh, & N. C. Spitzer (Eds.), *Fundamental Neuroscience (Fourth Edition)* (pp. 531-551). San Diego: Academic Press.

Herman, W. X., Smith, R. E., Kronemer, S. I., Watsky, R. E., Chen, W. C., Gober, L. M., . . . Horien, C. L. (2019). A switch and wave of neuronal activity in the cerebral cortex during the first second of conscious perception. *Cerebral Cortex, 29*(2), 461-474.

Hesselmann, G. (2013). Dissecting visual awareness with FMRI. *Neuroscientist, 19*(5), 495-508. doi: 10.1177/1073858413485988

Holmqvist, K., Nyström, M., Andersson, R., Dewhurst, R., Jarodzka, H., & Van de Weijer, J. (2011). *Eye tracking: A comprehensive guide to methods and measures*: OUP Oxford.

Hyder, F., Herman, P., Sanganahalli, B. G., Coman, D., Blumenfeld, H., & Rothman, D. L. (2011). Role of ongoing, intrinsic activity of neuronal populations for quantitative neuroimaging of functional magnetic resonance imaging-based networks. *Brain Connect, 1*(3), 185-193. doi: 10.1089/brain.2011.0032

Jervis, B. W., Nichols, M. J., Johnson, T. E., Allen, E., & Hudson, N. R. (1983). A fundamental investigation of the composition of auditory evoked potentials. *IEEE Trans Biomed Eng, 30*(1), 43-50. doi: 10.1109/tbme.1983.325165

Juravle, G., Heed, T., Spence, C., & Roder, B. (2016). Neural correlates of tactile perception during pre-, peri-, and post-movement. *Exp Brain Res, 234*(5), 1293-1305. doi: 10.1007/s00221-016-4589-5

Kang, O., & Wheatley, T. (2015). Pupil dilation patterns reflect the contents of consciousness. *Consciousness and cognition, 35*, 128-135.

Kida, T., Wasaka, T., Nakata, H., Akatsuka, K., & Kakigi, R. (2006). Active attention modulates passive attention-related neural responses to sudden somatosensory input against a silent background. *Exp Brain Res, 175*(4), 609-617. doi: 10.1007/s00221-006-0578-4

Kleiner, M., Brainard, D., & Pelli, D. (2007). What's new in Psychtoolbox-3? *Perception, 36*(14), 1-16.

Koch, C., & Laurent, G. (1999). Complexity and the nervous system. *Science, 284*(5411), 96-98.

Koivisto, M., Grassini, S., Salminen-Vaparanta, N., & Revonsuo, A. (2017). Different electrophysiological correlates of visual awareness for detection and identification. *Journal of Cognitive Neuroscience, 29*(9), 1621-1631.

Koivisto, M., Salminen-Vaparanta, N., Grassini, S., & Revonsuo, A. (2016). Subjective visual awareness emerges prior to P3. *European Journal of Neuroscience, 43*(12), 1601-1611.

Kountouris, D., Fritze, J., Blumm, R., Greulich, W., & Gehlen, W. (1984). Blink reflex and trigeminal nerve somatosensory evoked potentials: essentials in vascular brainstem diseases. *Monogr Neural Sci, 11*, 222-228. doi: 10.1159/000409215

Ku, Y., Ohara, S., Wang, L., Lenz, F. A., Hsiao, S. S., Bodner, M., . . . Zhou, Y. D. (2007). Prefrontal cortex and somatosensory cortex in tactile crossmodal association: an independent component analysis of ERP recordings. *PLoS One, 2*(8), e771. doi: 10.1371/journal.pone.0000771

Laeng, B., & Endestad, T. (2012). Bright illusions reduce the eye's pupil. *Proceedings of the National Academy of Sciences, 109*(6), 2162-2167.

Laeng, B., Sirois, S., & Gredebäck, G. (2012). Pupillometry: A window to the preconscious? *Perspectives on Psychological Science, 7*(1), 18-27. doi: 10.1177/1745691611427305

Latash, M. L. (2012). Fundamentals of motor control (1st ed. ed., pp. xii, 352 p. :). Amsterdam ;: Elsevier/Academic Press.

Lee, C. R., & Margolis, D. J. (2016). Pupil Dynamics Reflect Behavioral Choice and Learning in a Go/NoGo Tactile Decision-Making Task in Mice. *Front Behav Neurosci, 10*, 200. doi: 10.3389/fnbeh.2016.00200

Lefèvre, B. H. (1989). *Neuropsicologia infantil*: Sarvier.

Li, C. S., Yan, P., Bergquist, K. L., & Sinha, R. (2007). Greater activation of the "default" brain regions predicts stop signal errors. *Neuroimage, 38*(3), 640-648. doi: 10.1016/j.neuroimage.2007.07.021

Li, Q., Hill, Z., & He, B. J. (2014). Spatiotemporal dissociation of brain activity underlying subjective awareness, objective performance and confidence. *Journal of Neuroscience, 34*(12), 4382-4395.

Li, W., Motelow, J. E., Zhan, Q., Hu, Y. C., Kim, R., Chen, W. C., & Blumenfeld, H. (2015). Cortical network switching: possible role of the lateral septum and cholinergic arousal. *Brain Stimul, 8*(1), 36-41. doi: 10.1016/j.brs.2014.09.003

Lipp, O. V. (2002). Anticipation of a non-aversive reaction time task facilitates the blink startle reflex. *Biol Psychol, 59*(2), 147-162. doi: 10.1016/s0301-0511(02)00003-0

Lopez-Calderon, J., & Luck, S. J. (2014). ERPLAB: an open-source toolbox for the analysis of event-related potentials. *Frontiers in Human Neuroscience, 8*, 213 %@ 1662-5161.

Lopez-Ibor, J. J., Ortiz, T., & Lopez-Ibor, M. I. (2011). Perception, experience and body identity. *Actas Esp Psiquiatr, 39 Suppl 3*, 3-118.

Lu, X., & Hu, L. (2019). Electroencephalography, Evoked Potentials, and Event-Related Potentials. In L. Hu & Z. Zhang (Eds.), *EEG Signal Processing and Feature Extraction* (pp. 23-42). Singapore: Springer Singapore.

Luna, B., Velanova, K., & Geier, C. F. (2008). Development of eye-movement control. *Brain Cogn, 68*(3), 293-308. doi: 10.1016/j.bandc.2008.08.019

Lundy-Ekman, L. (2013). Introduction to Neuroscience. In L. Lundy-Ekman (Ed.), *NEuroscience-E-Book: Fundamentals for Rehabilitation*: Elsevier Health Sciences.

Luria, A. R. (1981). *Fundamentos da neuropsicologia*. São Paulo: Editora da Universidade de São Paulo.

Luu, P., & Ferree, T. (2000). Determination of the Geodesic Sensor Nets' Average Electrode Positions and their 10-10 International Equivalents. Technical Note. 2000, Eugene, Oregon, Electrical Geodesics: Inc.

Mak, L. E., Minuzzi, L., MacQueen, G., Hall, G., Kennedy, S. H., & Milev, R. (2017). The Default Mode Network in Healthy Individuals: A Systematic Review and Meta-Analysis. *Brain Connect, 7*(1), 25-33. doi: 10.1089/brain.2016.0438

Martinez-Conde, S., & Macknik, S. L. (2011). Microsaccades. In S. P. Liversedge, I. Gilchrist, & S. Everling (Eds.), *The Oxford Handbook of Eye Movements*. Bristol, UK: The University of Bristol.

Martinez-Conde, S., Macknik, S. L., Troncoso, X. G., & Hubel, D. H. (2009). Microsaccades: a neurophysiological analysis. *Trends Neurosci, 32*(9), 463-475. doi: 10.1016/j.tins.2009.05.006

McDowell, J. E., Brown, G. G., Lazar, N., Camchong, J., Sharp, R., Krebs-Thomson, K., . . . Geyer, M. A. (2006). The neural correlates of habituation of response to startling tactile stimuli presented in a functional magnetic resonance imaging environment. *Psychiatry Research: Neuroimaging, 148*(1), 1-10.

McGlone, F., & Reilly, D. (2010). The cutaneous sensory system. *Neuroscience & Biobehavioral Reviews, 34*(2), 148-159 %@ 0149-7634.

McGonigal, A., & Bartolomei, F. (2013). Consciousness, Epilepsy and Intracranial EEG (pp. 99-114). Berlin, Heidelberg: Springer Berlin Heidelberg.

Medathati, N. V. K., Desai, R., & Hillis, J. (2020). *Towards inferring cognitive state changes from pupil size variations in real world conditions.* Paper presented at the Eye Tracking Research and Applications Symposium (ETRA).

Melloni, L., Molina, C., Pena, M., Torres, D., Singer, W., & Rodriguez, E. (2007). Synchronization of neural activity across cortical areas correlates with conscious perception. *J Neurosci, 27*(11), 2858-2865. doi: 10.1523/JNEUROSCI.4623-06.2007

Michel, M., Beck, D., Block, N., Blumenfeld, H., Brown, R., Carmel, D., . . . Yoshida, M. (2019). Opportunities and challenges for a maturing science of consciousness. *Nat Hum Behav, 3*(2), 104-107. doi: 10.1038/s41562-019-0531-8

Miller, G. (2005). What is the biological basis of consciousness? *Science, 309*(5731), 79.

Mitra, P. (2007). *Observed brain dynamics*: Oxford University Press.

Montoya, P., & Sitges, C. (2006). Affective modulation of somatosensory-evoked potentials elicited by tactile stimulation. *Brain Res, 1068*(1), 205-212. doi: 10.1016/j.brainres.2005.11.019

Mückschel, M., Ziemssen, T., & Beste, C. (2020). Properties of lower level processing modulate the actions of the norepinephrine system during response inhibition. *Biol Psychol, 152*, 107862. doi: 10.1016/j.biopsycho.2020.107862

Mullen, T. (2012). CleanLine EEGLAB plugin. *San Diego, CA: Neuroimaging Informatics Toolsand Resources Clearinghouse (NITRC)*.

Muñoz, F., Reales, J. M., Sebastián, M. Á., & Ballesteros, S. (2014). An electrophysiological study of haptic roughness: Effects of levels of texture and

stimulus uncertainty in the P300. *Brain Research, 1562*, 59-68. doi: https://doi.org/10.1016/j.brainres.2014.03.013

Nani, A., Seri, S., & Cavanna, A. E. (2013). Consciousness and Neuroscience (pp. 3-21). Berlin, Heidelberg: Springer Berlin Heidelberg.

Nicolelis, M. A. L. (2011). *Beyond Boundaries: the new neuroscience of connecting brains with machines and how it will change our lives*. New York.

Niedermeyer, E., Da Silva, F. L., Niedermeyer, E., & Lopes Da Silva, F. H. (2004). *Electroencephalography : Basic Principles, Clinical Applications, and Related Fields*. Philadelphia, UNITED STATES: Wolters Kluwer.

Otero-Millan, J., Macknik, S. L., Serra, A., Leigh, R. J., & Martinez-Conde, S. (2011). Triggering mechanisms in microsaccade and saccade generation: a novel proposal. *Annals of the New York Academy of Sciences, 1233*(1), 107-116.

Palva, S., Linkenkaer-Hansen, K., Näätänen, R., & Palva, J. M. (2005). Early neural correlates of conscious somatosensory perception. *Journal of Neuroscience, 25*(21), 5248-5258.

Pelli, D. G. (1997). The VideoToolbox software for visual psychophysics: Transforming numbers into movies. *Spatial vision, 10*(4), 437-442 %@ 0169-1015.

Pins, D., & Ffytche, D. (2003). The neural correlates of conscious vision. *Cerebral Cortex, 13*(5), 461-474.

Piquado, T., Isaacowitz, D., & Wingfield, A. (2010). Pupillometry as a measure of cognitive effort in younger and older adults. *Psychophysiology, 47*(3), 560-569.

Pitts, M. A., Metzler, S., & Hillyard, S. A. (2014). Isolating neural correlates of conscious perception from neural correlates of reporting one's perception. *Frontiers in psychology, 5*, 1078.

Pitts, M. A., Padwal, J., Fennelly, D., Martínez, A., & Hillyard, S. A. (2014). Gamma band activity and the P3 reflect post-perceptual processes, not visual awareness. *Neuroimage, 101*, 337-350. doi: 10.1016/j.neuroimage.2014.07.024

Pleger, B., & Villringer, A. (2013). The human somatosensory system: from perception to decision making. *Prog Neurobiol, 103*, 76-97. doi: 10.1016/j.pneurobio.2012.10.002

Pliszka, S. R. (2004). *Neurociência para o clínico de saúde mental*: Artmed Editora.

Polich, J. (2007). Updating P300: An integrative theory of P3a and P3b. *Clinical Neurophysiology, 118*(10), 2128-2148. doi: https://doi.org/10.1016/j.clinph.2007.04.019

Purves, D., Augustine, G. J., Fitzpatrick, D., Hall, W. C., LaMantia, A.-S., Mooney, R. D., . . . White, L. E. (2018). *Neuroscience* (6th ed.). Suberland: Sinauer Associates.

Quirins, M., Marois, C., Valente, M., Seassau, M., Weiss, N., El Karoui, I., . . . Naccache, L. (2018). Conscious processing of auditory regularities induces a pupil dilation. *Sci Rep, 8*(1), 14819. doi: 10.1038/s41598-018-33202-7

Railo, H., Koivisto, M., & Revonsuo, A. (2011). Tracking the processes behind conscious perception: a review of event-related potential correlates of visual consciousness. *Consciousness and cognition, 20*(3), 972-983.

Ranade, S. S., Syeda, R., & Patapoutian, A. (2015). Mechanically Activated Ion Channels. *Neuron, 87*(6), 1162-1179. doi: 10.1016/j.neuron.2015.08.032

Ress, D., & Heeger, D. J. (2003). Neuronal correlates of perception in early visual cortex. *Nature neuroscience, 6*(4), 414-420.

Ríco, V. V., Goulart, P. R. K., Hamasaki, E., I.M., & Tomanari, G. Y. (2012). Percepção e Atenção. In M. M. C. Hübner (Ed.), *Fundamentos da Psicologia: temas*

clássicos de psicologia sob a ótica do comportamento. Rio de Janeiro: Guanabara Koogan.

Rogers, B. J. (2017). Perception

a very short introduction (pp. 1 online resource :). [Oxford] :: Oxford University Press.

Rose, D., & Brown, D. (2015). Idealism and materialism in perception. *Perception, 44*(4), 423-435. doi: 10.1068/p7927

Rossi, B., Vignocchi, G., Rossi, A., & Muratorio, A. (1989). Comparative study of pain perception and polysynaptic blink reflex responses in man. *Funct Neurol, 4*(1), 47-51.

Ruben, J., Schwiemann, J., Deuchert, M., Meyer, R., Krause, T., Curio, G., . . . Villringer, A. (2001). Somatotopic organization of human secondary somatosensory cortex. *Cereb Cortex, 11*(5), 463-473. doi: 10.1093/cercor/11.5.463

Rubinstein, B. B. (1997). Review of the self and its brain: an argument for interactionism by Karl R. Popper and John C. Eccles (1980). *Psychol Issues*(62-63), 531-540.

Sacks, O. W. (2010). *Vendo Vozes*. São Paulo: Companhia das Letras.

Saunders, J. A., & Backus, B. T. (2006). Perception of surface slant from oriented textures. *Journal of Vision, 6*(9), 3-3 %@ 1534-7362.

Sauseng, P., Klimesch, W., Gruber, W. R., Hanslmayr, S., Freunberger, R., & Doppelmayr, M. (2007). Are event-related potential components generated by phase resetting of brain oscillations? A critical discussion. *Neuroscience, 146*(4), 1435-1444. doi: 10.1016/j.neuroscience.2007.03.014

Schiffman, H. R. (2000). *Sensation and perception : an integrated approach* (5th ed.). New York: Wiley.

Schnakers, C., Laureys, S., & Boly, M. (2013). Neuroimaging of Consciousness in the Vegetative and Minimally Conscious States (pp. 117-131). Berlin, Heidelberg: Springer Berlin Heidelberg.

Schubert, R., Blankenburg, F., Lemm, S., Villringer, A., & Curio, G. (2006). Now you feel it—now you don't: ERP correlates of somatosensory awareness. *Psychophysiology, 43*(1), 31-40.

Searle, J. R. (2004). *Mind: A brief introduction*: oxford university press.

Shim, G., Oh, J. S., Jung, W. H., Jang, J. H., Choi, C.-H., Kim, E., . . . Kwon, J. S. (2010). Altered resting-state connectivity in subjects at ultra-high risk for psychosis: an fMRI study. *Behavioral and Brain Functions, 6*(1), 58. doi: 10.1186/1744-9081-6-58

Shumway-Cook, A. (2007). Motor control

translating research into clinical practice. In M. H. Woollacott (Ed.), (3rd ed. ed., pp. x, 612 p. :). Philadelphia :: Lippincott Williams & Wilkins.

Siegel, A. (2019). Essential neuroscience. In H. N. Sapru & H. Siegel (Eds.), (Fourth edition. ed., pp. 1 online resource (1 volume (various pagings)) :). Philadelphia :: Wolters Kluwer.

Siegle, G. J., Ichikawa, N., & Steinhauer, S. (2008). Blink before and after you think: Blinks occur prior to and following cognitive load indexed by pupillary responses. *Psychophysiology, 45*(5), 679-687.

Siegle, G. J., Steinhauer, S. R., Stenger, V. A., Konecky, R., & Carter, C. S. (2003). Use of concurrent pupil dilation assessment to inform interpretation and analysis of fMRI data. *Neuroimage, 20*(1), 114-124 %@ 1053-8119.

Sirois, S., & Brisson, J. (2014). Pupillometry. *Wiley Interdisciplinary Reviews: Cognitive Science, 5*(6), 679-692. doi: 10.1002/wcs.1323

Stehno-Bittel, L. (2013a). Physical and Electrical Properties of Cells in the Nervous System. In L. Lundy-Ekman (Ed.), *Neuroscience-E-Book: Fundamentals for Rehabilitation*: Elsevier Health Sciences.

Stehno-Bittel, L. (2013b). Synapses and synaptic transmission. In L. Lundy-Ekman (Ed.), *Neuroscince-E-Book: Fundamentals for Rehabilitation*: Elsevier Health Sciences.

Tallon-Baudry, C., & Bertrand, O. (1999). Oscillatory gamma activity in humans and its role in object representation. *Trends Cogn Sci, 3*(4), 151-162. doi: 10.1016/s1364-6613(99)01299-1

Tang, W., Liu, R., Shi, Y., Hu, C., Bai, S., & Zhu, H. (2020). From finger friction to brain activation: Tactile perception of the roughness of gratings. *J Adv Res, 21*, 129-139. doi: 10.1016/j.jare.2019.11.001

Tatler, B. W., Kirtley, C., Macdonald, R. G., Mitchell, K. M., & Savage, S. W. (2014). The active eye: Perspectives on eye movement research *Current trends in eye tracking research* (pp. 3-16): Springer.

Tononi, G., Boly, M., Massimini, M., & Koch, C. (2016). Integrated information theory: from consciousness to its physical substrate. *Nat Rev Neurosci, 17*(7), 450-461. doi: 10.1038/nrn.2016.44

Truini, A., Rossi, P., Galeotti, F., Romaniello, A., Virtuoso, M., De Lena, C., . . . Cruccu, G. (2004). Excitability of the Adelta nociceptive pathways as assessed by the recovery cycle of laser evoked potentials in humans. *Exp Brain Res, 155*(1), 120-123. doi: 10.1007/s00221-003-1785-x

van Hooijdonk, R., Mathot, S., Schat, E., Spencer, H., van der Stigchel, S., & Dijkerman, H. C. (2019). Touch-induced pupil size reflects stimulus intensity, not subjective pleasantness. *Experimental Brain Research, 237*(1), 201-210. doi: 10.1007/s00221-018-5404-2

Vigotski, L. S. (1998). *Pensamento e Linguagem* (2 ed.). São Paulo: Martins Fontes.

Walz, J. M., Goldman, R. I., Carapezza, M., Muraskin, J., Brown, T. R., & Sajda, P. (2015). Prestimulus EEG alpha oscillations modulate task-related fMRI BOLD responses to auditory stimuli. *Neuroimage, 113*, 153-163. doi: 10.1016/j.neuroimage.2015.03.028

Wernicke, C. (1969). *The symptom complex of aphasia.* Paper presented at the Proceedings of the Boston Colloquium for the Philosophy of Science 1966/1968.

Wetzel, N., Buttelmann, D., Schieler, A., & Widmann, A. (2016). Infant and adult pupil dilation in response to unexpected sounds. *Dev Psychobiol, 58*(3), 382-392. doi: 10.1002/dev.21377

Wyart, V., & Tallon-Baudry, C. (2008). Neural dissociation between visual awareness and spatial attention. *Journal of Neuroscience, 28*(10), 2667-2679.

Yamaguchi, S., & Knight, R. T. (1991). P300 generation by novel somatosensory stimuli. *Electroencephalography and Clinical Neurophysiology, 78*(1), 50-55. doi: https://doi.org/10.1016/0013-4694(91)90018-Y

Ye, M., Lyu, Y., Sclodnick, B., & Sun, H.-J. (2019). The P3 reflects awareness and can be modulated by confidence. *Frontiers in neuroscience, 13*, 510.

Zekveld, A. A., Koelewijn, T., & Kramer, S. E. (2018). The Pupil Dilation Response to Auditory Stimuli : Current State of Knowledge. *22*, 1-25. doi: 10.1177/2331216518777174

Zola-Morgan, S. (1995). Localization of brain function: the legacy of Franz Joseph Gall (1758-1828). *Annu Rev Neurosci, 18*, 359-383. doi: 10.1146/annurev.ne.18.030195.002043

Appendix 1 – IRB approval

Yale

Human Research Protection Program
Institutional Review Boards
FWA00002571
25 Science Park – 3rd Fl., 150 Munson St.
New Haven CT 06520-8327

Telephone: 203-785-4688
http://www.yale.edu/hrpp

August 16, 2019

APPROVAL OF RESPONSE TO REVISIONS REQUESTED AT FULL BOARD

Modification Required Date: 8/7/2019

Final Approval Date: 8/16/2019

Expiration Date: 8/18/2020

Investigator:	Hal Blumenfeld
Type of Review:	Modification and Continuing Review
Title of Study:	Understanding Consciousness and Information Processing
IRB Protocol ID:	1107008859
Submission ID:	MODCR00004679
Committee Name:	Human Investigation Committee 1

Research activities associated with this submission are approved and may begin consistent with the terms of IRB approval.

The IRB continues to find that the research presents no more than minimal risk to subjects as per 45 CFR 46 102(i), and no greater than minimal risk in the minor subjects as per 45 CFR 46.404.

The modification updates the recruitment target, increases the payment value for participants completing the sensory awareness task from $20 to $40, adds the use of needle scalp electrodes for a subset of adult participants in the deep brain stimulation part of this study, and adds use of Yale Fitkin Memorial Pavilion EEG Laboratory as a study location. These changes result in minor changes to the consent form.

The IRB finds the modification does not affect subjects' rights or welfare or change subjects' willingness to participate in the study, therefore, reconsenting of subjects is not required.

The PI is reminded that changes to the adult consent must not be made in the Spanish version and be submitted to the IRB for approval before use.

Yale

Human Research Protection Program
Institutional Review Boards
FWA00002571
25 Science Park – 3rd Fl., 150 Munson St.
New Haven CT 06520-8327

Telephone: 203-785-4688
http://www.yale.edu/hrpp

See the next pages for important reminders and the list of IRB approved documents.

Yale

Human Research Protection Program
Institutional Review Boards
FWA00002571
25 Science Park – 3rd Fl., 150 Munson St.
New Haven CT 06520-8327

Telephone: 203-785-4688
http://www.yale.edu/hrpp

IMPORTANT REMINDERS:

- By 6/19/2020, you are to submit documentation for a continuing review.
- You can submit a request to close research (end the IRB's oversight) when:
  - The protocol is permanently closed to enrollment,
  - All subjects have completed all protocol related interventions and interactions, and
  - Analysis of private identifiable information is completed.
- Changes must be submitted with a modification and approved by the IRB prior to implementation except to eliminate immediate hazards to participants. This includes changes to study procedures, informed consent documents, recruitment activities or study personnel.
- Information that requires prompt reporting to the IRB must be done so within 5 days of the PI becoming aware of the event (see Policy 710: Reporting Unanticipated Problems Involving Risks to Subjects or Others, including Adverse Events). This includes potential serious noncompliance, continuing noncompliance, and unanticipated problems to subjects or others.
- In conducting this activity, you should refer to and follow the Investigator Manual (HRP-103) as applicable, which can be found in the IRB Library within the IRB system.

Yale

Human Research Protection Program
Institutional Review Boards
FWA00002571
25 Science Park – 3rd Fl., 150 Munson St.
New Haven CT 06520-8327

Telephone: 203-785-4688
http://www.yale.edu/hrpp

IRB REVIEW REFLECTS:

- Adult Patient Consent Form 8_11_19.pdf, Category: Consent Form;
- 1107008859 Protocol 8_11_2019.pdf, Category: IRB Protocol;
- Adolescent Patient Consent Form 4_15_2019.pdf, Category: Consent Form;
- Healthy Adult Consent Form 4_15_2019.pdf, Category: Consent Form;
- Parental Permission Form 4_15_2019.pdf, Category: Consent Form;

Please keep this letter with your copy of the approved protocol documents.

Appendix 2 – PsychStairCase pipeline

```
1 function fhndl = MinExpEntStair(mode)
2 % Minimum Expected Entropy Staircase
3 %
4 % Caution: Currently only works with Matlab, not with GNU/Octave!
5 %
6 % The staircase gives suggestions for which probe value to test next,
7 % choosing the probe that will provide the most information (based on the
8 % principle of minimum entropy = maximally unambiguous probability
9 % distribution). Probes are chosen from a set of possible probe values
10 % provided at staircase init, and their use is evaluated based on the
11 % expected amount of information gain given a space of PSE and slope values
12 % to test over.
13 %
14 % By default, a psychometric function ranging from 0% to 100% is used, as
15 % is suitable for discrimination experiments with a standard in the middle
16 % of the possible stimulus parameter range. For other paradigms, such as
17 % n-AFC detection tasks, one can set the guessrate input during staircase
18 % init to 1/num_alternatives, e.g. .5 when doing a 2IFC detection task.
19 % This guess rate is thus not the rate at which participants guess instead
20 % of do your task (thats the lapse rate), it the minimum rate of correct
21 % responses as determined by your design. NB: below discussion is based on
22 % the default psychometric function with the full range, but all points are
23 % equally valid for a scaled psychometric function.
24 %
25 % It is recommended to have the staircase determine the optimal next probe
26 % based on only a random subset of the response history (see options
27 % 'toggle_use_resp_subset' and 'toggle_use_resp_subset_prop'). This makes
28 % its operation more robust for response errors and also avoids probe
29 % oscillations when the fit estimate is converging.
30 % When we are close to convergence, probes will tend to be near the 25% and
31 % 75% points. If a probe is 25% and you answer '1' (pedestal faster, which
32 % is likely, because it's near the correct 25% point), then for the next
33 % trial the peak in expected entropy reduction will generally be the 75%
34 % point, and vice versa. This can lead to undesirable probe sequences where
35 % the correct response alternates 0,1,0,1,0,1. If you choose a random
36 % subset, this will completely eliminate the problem. If the staircase has
37 % converged to where there are two almost equal expected entropy minima,
38 % then small variations due to the selection of subsets will randomly vary
39 % which minimum emerges as lowest.
40 % This strategy does not significantly affect optimal operation of the
41 % staircase. Lots of probe values provide useful information. Therefore, it
42 % is not crucial to have a highly accurate estimate of likelihoods, so
43 % relatively few trials are sufficient (less than are needed to for final
44 % estimates of PSE and DL). Throwing out trials for the staircase
45 % computation yields robustness without much cost.
46 %
47 % Another option would be to load a non-uniform prior on the space of
48 % possible location/mean/PSE and dispersion/slope parameters (known as mu
49 % and sigma respectively for a cumulative Gaussian - see option
50 % 'loadprior'). Probe sampling will then stay reasonable in early trials
51 % even if there were a couple bad responses. But this strategy is not as
52 % robust as using a random subset -- bad trials will continue to have an
53 % effect throughout.
54 %
55 % In absence of anything to base the optimal probe value on, the first
```

```
56 % probe is chosen randomly from the set of possible probes. When a prior
57 % was loaded, a likelihood distribution is available based on which the
58 % optional probe value can be computed. If for any other reason choosing
59 % the next probe based on the measure of minimum expected entropy fails,
60 % the staircase will fall back on the same random probe sampling strategy.
61 % There is an option to set the first probe value to be tested, which, for
62 % the first trial only, will overrule both of the above probe choice
63 % strategies. This can be useful if you want to be sure that the first
64 % trial is an easy one so the participant knows what to expect.
65 %
66 % Another measure for robustness is to choose a small lapse rate. If lapse
67 % would be zero and a response error is made by the observer, immediately a
68 % whole range of mean-slope combinations becomes impossible. If lapse rate
69 % is non-zero, these would still have a non-zero probability and the
70 % staircase can rebound. Therefore a lapse rate of 5% or even more
71 % depending on task difficulty is always recommended. NB: in the default
72 % discrimination setup of the staircase (guessrate is not specified or set
73 % to 0), half of the lapse rate is taken off the bottom of the psychometric
74 % function and half is taken off the top. So if the lapse rate is 0.05, the
75 % psychometric function will range from 0.025 to 0.975. In the setup for a
76 % n-AFC detection experiment when the psychometric function has a lower
77 % bound of 1/num_alternatives, the lapse rate is taken off the top. So when
78 % the guess_rate is set to .5 (2AFC) and the pase rate is set to .05, the
79 % psychometric function will range from 0.05 to 0.95.
80 % Note that the staircase does not support a 0 lapse rate in the first
81 % place as it works with log-probability and we get in trouble if we would
82 % take the log of a 0 probability. Any lapse rate lower than 1e-10 will be
83 % adjusted to 1e-10 upon calling the 'init' function.
84 %
85 % If the staircase gets stuck at one of the bounds of the probe set, check
86 % that the sign of the slope space matches the expected sign of the
87 % response. E.g., lets look at an experiment in which you are doing 2IFC
88 % task in which the observer is asked to report which interval contained
89 % the faster motion. If the observer choses the test over the pedestal
90 % interval the response is 1, if the observer chosen the pedestal to be
91 % faster, the response is 0. All slopes in the set would in this case be
92 % positive as the low end of the probe space (slow speeds) is associated
93 % with response 0 and the high end with response 1. If we however asked the
94 % observer to indicate the slower interval, the slopes in our slope set
95 % would not match the task, and the staircase would get stuck at one of the
96 % probe bounds. In this case, the lower end of the probe space is
97 % associated with the response 1 and the higher end with the response
98 % 0--we'd thus have a negative slope for the fitted cumulative probability
99 % function.
100 %
101 % The staircase currently only supports logistic and cumulative Gaussian
102 % (default) psychometric functions (see 'set_psychometric_func'), but
103 % others could easily be implemented. Changes should be needed only to the
104 % function "fit_a_point" at the bottom of this mfile, providing that the
105 % function is characterized by two parameters (which do not necessarily
106 % have to be PSE and slope, though that is the terminology here.
107 % Should you implement such a function, please do send me your code at
108 % dcnieho @at@ gmail.com.
109 %
110 % The above discussion assumes that response inputs to 'process_resp' are
```

```
111 % either 0 or 1 (see note above about their meaning) though in practice
112 % anything larger than 0 is treated as 1 and anything lower than 0,
113 % including 0, is treated as 0. the staircase can thus easily be integrated
114 % with programs that use a 1, -1 response scheme.
115 %
116 % For actual offline fitting of your data, you would probably want to use a
117 % dedicated toolbox such as Prins, N & Kingdom, F. A. A. (2009) Palamedes:
118 % Matlab routines for analyzing psychophysical data.
119 % http://www.palamedestoolbox.org. instead of using the function parameters
120 % or PSE and DL returned from staircase functions 'get_fit' and
121 % 'get_PSE_DL'.
122 % Also note that while the staircase runs far more robust when a small
123 % lapse rate is assumed, it is common to either fit the psychometric
124 % function without a lapse rate, or otherwise with the lapse rate as a free
125 % parameter (possibily varying only over subjects, but not over conditions
126 % within each subject).
127 %
128 %
129 % References:
130 %  Based on the Minimum expected entropy staircase method developed by:
131 %  Saunders JA & Backus BT (2006). Perception of surface slant from
132 %    oriented textures. Journal of Vision 6(9), article 3
133 %
134 %  Discussions of conceptually similar staircases can be found in:
135 %  Kontsevich LL & Tyler CW (1999). Bayesian adaptive estimation of
136 %    psychometric slope and threshold. Vision Res 39(16), pp. 2729-37
137 %  Lesmes LA, Lu ZL, Baek J & Albright TD (2010). Bayesian adaptive
138 %    estimation of the contrast sensitivity function: The quick CSF method.
139 %    Journal of Vision 10(3), article 17
140 %
141 %
142 % USE:
143 % Calling this function creates a staircase instance. The interface of the
144 % staircase is accessed through the returned function handle. You can
145 % create as many instances as you like by calling this function, each
146 % instance has its own internal memory/history. In that sense this is
147 % really OO (I'm not happy with MATLAB's OO features and also want to be
148 % compatible with old versions, hence the below paradigm).
149 % When interacting with the staircase through the function handle, the
150 % first argument is a string that identifies the action you want to perform
151 % (you can think of this as the string containing the name of the member
152 % function to be called) and optionally any other arguments that are needed
153 % for the call. See MESDemo for an example and the comments below for use
154 % of the different staircase functions.
155
156 % Copyright (c) 2011 by DC Niehorster and JA Saunders
157
158 % The demo and MinExpEntStair use nested functions internally, something
159 % not supported by Octave, so this is a no-go unless somebody rewrites this
160 % stuff:
161 if IsOctave
162     error('Sorry, this function does not yet work on GNU/Octave.');
163 end
164
165 % private member variables
```

```
166 probeset    = [];          % possible probe values to be tested
167 aset        = [];          % pse's tested (and fitted)
168 bset        = [];          % slopes fitted
169 agrid       = [];
170 bgrid       = [];
171 lapse_rate  = [];          % lapse/mistake rate
172 guess_rate  = [];          % guess rate
173 phist       = [];          % probe history
174 rhist       = double([]);  % response history (0 or 1)
175 loglik      = [];
176 lik         = [];
177 g0          = [];
178 g1          = [];
179 % likelihood lookup table
180 qUseLookup  = [];          % can explicitly be set to true or false by user with
181 likLookup   = [];
182 qLookupCompressed = false;  % lots of overlap between likelihoods for different probe values, compute and store in a format↙
making use of this overlap
183
184 % option: use a subset of all data for choosing the next probe, default values:
185 quse_subset = false;        % use limited subset for computing next probe? Limited subset by discarding a fixed number of trials
186 quse_subset_perc = false;   % same as above, but instead use a percentage of the available data
187 minsetsize  = 10;           % minimum size to start subsetting
188 subsetsize  = 3;            % subset contains subsetsize less datapoints than full dataset
189 percsetsize = .8;           % percentage of data in set used
190
191 % option: set the value to test if probe history is empty
192 first_value = [];           % first value to test instead of random or by prior
193
194 % psychometric function that is used (default)
195 psychofunc     = [];
196 psychofuncStr  = 'cumGauss';
197
198 % subfunction
199 if nargin<1 || strcmpi(mode,'legacy')
200     fhndl = @MinExpEntStair_internal;
201     external_funs     = {@init, @loadhistory, @loadprior, @toggle_use_resp_subset, @toggle_use_resp_subset_prop,↙
@set_first_value, @set_use_lookup_table, @get_use_lookup_table, @set_psychometric_func, @get_psychometric_func,↙
@get_next_probe, @process_resp, @get_history, @get_fit, @get_PSE_DL};
202     external_funs_str = cellfun(@(x) strrep(func2str(x),[mfilename '/''],''),external_funs,'uni',false);
203 elseif strcmpi(mode,'v2')
204     % setup function handles
205     fhndl.init                      = @init;
206     fhndl.loadhistory               = @loadhistory;
207     fhndl.loadprior                 = @loadprior;
208     fhndl.toggle_use_resp_subset    = @toggle_use_resp_subset;
209     fhndl.toggle_use_resp_subset_prop   = @toggle_use_resp_subset_prop;
210     fhndl.set_first_value           = @set_first_value;
211     fhndl.set_use_lookup_table      = @set_use_lookup_table;
212     fhndl.get_use_lookup_table      = @get_use_lookup_table;
213     fhndl.set_psychometric_func     = @set_psychometric_func;
214     fhndl.get_psychometric_func     = @get_psychometric_func;
215     fhndl.get_next_probe            = @get_next_probe;
216     fhndl.process_resp              = @process_resp;
217     fhndl.get_history               = @get_history;
```

```
218     fhndl.get_fit                   = @get_fit;
219     fhndl.get_PSE_DL                = @get_PSE_DL;
220
221 end
222
223 % public interface
224     function [varargout] = MinExpEntStair_internal(mode,varargin)
225         % get internal function to run
226         qFun = strcmp(mode,external_funs_str);
227         if any(qFun)
228             % run function
229             [varargout{1:nargout}] = external_funs{qFun}(varargin{:});
230         else
231             error('MinExpEntStair: mode "%s" unknown',mode);
232         end
233     end
234
235     % init
236     function [] = init(probeset_,meanset,slopeset,lapse_rate_,guess_rate_)
237         probeset            = probeset_;
238         aset                = meanset;
239         bset                = slopeset;
240         [agrid,bgrid]       = meshgrid(aset,bset);
241         % init with uniform probability, normalized
242         loglik              = zeros(size(agrid)) - log(numel(agrid));
243         lik                 = ones(size(agrid))./numel(agrid);
244         % lapse rate and guess rate
245         lapse_rate          = lapse_rate_;
246         % the lapse rate cannot be exactly 0 as the computed
247         % probability must not be exactly 0 so we can work with
248         % log(prob) without trouble, so set it to 1e-10 at least.
249         lapse_rate          = max(lapse_rate,1e-10);
250         % guess rate is optional, if not specified we assume a 2IFC
251         % discrimination experiment where the guess rate is
252         % irrelevant as function goes from always one option at the
253         % one end to always the other option at the other end.
254         if nargin<5
255             guess_rate = 0;
256         else
257             guess_rate = guess_rate_;
258         end
259
260         % lapse rate:
261         % 1. for a discrimination setup (guess_rate==0) the
262         % lapserate basically means that instead of ranging from 0
263         % to 1, the psychometric function ranges from lapse_rate/2
264         % to 1-lapse_rate/2
265         % 2. for a detection setup, the lower bound is guess_rate
266         % and the upper bound is 1-lapse_rate
267
268         % lower bound of pyschometric function
269         % and
270         % range of pyschometric function
271         if guess_rate==0
272             g0 = lapse_rate/2;
```

```
273         g1 = 1 - lapse_rate;
274       else
275         g0 = guess_rate;
276         g1 = 1 - lapse_rate - guess_rate;
277       end
278
279       set_psychometric_func(psychofuncStr);   % calls precomputeLikelihoods()
280     end
281
282
283     %%% load bunch of previously run trials (need probes and
284     %%% responses)
285     function [] = loadhistory(probes,responses)
286       phist              = probes;
287       rhist              = responses;
288
289       % refit likelihood up to this point
290       [loglik,lik]       = fit_all(phist,rhist);
291     end
292
293
294
295     %%% load a prior likelihood, so that first probe is not chosen
296     %%% randomly and you can influence evolution of the fit
297     function [] = loadprior(priorlik_)
298       assert(all(loglik(:)==-log(numel(agrid))),'Cannot load prior if we have a likelihood already'); % this tests if it is not default↙
inited
299
300       priorlik = priorlik_;
301       assert(size(priorlik,1)==length(bset),'Number of rows in prior much match length of slope set')
302       assert(size(priorlik,2)==length(aset),'Number of columns in prior much match length of mean set')
303       assert(all(priorlik(:)>=0),'Loaded prior is not expected to be a log likelihood (that is: all your probabilities should be larger↙
than or equal to 0!)');
304
305       loglik  = normalize_loglik(log(priorlik));
306       lik     = exp(loglik);
307     end
308
309
310     %%% use subset of data for computing next probe
311     function [varargout] = toggle_use_resp_subset(minsetsize_,subsetsize_)
312       % option: extract a probe and response subset for choosing
313       % the next probe, and fit just those
314       % when lots of trials ran, entropy function often has two
315       % local minima, with their relative values switch back and
316       % forth. This will lead to large oscillations in the probe
317       % value being tested (one trial a probe from the beginning
318       % of set, next trial a probe from the end and the from
319       % beginning of set again).
320       % We want to avoid these oscillations in probe values,
321       % therefore we select a limited subset of data to calculate
322       % the best next probe.
323       quse_subset  = ~quse_subset;
324       assert(~(quse_subset && quse_subset_perc));
325       if nargin>0 % change defaults
```

```
326         minsetsize = minsetsize_;
327         subsetsize = subsetsize_;
328     end
329     varargout{1} = quse_subset;
330     varargout{2} = minsetsize;
331     varargout{3} = subsetsize;
332 end
333
334
335 %%% use subset of data for computing next probe
336 function [varargout] = toggle_use_resp_subset_prop(minsetsize_,percsetsize_)
337     % same as above, but now always use a proportion of the
338     % available data
339     quse_subset_perc  = ~quse_subset_perc;
340     assert(~(quse_subset_perc && quse_subset));
341     if nargin>0 % change defaults
342         minsetsize  = minsetsize_;
343         percsetsize = percsetsize_;
344     end
345     varargout{1} = quse_subset_perc;
346     varargout{2} = minsetsize;
347     varargout{3} = percsetsize;
348 end
349
350
351 %%% set the first value to test. Normally the first is chosen
352 %%% randomly or by using the prior that you loaded. If you prefer
353 %%% to start at a fixed value, use this.
354 function [] = set_first_value(first_value_)
355     first_value = first_value_;
356     if ~isempty(phist)
357         warning('the first trial has already been run. Setting the first value now is pointless and it''ll be ignored');
358     end
359 end
360
361
362 %%% if set to true or false, for (not) using of a precomputed lookup
363 %%% table instead of evaluating the psychometric function all the time.
364 %%% call this before calling init as lookup table computation is
365 %%% triggered at end of init
366 function [] = set_use_lookup_table(qUseLookup_)
367     qUseLookup = qUseLookup_;
368     if qUseLookup && isempty(likLookup)
369         precomputeLikelihoods();
370     end
371 end
372 %%% get if lookup table is currently used.
373 function varargout = get_use_lookup_table()
374     varargout{1} = qUseLookup;
375 end
376
377
378 %%% set the psychometric function to be used (default cumulative
379 %%% Gaussian). Can be called at any time (but it will refit all
380 %%% the data already present and thus remove the effect of any
```

```
%%% priors).
function [] = set_psychometric_func(funcID)
    % currently supported:
    %  'cumGauss' - Cumulative Gaussian
    %  'logistic' - logistic function
    switch funcID
        case 'cumGauss'
            psychofunc = @(x,a,b) normcdf((x-a)./b);

            %       1  [           x - a      ]
            %   P = --- [ 1 + erf( ---------- ) ],
            %       2  [         b*sqrt(2)    ]
            % where a and b are known as the mean (mu) and the standard
            % deviation (sigma)
            % http://en.wikipedia.org/wiki/Normal_distribution

        case 'logistic'
            psychofunc = @(x,a,b) 1./(1+exp(-(x-a)./b));

            %             1
            % P =   -------------------,
            %            -(x - a)/b
            %       1 + e^
            %
            % where a and b are known as the mean (mu) and b is
            % proportional to the standard deviation (s)
            % http://en.wikipedia.org/wiki/Logistic_distribution

        otherwise
            error('Psychometric function "%s" not supported',funcID);
    end
    psychofuncStr = funcID;
    % recompute lookup table
    precomputeLikelihoods();
    % if there's any data already, refit it using the new
    % psychometric func. This would remove the effect of any
    % priors!
    if ~isempty(phist)
        ndata = min(length(phist),length(rhist));
        [loglik,lik]    = fit_all(phist(1:ndata),rhist(1:ndata));
    end
end
%%% get the psychometric function that is currently used.
function [varargout] = get_psychometric_func()
    % currently possible outputs:
    %  'cumGauss' - Cumulative Gaussian
    %  'logistic' - logistic function
    varargout{1} = psychofuncStr;
end


%%% given history, get which probe is best to test next
function [p,entexp,indmin] = get_next_probe()
    if isempty(phist) && ~isempty(first_value)
        % first trial and user requested a specific probe value to be tested
```

```
436         p               = first_value;
437         [entexp,indmin]  = deal([]);
438       else
439         [p,entexp,indmin]   = getnextprobe;
440         if isempty(p) || isscalar(unique(loglik))
441           % if we couldn't compute expected entropy, or we have a
442           % uniform likelihood on which calculation was based
443           % (useless prior info, such as default inited), fall
444           % back on random probe selection
445           p                 = probeset(round(RandLim(1,1,length(probeset))));
446           [entexp,indmin]     = deal([]);
447         end
448       end
449       phist          = [phist p];
450   end
451
452
453   %%% fit likelihoods for new response
454   function [] = process_resp(resp) % resp on current trial
455     rhist(end+1)    = resp;
456     [loglik,lik]    = fit_additional_data_point(loglik,phist(end),rhist(end));
457   end
458
459
460   %%% retrieve probe and response history
461   function [varargout] = get_history()
462     varargout{1}    = phist;
463     varargout{2}    = rhist;
464   end
465
466
467   %%% get fitted a (PSE) and b (slope) parameters and loglik.
468   %%% This returns the fit of all data, also when subsetting is
469   %%% enabled.
470   function [varargout] = get_fit()
471     kmin           = find(loglik == max(loglik(:))); % most likely combination(s) of PSE and Slope
472     varargout{1}    = mean(agrid(kmin));
473     varargout{2}    = mean(bgrid(kmin));
474     varargout{3}    = loglik;
475   end
476
477
478   %%% get fitted PSE and DL (distance of 75% point from the 50%
479   %%% point) and loglik. This returns the fit of all data, also
480   %%% when subsetting is enabled.
481   %%% This function is meant to be used for discrimination
482   %%% experiments only (hence the terminology), although it will
483   %%% return the inflection point and the distance between the
484   %%% points that are equivalent to the 50% and 75% points after
485   %%% scaling the psychometric function for all setups.
486   function [varargout] = get_PSE_DL()
487     [varargout{1:3}] = get_fit();
488     % convert b (dispersion) parameter to DL
489     switch psychofuncStr
490       case 'cumGauss'
```

```
491             varargout{2} = varargout{2} * erfinv(.5)*sqrt(2);
492         case 'logistic'
493             varargout{2} = varargout{2} * log(3);
494         otherwise
495             error('Psychometric function "%s" not supported',psychofuncStr);
496     end
497 end
498
499
500 % helpers (private functions, can only be called from the public
501 % functions above)
502 function [p,entexp,indmin] = getnextprobe
503     if length(rhist)>minsetsize && (quse_subset || quse_subset_perc)
504         % select subset and fit
505         if quse_subset_perc
506             ind = NRandPerm(length(rhist),round(length(rhist)*percsetsize)); % select percentage of set
507         else
508             ind = NRandPerm(length(rhist),length(rhist)-subsetsize); % select set minus a few data points
509         end
510         [thellik,thelik] = fit_all(phist(ind),rhist(ind));
511     else
512         % use likelihoods already fitted for all available data
513         thelik  = lik;
514         thellik = loglik;
515     end
516
517     entexp  = zeros(1,length(probeset));
518     for ksamp = 1:length(probeset)
519         % p values for each possible model
520         % these are used in multiple steps
521         pvalsamp    = fit_a_point(probeset(ksamp),1);
522
523         % expected value is sum, weighted by lik
524         pval        = sum(pvalsamp(:).*thelik(:));
525
526         % two possibilities for next response, 0 or 1
527         % each would make a diff new likelihood function
528         newloglik0  = thellik(:) + log(1 - pvalsamp(:));
529         newloglik1  = thellik(:) + log(    pvalsamp(:));
530
531         % important! need to normalize
532         newloglik0  = normalize_loglik(newloglik0);
533         newloglik1  = normalize_loglik(newloglik1);
534
535         % 0 and 1 for next response each has an entropy
536         ent0        = sum(-exp(newloglik0).*newloglik0);
537         ent1        = sum(-exp(newloglik1).*newloglik1);
538
539         % probability pval of 0, probability (1-pval) of 1
540         % use these to get expected value of entropy
541         entexp(ksamp)  = ent0*(1-pval) + ent1*pval;
542     end
543
544     indmin      = find(entexp == min(entexp),1);
545     p           = probeset(indmin);
```

```
546 end
547
548 function [loglik,lik] = fit_additional_data_point(loglik,probe,resp)
549     % get likelihood of current point
550     currlik = fit_a_point(probe,resp);
551     % multiply with previous likelihoods
552     loglik  = loglik + log(currlik);
553
554     % normalize
555     loglik  = normalize_loglik(loglik);
556     lik     = exp(loglik);
557 end
558
559 function [loglik,lik] = fit_all(probes,resps)
560
561     if length(probes) ~= length(resps)
562         error('Number of probe values and responses does not match');
563     end
564
565     if strcmp(psychofuncStr,'cumGauss')
566         % we have a fast one for this!
567         loglik = FitCumGauss_MES(probes,resps,aset,bset,lapse_rate,guess_rate);
568     else
569
570         loglik = zeros(size(agrid));
571         for p=1:length(probes)
572             loglik = fit_additional_data_point(loglik,probes(p),resps(p));
573         end
574     end
575
576     % normalize
577     loglik  = normalize_loglik(loglik);
578     lik     = exp(loglik);
579 end
580
581 function pval = fit_a_point(probe,resp)
582     if qUseLookup
583         qProbe = probeset==probe;
584         if qLookupCompressed
585             pval = likLookup(:,[(end-length(aset)+1):end]-find(qProbe)+1);
586         else
587             pval = likLookup(:,:,qProbe);
588         end
589     else
590         pval = evalLikelihood(probe);
591     end
592     % if response was wrong flip probs
593     if resp <= 0
594         pval = 1-pval;
595     end
596 end
597
598 function [] = precomputeLikelihoods()
599     if isempty(aset)
600         % called before init, parameter space not known yet, nothing to
```

```
601         % do here
602         return;
603       end
604       if ~isempty(qUseLookup) && ~qUseLookup
605         % were not using lookup tables by users request, return
606         return;
607       end
608
609       % determine if we want to precompute
610       % first see if compressed format is possible. It is if same
611       % stepsize for probeset and aset, as there is then significant
612       % overlap between the pvalues for each probe level (could extend
613       % this to one being multiples of the other...)
614       stepP = mean(diff(probeset));
615       stepA = mean(diff(aset));
616       qLookupCompressed = abs(stepP-stepA)<=2*eps;
617
618       % use lookup if compressed possible, or if table would be small,
619       % or if user asked for it.
620       if  (isempty(qUseLookup) && (...
621             qLookupCompressed || ...              % same stepsize for probeset and aset
622             numel(agrid)*length(probeset)/128/1024<3)...% small lookup table (by some arbitrary standard of what is small, which↙
in this case is less than 3 mb)
623             ) ||...
624           (~isempty(qUseLookup) && qUseLookup)          % user asked for it
625
626         qUseLookup = true;
627
628         nProbe = length(probeset);
629         if qLookupCompressed
630           [tempAGrid,tempBGrid] = meshgrid(linspace(probeset(1)-aset(1,end),probeset(end)-aset(1,1),length(aset)+length↙
(probeset)-1),bset);
631           likLookup = g0 + g1*psychofunc(0,tempAGrid,tempBGrid);
632         else
633           likLookup = zeros([size(agrid) nProbe]);
634           for p=1:nProbe
635             likLookup(:,:,p) = evalLikelihood(probeset(p));
636           end
637         end
638       else
639         qUseLookup = false;
640       end
641
642     end
643
644     function pval = evalLikelihood(probe)
645       % evaluate psychometric function, incorporate lapse rate and guess rate
646       pval = g0 + g1*psychofunc(probe,agrid,bgrid);
647     end
648
649     function loglik  = normalize_loglik(loglik)
650       loglik  = loglik - log(sum(exp(loglik(:))));
651     end
652 end
```

Appendix 3 – Task timeline checklist

Tactile taks+ pupillometry + hdEEG checklist
ID:_____ Date:_____Hand:_____

Connections Tactile + pupillometry:
☐ Amplifier to outlet
☐ Cart to outlet
☐ Plug camera
☐ HDMI from Atlantica to Amplifier
☐ Ethernet from Amplifier to tactors
☐ Ethernet + thunderbolt from Eyelink to mac
☐ VGA + thunderbolt from Eyelink to mac
☐ USB to Button Box
☐ USB to Arduino
☐ Flashdrive to clonerbox

Steps 1:
☐ Consent
Measure head
☐ Circumference 2X (from nasion to one finger over the inion) - choose net – write net size
☐ Sagittal measurement - mark halfway from nasion to inion
☐ Coronal measurement – mark the preauriculars and halfway between them, crossing by the sagittal mark

☐ Place net
☐ Connect net to arm
Set-up computer
☐ Open net station
☐ Start new session
☐ Choose *Sharif_4markers_2.0*
☐ Click on rename
☐ Create a new folder under Test Data>>Blumenfeld>>Tactile>> *SubjectID*
☐ Name the session 000XX_Session1 (alphanumeric code)
☐ Measure Net Impedances (ideal 70)
☐ Gel the net
☐ Click on *save and close*
☐ Open net impedances again, change to 40, and just close.
☐ Click on Panels>>Waveform
☐ Click on ball on bottom of the screen and check if the clock moves = it is recording
☐ Check the TTL pulses
☐ Start recording from clonerbox

Net size:_____ Room Lighting:_____

Connections Tactile + hdEEG
☐ Connect both sides of time bus cable (green)
☐ Connect USB B to bottom box (beige)
☐ Disconnect 128 cable and connect 256 to top amp (both cables from the same arm should be connected)
☐ Connect VGA from Arduino to bottom amp

Steps 2:
☐ Start the task
☐ Check if the person is feeling all fingers
☐ Calibrate
☐ Validate
☐ Click on *OUTPUT/RECORD*
☐ Do drift correct
☐ Click on OUTPUT/RECORD
☐ Start task
☐ Observe p100cp, if it starts to go to low, readjust the fingers in the straps.
Runs check
☐ Run 1
☐ ***Check Room lighting*** – write here_____
☐ Calibrate? ☐ Run 2
☐ Calibrate? ☐ Run 3
☐ Calibrate?
☐ Check clock, if time> 45 min, restart the EEG file
☐ Run 4
☐ Stop clonerbox recording
☐ Do photogrammetry
☐ Name photogrammetry file 000XX_GPS
☐ Let person clean up
☐ Pay

Disconnect
☐ Both sides of time cable
☐ USB B from bottom amp
☐ 256 from top amp and connect the 128 one
☐ VGA from bottom amp

Clean net
☐ Take all the gel with warm spray nozzle
☐ Let for 1 minute in disinfectant
☐ Rinse in bucket 6 times 10
☐ Rinse in bucket with distilled water 1 time 10